



# A Platform for Controlled Myelination:

An Investigation into Patterned  
Oligodendrocyte Growth

Rosey Rasoda  
Department of Biomedical Engineering  
McGill University, Montreal  
December 2015

A thesis submitted to McGill University in partial fulfillment of the requirements of  
the degree of Master of Engineering.

© Rosey Rasoda 2015

## Acknowledgements

Firstly, I would like to thank my supervisor, Dr. Maryam Tabrizian, for her continual support and guidance. Thank you for inviting me into your lab, for encouraging my work, and for helping me to always keep moving forward in my project.

I would also like to thank Dr. Mina Mekhail for all his advice and guidance throughout my project. From the project concept to the finer points of cell culture, thank you for always sharing your ideas and skills with me - your support has been invaluable. (And, of course, thank you for helping me re-adjust my expectations for working with primary cells!)

To the entire Biomat'X laboratory (past, present, and honorary), thank you not only for sharing your time, knowledge, and immense talent with me, but also for making my time at McGill unforgettable. I couldn't have asked for a warmer, sweeter, or smarter group of people to spend these last two(-ish) years with. Thank you!

Additional thanks goes to Dr. Guillermina Almazan and her entire lab for sharing their vast expertise and for kindly providing primary cells, cell culture reagents, and laboratory space. I would like to extend a special thank you to Li-Chun (Lydia) Wang for her endless support and assistance. For everything, from performing extra dissections to letting me into the lab on weekends, I could not have completed this work without your help. Most of all, thank you for always taking the time to answer my countless questions –your patience and expertise know no bounds!

And to my family, thank you for your visits, your calls, your care packages, and your belief in me. It made being away not feel that far away.

## Abstract

Through myelination, specialized glial cells, including oligodendrocytes in the central nervous system, wrap membrane processes around neuronal axon segments forming multilamellar myelin sheaths. As it is critical to normal motor and cognitive function, furthering the understanding of myelin formation and function as well as degeneration and dysfunction is of high importance. By and large, *in vitro* myelination studies involve unstructured co-cultures of neuronal and glial cells. However, these systems are often beset by difficulties in consistent replication, control on a single cell level, and microenvironment manipulation. With innovations in techniques to control cell growth, investigations of structured co-cultures are becoming more common. One favoured technique is microcontact printing, hailed for its speed, simplicity, and low-cost. Currently, however, structured myelination co-cultures tend to focus only on controlling the growth of neurons, not glial cells.

As such, the primary objective of this study is to direct the growth and development of oligodendrocytes upon patterns of microcontact printed bio-inks, each containing antibodies commonly used to identify oligodendrocyte cells: alpha platelet derived growth factor receptor antibodies and A2B5 antibodies, each alone or combined with O4 antibodies. For each of the four bio-inks tested, oligodendrocytes showed high levels of pattern adherence (>80%) and differentiation (>90%) after five days in culture. Building upon these successful results, the secondary objective, to investigate the feasibility of a structured co-culture platform, was begun. With respect to neuron growth, patterned laminin was found to successfully direct axon extension and maintain neuron attachment for 2 weeks in culture. Additionally, the four glial bio-inks were able to support patterned oligodendrocyte maturation in pure and co-culture

environments. Finally, the investigated co-culture conditions, including the presence of patterned proteins and antibodies, were found to permit myelination.

## Résumé

La myélinisation est un procédé par lequel des cellules gliales spécialisées, telles les oligodendrocytes du système nerveux central, enveloppent de leur membrane cellulaire des axones, formant ainsi des gaines de myéline multi-lamellaires. Du fait de l'importance de la myéline pour les fonctions motrices et cognitives, l'étude de sa formation et son fonctionnement, ainsi que sa dégénérescence et dysfonctionnement est cruciale. En général, les études de myélinisation in vitro utilisent des co-cultures non-structurées de cellules gliales et neuronales. Néanmoins, les performances de ces systèmes sont limitées dans le cas de la réplication régulière, du contrôle à l'échelle unicellulaire et de la manipulation de microenvironnement. Grâce aux innovations techniques pour le contrôle de la croissance cellulaire, les études de co-culture structurées deviennent de plus en plus fréquentes. Une méthode de choix est l'utilisation d'impression par contact à l'échelle micrométrique, reconnue pour son efficacité, sa simplicité et de son prix abordable. Pour autant, la myélinisation structurée de co-cultures se limite à présent uniquement à la croissance des neurones, et non sur celle des cellules gliales.

En tant que tel, l'objectif primordial de cette étude est de diriger la croissance et le développement des oligodendrocytes sur des motifs de bio-encre à l'aide d'impression par microcontact, chacune contenant des anticorps couramment utilisés pour identifier les oligodendrocytes: les plaquettes alphas dérivées des anticorps de récepteur de facteur de croissance et les anticorps A2B5, soit seuls ou conjugués aux anticorps O4. Sur chacune des quatre bio-encres étudiée, les oligodendrocytes ont démontré des niveaux élevés d'adhérence au motif (>80%) et de différenciation (>90%) au bout de cinq jours en culture. À partir de ces

résultats, l'objectif secondaire, une enquête sur plateforme de co-culture, a été menée. Quant aux cultures de neurones, les résultats ont montré que les motifs de laminine pouvaient diriger avec succès l'extension de l'axone et maintenir l'adhérence neuronale pendant deux semaines en conditions de culture. De plus, les quatre bio-encres gliales étaient en mesure de supporter la maturation des oligodendrocytes en environnement pur et en co-culture. Enfin, les conditions de co-cultures testées, impliquant la présence de motifs de protéines et d'anticorps, ont révélé que la myélinisation était possible.

# Table of Contents

Acknowledgements.....	ii
Abstract .....	iii
Résumé .....	v
Table of Contents.....	vii
List of Figures .....	x
List of Tables .....	xi
List of Abbreviations .....	xii
Chapter 1. Background .....	1
1.1. Myelination in the Central Nervous System .....	1
1.1.1. Myelination .....	1
1.1.2. Oligodendrocytes.....	5
1.1.3. <i>In Vitro</i> Myelination Co-Cultures .....	11
1.2. Microcontact Printing .....	15
1.2.1. Development of Soft Lithography.....	15
1.2.2. Patterning Proteins .....	16
1.2.3. Competing Technologies.....	18
1.2.4. Applications of Microcontact Printing .....	22
1.3. Structured <i>In Vitro</i> Myelination Co-Cultures .....	27
1.3.1. Recent Examples in the Literature.....	27
Chapter 2. Motivation and Objectives.....	33
2.1. Motivation.....	33
2.2. Objectives.....	34
Chapter 3. Materials and Methods.....	36
3.1. Microcontact Printing .....	36
3.1.1. Stamp Photomask.....	36
3.1.2. Stamp Fabrication .....	36
3.1.3. Microcontact Printing Procedure .....	38
3.1.4. Bio-inks and Blocking Agents .....	41
3.2. Cell Culture .....	42
3.2.1. Oligodendrocyte Culture.....	43
3.2.2. Neuron Culture .....	44

3.2.3.	Neuron-Oligodendrocyte Co-Culture.....	46
3.3.	Analysis.....	46
3.3.1.	Immunostaining.....	46
3.3.2.	Cell Survival.....	47
3.4.	Imaging.....	47
3.4.1.	OPC Differentiation Quantification.....	47
3.4.2.	OPC Viability Quantification .....	48
3.5.	Statistical Analysis .....	48
Chapter 4.	Experimental Rationale.....	49
4.1.	Stamp Design.....	49
4.1.1.	Oligodendrocyte Culture.....	49
4.1.2.	Neuron Culture .....	50
4.2.	Bio-Ink Choice.....	50
4.2.1.	Oligodendrocyte Culture.....	50
4.2.2.	Neuron Culture .....	53
Chapter 5.	Results.....	54
5.1.	Oligodendrocyte Culture.....	54
5.1.1.	Pattern Adherence.....	54
5.1.2.	OPC Differentiation.....	61
5.1.3.	OPC Viability.....	63
5.2.	Neuron Culture.....	64
5.2.1.	Neuron Attachment and Pattern Adherence .....	64
5.3.	Neuron-Oligodendrocyte Co-Culture.....	69
5.3.1.	Cross-Printing.....	69
5.3.2.	Pattern Maintenance .....	70
5.3.3.	Myelination .....	73
Chapter 6.	Discussion.....	75
6.1.	Oligodendrocyte Culture.....	75
6.2.	Neuron Culture.....	78
6.3.	Neuron-Oligodendrocyte Co-Culture.....	82
Chapter 7.	Conclusions and Future Work.....	85
References	.....	87
Appendix A	.....	94

Appendix B .....	95
Appendix C .....	96

## List of Figures

Figure 1-1. Oligodendrocyte myelination. ....	3
Figure 1-2. Oligodendrocyte development.....	7
Figure 1-3. Croissant mechanism of myelination. ....	9
Figure 1-4. Traditional myelination co-cultures. ....	14
Figure 1-5. Different patterning techniques. ....	19
Figure 1-6. Examples of controlling cell growth using microcontact printing.....	24
Figure 1-7. Examples of structured cell growth and structured myelination.....	30
Figure 2-1. Grid design for a controlled myelination platform.....	34
Figure 3-1. Flowchart of the basic photolithography process.....	38
Figure 3-2. Flowchart of the microcontact printing process. ....	40
Figure 4-1. Markers present at different developmental stages of the oligodendrocyte cell lineage, in rodents. ....	51
Figure 5-1. Oligodendrocyte adherence to patterned anti-PDGFr- $\alpha$ . ....	55
Figure 5-2. Oligodendrocyte adherence to patterned anti-PDGFr- $\alpha$ /O4. ....	56
Figure 5-3. Oligodendrocyte adherence to patterned anti-A2B5.....	57
Figure 5-4. Oligodendrocyte adherence to patterned anti-A2B5/O4. ....	58
Figure 5-5. Oligodendrocyte adherence to the positive control, unpatterned poly-L-ornithine. ....	59
Figure 5-6. Oligodendrocyte adherence to patterned anti-PDGFr- $\alpha$ diluted in PBS and SFM. ....	60
Figure 5-7. OPC differentiation after 5 days on patterned bio-inks. ....	62
Figure 5-8. OPC viability after 5 days on patterned bio-inks. ....	63
Figure 5-9. Neuron attachment to collagen-I. ....	65
Figure 5-10. Neuron attachment to laminin patterns at day 3 and day 13.....	66
Figure 5-11. Neuron attachment to laminin at day 28. ....	66
Figure 5-12. Neuron culture on plastic coverslips. ....	68
Figure 5-13. Cross-printed pattern. ....	69
Figure 5-14. Oligodendrocyte adherence to patterns printed 0 days and 23 days before cell seeding.....	71
Figure 5-15. Oligodendrocyte adherence to antibodies on co-culture substrates, patterned 21 days before cell seeding.....	72
Figure 5-16. Successful myelination of mature axons by oligodendrocytes. ....	74
Figure 6-1. Designs for networked neuronal growth. ....	80
Figure 6-2. Overgrowth of neuron attachment on patterned laminin at day 28. ....	80
Figure 6-3. Alternate designs for controlled myelination platforms.....	83

## List of Tables

Table 3-1. Serum-free media components .....	44
Table 3-2. N1 media components.....	45

## List of Abbreviations

$\mu$ CP	microcontact printing
$\mu$ FN	microfluidic network
AFM	atomic force microscopy
DPN	dip-pen nanolithography
PDMS	polydimethylsiloxane
CNS	central nervous system
PNS	peripheral nervous system
OPC	oligodendrocyte progenitor cell
DRG	dorsal root ganglion
UV	ultraviolet light
DMEM/F12	Dulbecco's modified Eagle medium/Ham's F12 medium
ddH <sub>2</sub> O	double distilled water
PBS	phosphate buffered saline
PBS*	phosphate buffered saline with magnesium and calcium
SFM	serum-free media, composition listed in Table 3-1
N1	N1 media, composition listed in Table 3-2
$X \times Y \mu\text{m}$	pattern of parallel lines, $X \mu\text{m}$ thick with $Y \mu\text{m}$ spacing between lines
anti- $X/Y$	mixture of antibody $X$ and antibody $Y$
(anti-)PDGFr- $\alpha$	alpha platelet derived growth factor receptor (antibody)
(anti-)O4	oligodendrocyte marker O4 (antibody)
(anti-)A2B5	A2B5 marker (antibody)
anti-trkA	tropomyosin receptor kinase A antibody
(anti-)GalC	galactocerebroside (antibody)
(anti-)MBP	myelin basic protein (antibody)
anti-N52	neurofilament N52 antibody
AraC	cytosine-1-b-D-arabinofuranoside
PLL-g-PEG	poly(L-lysine)-grafted-poly(ethylene glycol)

# Chapter 1. Background

## 1.1. Myelination in the Central Nervous System

### 1.1.1. Myelination

Within complex nervous systems, there exists an intricate system of neuronal and glial cells [11]. Glial cells generally outnumber neurons, comprising 65% of the total cells in rodent brains and 90% in human brains [3, 12]. Despite this, historically, careful attention was only ever paid to neuronal cells, with glial cells considered ‘nervenkitt’ –literally meaning nerve glue– and thought to act as connective tissue in the brain [3, 12, 13]. Today, glial cells are known to provide a much more critical role, with neuron-glial interactions essential to normal development within the nervous system [14]. Lacking electrical excitability, glial cells are thought to “support and moderate neuronal function” [11], necessary for both the maturation of neurons and overall functioning of the nervous system [3]. Specifically, this support is thought to manifest in roles affecting the plasticity of neural synapses, the functionality of axons, and the facilitation of neuron connectivity [12]. Primarily, glial cells consist of microglia and macroglia, the latter of which includes oligodendrocytes, Schwann cells, and astrocytes. Within the central nervous system, microglia are known to play important roles in homeostasis and immunological responses, and astrocytes are known to play key roles in connecting neurons to blood vessels as well as modulating neurotransmitters and the external ionic environment [14]. The remaining major glial cells are oligodendrocytes and Schwann cells. Among their many roles, they are known primarily as myelinating cells –with oligodendrocytes

myelinating neurons within the central nervous system (CNS) and Schwann cells performing the equivalent function within the peripheral nervous system (PNS).

Myelination, as illustrated in Figure 1-1, is the process by which these specialized glial cells extend their plasma membranes to ensheath neuronal axons in distinct segments [15]. These myelin sheaths, formed of multiple layers of glial membrane, act as electrical insulators, allowing for the saltatory conduction of action potentials along an axon [12, 13, 16]. Each section of myelin sheath, or internode, insulates the axonal membrane, increasing the transverse resistance along the length of the sheath and causing sodium channels to cluster in the short, unmyelinated regions between the internodes, referred to as nodes of Ranvier [2, 17]. This allows action potentials to rapidly propagate along the myelinated axon from one node of Ranvier to another [2, 12, 17, 18]. In other words, the action potential 'jumps' from one node to the next in lieu of a measured progression along the entire length of the axon, as is the case for unmyelinated axons [3]. This rapid impulse propagation, known as saltatory conduction, increases the speed of signal conduction in myelinated axons by a factor between 20 and 100 [2]. Similarly, this saltatory conduction also provides a level of energy saving, as the need to maintain the resting potential of the axonal membrane, using ATP dependent ion channels, is also reduced [2]. Thus, myelination enables the fast and efficient propagation of electrical signals through the nervous system [12]. As such conduction is necessary for normal motor, sensory and cognitive function, the importance of proper myelination cannot be overstated [2, 19].

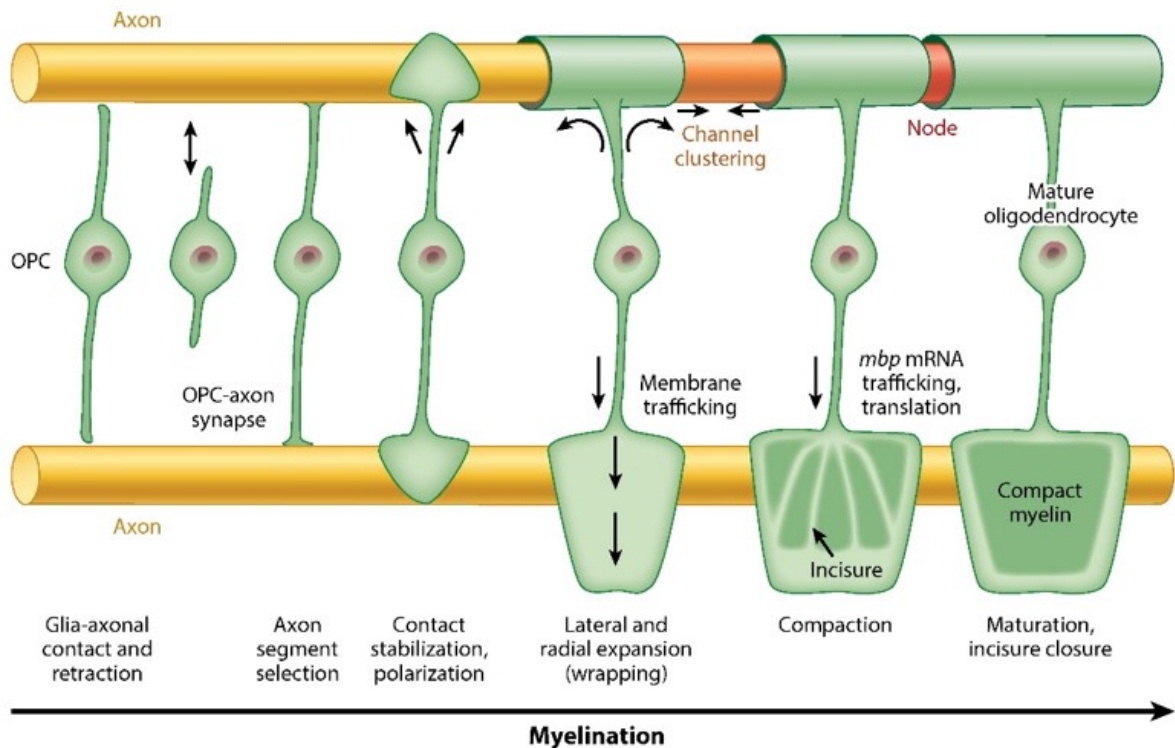


Figure 1-1. Oligodendrocyte myelination.

This image depicts the major steps involved in oligodendrocyte maturation and myelination, as illustrated by Nave and Werner [2]. Adapted from [2], copyright © 2014, Annual Reviews.

Myelin itself is a white, fatty substance, rich in lipids including cholesterol [20]. It contains only 40% water, in contrast to the 80% seen with the largely unmyelinated grey matter [13]. By dry weight, myelin consists of approximately 70-80% lipids and 20-30% proteins, a feature quite unique to myelin and largely reversed in other cell membranes [3, 13, 21]. Taken together, this low water and high lipid composition allows myelin to function as a successful electrical insulator for axons [3]. Moreover, the high levels of cholesterol, approximately 25%, are thought to play an important role in the expansion of myelin and are considered a rate-determining factor in myelination [2]. Of the remaining lipid concentration, galactocerebroside

(GalC) seems to be a major constituent [21, 22]. With respect to proteins, myelin basic protein (MBP) is a relatively large component [3, 22]. However, the full protein composition in the PNS and CNS differ, with glycoproteins being favoured in the former and basic proteins favoured in the latter [22]. In the PNS, the major protein component is myelin protein zero (P0) at 50-70%, with MBP following at 5-15% [22]. In the CNS, the major protein component is proteolipid protein (PLP) at 50% followed by MBP at 30% [3]. It is worth noting that MBP is a strict requirement for healthy, compact myelination in the CNS but not in the PNS [2].

With its complex structure and role in rapid impulse propagation, it is clear that myelination plays an important role in the nervous system. With myelinated white matter comprising 40% of the brain, its ubiquitous presence in the CNS suggests the indispensable nature of myelin [15]. As is often posited, myelin is not simply an inert electrical insulator but a mainstay in the normal development of the nervous system, playing a role in both the maintenance and functionality of axons [12, 13, 20]. Thus, it follows that disrupted myelination can result in deleterious effects to motor and sensory functions and underlie a number of neurological disorders [23, 24]. For example, in the CNS, abnormal myelination can result from dysmyelinating disorders including leukodystrophies such as Pelizaeus-Merzbacher disease [2]. Similarly, damaged myelination can result from trauma such as spinal cord injuries or from demyelination as found in multiple sclerosis [2, 20, 21]. Charcot-Marie-Tooth neuropathy and Guillain-Barré syndrome are additional demyelinating disorders found in the PNS [2]. Each of these can have significant impacts on sufferers, resulting in pain, severe loss of muscle function, or even neurological disability [20].

However, neither the morphogenesis of myelinated nerves nor the mechanisms of myelin dysfunction is completely understood [3, 23]. Moreover, although the importance of axon-glia support is often discussed, the underlying mechanisms are still being investigated [11]. In fact, the regulatory signals for CNS myelination have yet to be fully identified [13, 24]. For such reasons, the continued study of myelination is a critical step in furthering its understanding, from the basic science of myelination generation and degeneration to the causes and treatments of its dysfunction.

### 1.1.2. Oligodendrocytes

Within the CNS, the complexity of the axon-glia relationship still presents a number of unanswered questions. For example, although a single-key regulator has been found in the PNS (neuregulin-1), the exact myelination triggers in the CNS are still not known [13, 17]. Similarly, the myelination axon selection process in the CNS is not as clearly defined as in the PNS [13]. Thus, the continued study of CNS myelination can help to address some of these remaining questions. To that end, it is important to better understand one of the key players in CNS myelination, oligodendrocytes. As, in large part, the general understanding of oligodendrocytes is derived from their study in rodents, observations drawn using these models will be discussed here [17].

In order to acquire myelination abilities, these glial cells must undergo a process of differentiation, maturing from oligodendrocyte progenitor cells (OPCs) into myelin producing oligodendrocytes [1]. These OPCs originate from within the ventral ventricular zone, and through proliferation and migration, move throughout the CNS [17, 25, 26]. As this

differentiation must be co-ordinated with the development process of neurons, its initiation and control is thought to be mediated by neuronal signals –although the exact signalling pathways have yet to be fully identified [12, 13]. As the differentiation process progresses, OPCs begin to lose their migratory and proliferation capacities [1]. Once settled, these cells undergo a four stage differentiation process, illustrated in Figure 1-2 below. This maturation from OPC to pre-oligodendrocyte to immature oligodendrocyte to mature oligodendrocyte manifests morphologically as well. That is, the OPCs begin as bipolar cells and differentiate into post-mitotic, multi-processed, mature oligodendrocytes [1]. At this mature stage, oligodendrocytes are capable of myelination, and even when outside the vicinity of neurons, still form a myelin-like membrane [3]. The timing of this differentiation process is of vital importance; as mature oligodendrocytes are largely unable to re-position or postpone myelination, it is essential that they are correctly situated before differentiation [13]. Similarly, the window of myelin synthesis is relatively brief, and mature oligodendrocytes cannot re-acquire this myelination ability [17].

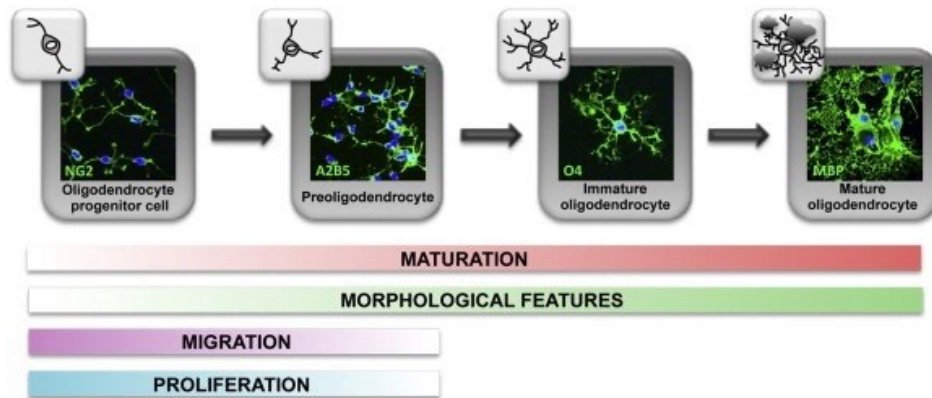


Figure 1-2. Oligodendrocyte development.

In this image, the four stages of oligodendrocyte maturation are depicted by Barateiro *et al.* [1], with accompanying illustrations of morphological features. Adapted with permission from [1], copyright © 2014, Elsevier.

In the PNS, each Schwann cell attaches to a single axon during myelination, creating a one-to-one ratio of Schwann cell to internode [15, 22]. In contrast, a single oligodendrocyte can ensheath over 60 separate axon segments [15, 16]. Moreover, the multiple myelin sheaths are formed in tandem, with the process allowed only a brief time frame of approximately 12 to 18 hours [17]. It should be noted that some oligodendrocytes are found to myelinate multiple small-diameter axons, forming short internodes, whereas others myelinate only a select few large-diameter axons, forming longer internodes and thicker myelin sheaths [15]. By and large, the average oligodendrocyte appears to form 20 to 60 internodes, with an average length between 20 and 200  $\mu\text{m}$  –although possibly as high as 1,500  $\mu\text{m}$  [13, 15].

The selection of which axons a glial cell will myelinate appears to be, at least in part, due to axons features, with one significant characteristic being size [27]. In the PNS, there is a strict size relationship with Schwann cells only myelinating axons with a diameter of 1  $\mu\text{m}$  or higher

[2, 15]. In the CNS, oligodendrocytes can myelinate any axons with a diameter greater than 0.2  $\mu\text{m}$ ; however, the threshold is actually thought to vary between 0.4 and 1.2  $\mu\text{m}$  [2, 15]. That is, studies have shown that with diameters between 0.2 and 0.8  $\mu\text{m}$ , axons may or may not be myelinated by oligodendrocytes [15]. This suggests that additional signaling factors are responsible for CNS myelination, such as electrical activity [2, 13, 17, 19] and OPC density [2, 26]. Although electrical activity has been seen to promote CNS myelination, it is not strictly necessary. In fact, studies have shown oligodendrocytes to form what are essentially myelin sheaths around electrospun polystyrene nanofibers [28], micropillar arrays [8], and even paraformaldehyde fixed axons [26]. These studies also reinforce the idea that in contrast to Schwann cells, oligodendrocytes do not require the adhesion molecules or growth factors found on axons in order to promote myelination [13].

Although comprising an intricate series of events, the general process of CNS myelination can be summed up through the illustration in Figure 1-1. However, the exact mechanism of CNS myelination is not fully understood due to the difficulties in obtaining high quality images and tissue preparations [15]. However, with the use of novel advancements in confocal live imaging and high pressure freezing, further detailed analyses of myelin sheath formation have become possible [6, 15]. In their 2011 live imaging study, Sobottka *et al.* [6] suggested the 'croissant' method for the formation of the myelin sheath. In this method, depicted in Figure 1-3, the oligodendrocyte process begins to open up as a triangular tongue and wraps around an axon; upon contact, it begins spreading laterally along the length of the axon [6]. From this single oligodendrocyte extension, new layers are formed atop one another, coiling around the axon and thickening the myelin sheath [6]. In their 2014 study, Snaidero *et*

*al.* [29] built upon these findings and provided additional evidence of the myelin sheath forming from a single triangular membrane extension expanding laterally while wrapping around the axon [15]. However, they suggest that within this coiling, new layers are found underneath the previous layers. That is the layer with the largest lateral width is in contact with the oligodendrocyte cell body and that with the shortest lateral width is in contact with the axon [15]. In either case, the lateral edges of each internode is a spiralling or helical coiling pattern, similar to the dough edges of a croissant [6, 15]. These theories on myelin formation each support characteristics of the myelin sheath not addressed in previous theories. These include the non-homogenous surface of the myelin sheath, the inconsistent numbers of myelin layers along the internode, and the bidirectional coiling –each explained by the simultaneous wrapping and lateral spreading of a single oligodendrocyte membrane extension [6, 12, 13, 15].

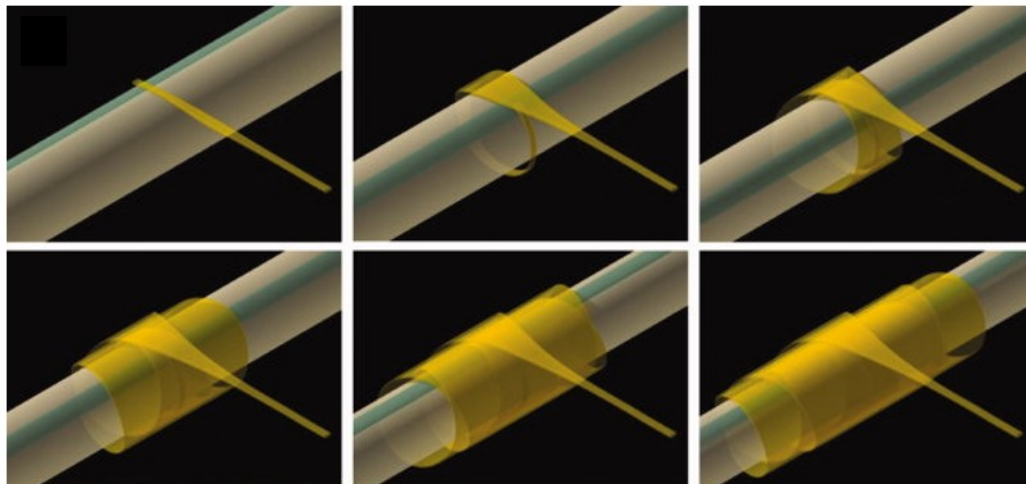


*Figure 1-3. Croissant mechanism of myelination.*

The following illustrates the ‘croissant’ mechanism of myelination suggested by Sobottka *et al.* [6]. The oligodendrocyte process is shown in yellow and the axon is shown in grey. Note the bi-directional lateral coiling, similar to that seen at the edges of a croissant. Adapted with permission from [6], copyright © 2011, John Wiley and Sons.

It must be said that the transformation process required to turn the plasma membrane into myelin is an undoubtedly complex, multifaceted undertaking. These multilamellar myelin sheaths can comprise up to 100-160 layers, necessitating an immense output from the myelinating oligodendrocytes [2, 13]. Estimates suggest that the myelin membrane can grow up to 5,000  $\mu\text{m}^2$  per day, with a single oligodendrocyte producing up to 2,000,000  $\mu\text{m}^2$  of myelin [2, 13]. Capable of producing up to 3 times its weight in myelin and up to 100 times its weight in supporting membrane each day, oligodendrocytes have extraordinary levels of membrane development, far exceeding any other cell type [13, 15].

Although a major facet of its functionality, oligodendrocytes are thought to have a number of additional roles distinct from the formation and maintenance of myelin [3]. Namely, oligodendrocytes are thought to offer axonal support beyond myelination, aiding in functional integrity and survival [11]. Firstly, oligodendrocytes are believed to provide trophic support to axons [2, 12, 17]. Moreover, their metabolic activity is thought to be linked with that of neuronal axons, maintaining axon structure and function through aerobic glycolysis [2, 12, 13]. In fact, it has been suggested that neurodegeneration may befall a system without oligodendrocyte metabolic support [12]. Furthermore, additional functionality is suggested by 'satellite' oligodendrocytes, often found in grey matter with their cell bodies in close association with a neuron but distinct from any myelin sheath [3, 13]. These cells are suggested to regulate the microenvironment around their associated neuron, possibly establishing an interdependency [3, 13].

### 1.1.3. *In Vitro* Myelination Co-Cultures

The intricacies of communication between neuronal and glial cells, including signalling pathways, are thought to be key to furthering the knowledge base surrounding CNS physiology and myelination in particular [28, 30]. With myelin considered critical to healthy motor, sensory and cognitive function [2], the consequences of myelin dysfunction can be quite severe. As such, understanding the mechanisms behind normal myelin formation, disease or trauma based myelin degeneration, and potential myelin regeneration are areas of great interest [2, 8, 12, 23]. Such knowledge is key not only to enhancing the basic science behind such processes but also to driving the development of treatments for dysfunction [2]. To aid such progress, suitable *in vitro* platforms for studying myelination and axon-glial interaction are necessary [2, 8].

Although *in vivo* studies would more faithfully replicate CNS mechanisms, the added cost and time involved are factors to consider. Rodent models, in particular, are beset by minimal offspring and an extended gestational period of approximately 20 days [31]. Although zebrafish have emerged as a “rapid and inexpensive” [31] *in vivo* myelination model comparable to rodent models, it is worth noting that the “inaccessibility and complexity” [32] of the CNS can introduce a number of confounding effects into *in vivo* studies. Thus, high-throughput *in vitro* studies may still be preferable systems for initial investigations.

For *in vitro* studies of CNS myelination, post-natal OPCs co-cultured with purified sensory neurons [27, 32, 33] or CNS neuron explants/cell aggregates [34] are most commonly employed [35, 36]. However, the use of explants and aggregates can present a number of practical limitations for *in vitro* cultures, including difficulties establishing firm substrate

attachment [35]. Moreover, the sheer density of cells has itself proven challenging to manage, as the identifying of individual cells and imaging of thicker tissues can be difficult [35, 37]. Similarly, with the multitude of cell layers found in these samples, it can be harder to ensure reagents reach cultured cells, potentially hampering future quantifications [37]. Furthermore, non-purified cultures may contain additional cell types that can obfuscate findings [32]. For such reasons, the use of purified sensory neurons, including dorsal root and retinal ganglion neurons, are considered among the “most sophisticated” co-culture models [36]. It should be noted that these are not technically considered CNS neurons as ganglia cell bodies do not lie within the CNS and their neurites can extend into both the CNS and PNS [1, 35]. However, many studies still consider these appropriate models [33, 38, 39]. It has also been reported that the myelin formations in rodent and mouse co-cultures of oligodendrocytes and dorsal root ganglion cells (DRGs) have similar characteristics to CNS myelination (i.e. internode lengths similar to those found in the frontal cortex) [1]. Despite co-culture protocols involving CNS neurons (including those derived from the hippocampus [36] and cerebral cortex [37]), DRG-oligodendrocyte co-cultures remain “one of the most universally used myelination models” [37].

It is undoubtedly true that *in vitro* neuron-oligodendrocyte co-cultures [26, 27, 32, 40] have been instrumental in the study of the CNS processes –including the molecular and biochemical cues involved in oligodendrocyte differentiation and myelination formation [23, 32]. Despite the wealth of knowledge gained from these traditional co-cultures, their lack of structure –that is, a level of control or underlying design directing cell growth– can present a few challenges. In these traditional co-cultures, the oligodendrocytes and neurons are

indiscriminately dispersed; however, this randomized growth is ill-suited to studying local or single cell level interactions [35, 37]. As seen in Figure 1-4, myelination in this type of dense co-culture is often quite difficult to visually evaluate due to the uncontrolled neuronal network and random oligodendrocyte placement. Not only can it be difficult to distinguish the individual cells involved in myelination, but the reproducibility and throughput of such investigations can also be an issue [8, 28]. For example, in their traditional myelination co-culture, Pang *et al.* [37] reported evaluation difficulties due to both mature oligodendrocyte cell bodies and myelinating oligodendrocyte processes staining positive for MBP. Such issues may be eased with a co-culture structured to a finer degree, where the positions of oligodendrocytes and neurons can be controlled. For example, being able to accurately predict points of myelination and thus, easily visually identify myelin from cell bodies can limit the amount of post-processing necessary and perhaps improve the accuracy of quantification techniques. Pang *et al.* [37] also commented on the inaccuracy of measuring total protein concentrations to represent myelin creation for the same reason. This too offers support for a more structured co-culture with *a priori* knowledge of cell growth and stronger visual cues for areas of myelination. Furthermore, investigating neuron-glia interaction can be difficult without a measure of localized environmental control [23, 24, 33, 35]. Generally, such control is dependent on first directing cell growth.

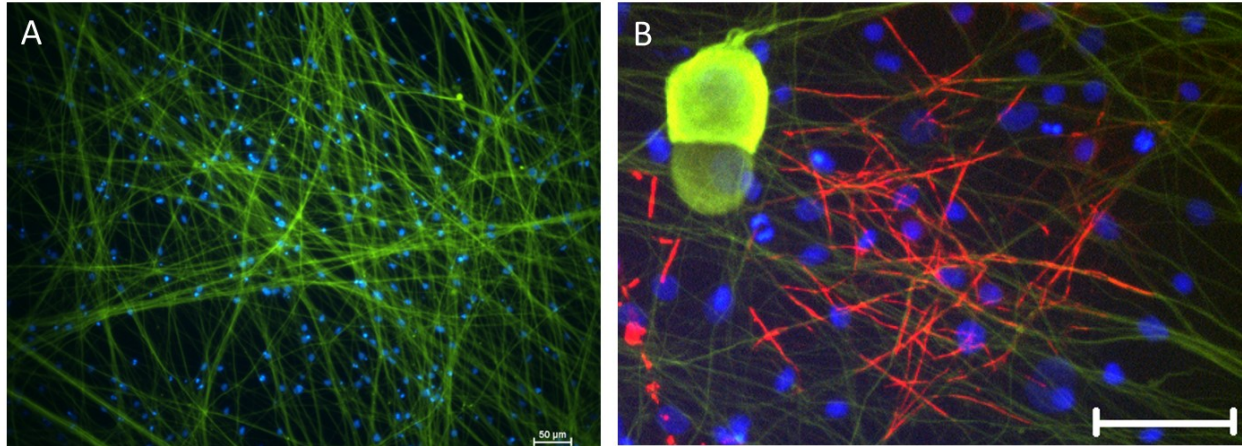


*Figure 1-4. Traditional myelination co-cultures.*

The following represents a typical, unstructured co-culture. Nuclei are seen in blue (Hoechst stain), neurons in green (anti-N52 stain), and myelin sheaths in red (anti-MBP stain). Image (A) shows an intricate network of neurons and oligodendrocytes. Image (B) shows the first stages of a dense network of myelination. Scale is 50 µm for all images.

With the advent of micro- and nano- scale technologies leading the development of micro-electro-mechanical devices and lab-on-a-chip systems, the ease and simplicity of interfacing with cell cultures at a micron scale is ever increasing. In particular, the control over localized cellular growth and microenvironmental conditions have been improved with a variety of microscale engineering technologies [41]. One popular patterning method is microcontact printing in which a rubber-like stamp is 'inked' with a solution of interest and applied to a substrate, transferring the 'ink' pattern. This technique has been successfully applied to a variety of applications including surface functionalization and bio-molecule patterning [42]. In particular, the microcontact printing of biological materials has been successfully used in studies of cell behaviour, growth, and development. With the capability to control cell growth, this technique has been shown to be useful in the structuring of culture platforms. To that end, a review of microcontact printing will be presented in the next section.

## 1.2. Microcontact Printing

### 1.2.1. Development of Soft Lithography

The micropatterning of substrates has long been considered a popular technology across a variety of fields, although its foundation is firmly rooted in the microelectronics industry [42, 43]. Of particular note was the development of photolithography, the “workhorse of microfabrication,” capable of creating features in both the micro- and nano- scales [44]. Generally involving the use of a photomask to develop a desired pattern onto a layer of deposited photoresist, photolithography is a mainstay in the semiconductor industry [44, 45]. However, photolithography has also successfully been applied to the biological field, with the fabrication of DNA arrays [46] being an example of particular note [42]. Despite this success, photolithography would appear rather ill-suited to the biological field. The cleanroom conditions commonly required for photolithography are both expensive and generally incompatible with organic systems including proteins or cells; moreover, this technique is not suited to altering surface chemistries or addressing curved surfaces [42, 44].

To address such issues, Whitesides *et al.* [42] pioneered a straightforward method to simply and rapidly replicate the patterns created through photolithography, extending the reach of conventional techniques. Termed soft lithography, the crux of this system is the use of an elastomer to cast replicas of photolithography-created micro-features [42, 45]. Using these elastomer replicas as stamps, the patterning technique of microcontact printing ( $\mu$ CP) was established. The  $\mu$ CP process has three main steps: submerging the elastomer surface in a solution of the substance of interest or ‘ink’, allowing the substance of interest to deposit onto the elastomer surface, and stamping the ‘inked’ elastomer onto a substrate, transferring the

deposited 'ink' onto the substrate in the design replicated on the elastomer surface [42]. With such a system, a single photolithography-created structure (or master) is required. This not only reduces expenses by requiring only a single cleanroom visit, but it also allows patterning of cleanroom incompatible organic systems. Moreover, as the patterning can be done in standard laboratory conditions, a variety of inks can be used to modify surface properties. Finally, the soft, pliable elastomer replicas can be used to pattern a variety of surfaces, including those that are curved.

By and large, the most widely employed elastomer is polydimethylsiloxane (PDMS), and its use provides a number of advantages for  $\mu$ CP [47]. Firstly, it is both inexpensive and readily commercially available, making it an attractive material to work with [42, 48]. Moreover, it is non-toxic, permeable to gases, chemically inert, and biocompatible making it suitable for cell culture applications [49-51]. Adding to its versatility, the hydrophobic surface of PDMS can be inked with a number of different coatings, including a variety of functional groups [48]. Furthermore, the flexible nature of PDMS allows patterning of relatively large areas as well as non-planar surfaces [49].

### 1.2.2. Patterning Proteins

In their defining paper, Kumar and Whitesides [52] used microcontact printing to pattern self-assembled monolayers of alkanethiols on gold-coated surfaces; as the patterned thiol layer protects gold from etching, this technique was capable of creating well-defined gold features. Shortly following this, Bernard *et al.* [53] extended this microcontact printing

technique to the patterning of proteins and other bioactive molecules. With this advancement, microcontact printing has gained greater interest within the field of cell biology [43].

By and large, the use of elastomer stamps readily allows the concentration and reversible adsorption of proteins onto its surface; however, the exact physiochemical events directing the transfer during the stamping process are not fully understood [54, 55]. Empirically, it was found that in order to microcontact print proteins, successful movement of the protein pattern requires an initial surface of low-energy –such as the naturally hydrophobic surface of a PDMS elastomer stamp– and a final surface of high-energy –such as the hydrophilic surface of an oxygen plasma treated glass substrate [54, 56]. With this configuration, homogenous and effective protein transfer is possible due to the conformal contact between the flexible elastomer and hard substrate during printing [56]. As such, the technique of  $\mu$ CP is shown to accurately transfer high-resolution patterns with precise placement [57, 58]. Moreover, these printed protein patterns show high levels of stability and reproducibility, with the adsorbed proteins showing little to no surface diffusion [54, 58, 59]. Furthermore, studies have shown that despite the mechanical forces present in the stamping process, proteins retain their biological activity following  $\mu$ CP, although conformal changes are possible [59, 60]. Similarly, the microcontact printing of antibodies has been shown to result in minimal decreases in functionality, with antibodies able to retain high levels of capture efficiency post printing - approximately 90% [47, 56].

### 1.2.3. Competing Technologies

In addition to microcontact printing, a number of alternate patterning techniques are also being used today. Three leading methods include microfluidic networks, dip-pen nanolithography, and inkjet printing [61-63]. Microfluidic networks can be constructed in a similar method to  $\mu$ CP stamps, cast in elastomer from a photolithographic master with microscale channel designs. Once these casts are bound to a substrate, a microfluidic network is realized, capable of laminar flow and patterning through physical adsorption [64, 65]. Dip-pen nanolithography is a scanning probe method in which an atomic force microscopy (AFM) tip is coated in the solution of interest and used to physically pattern a surface [66]. Inkjet printing adapts this common office technology to print a range of biological solutions, including those containing cells, through non-contact deposition [62, 67]. These four techniques are depicted in Figure 1-5 below.

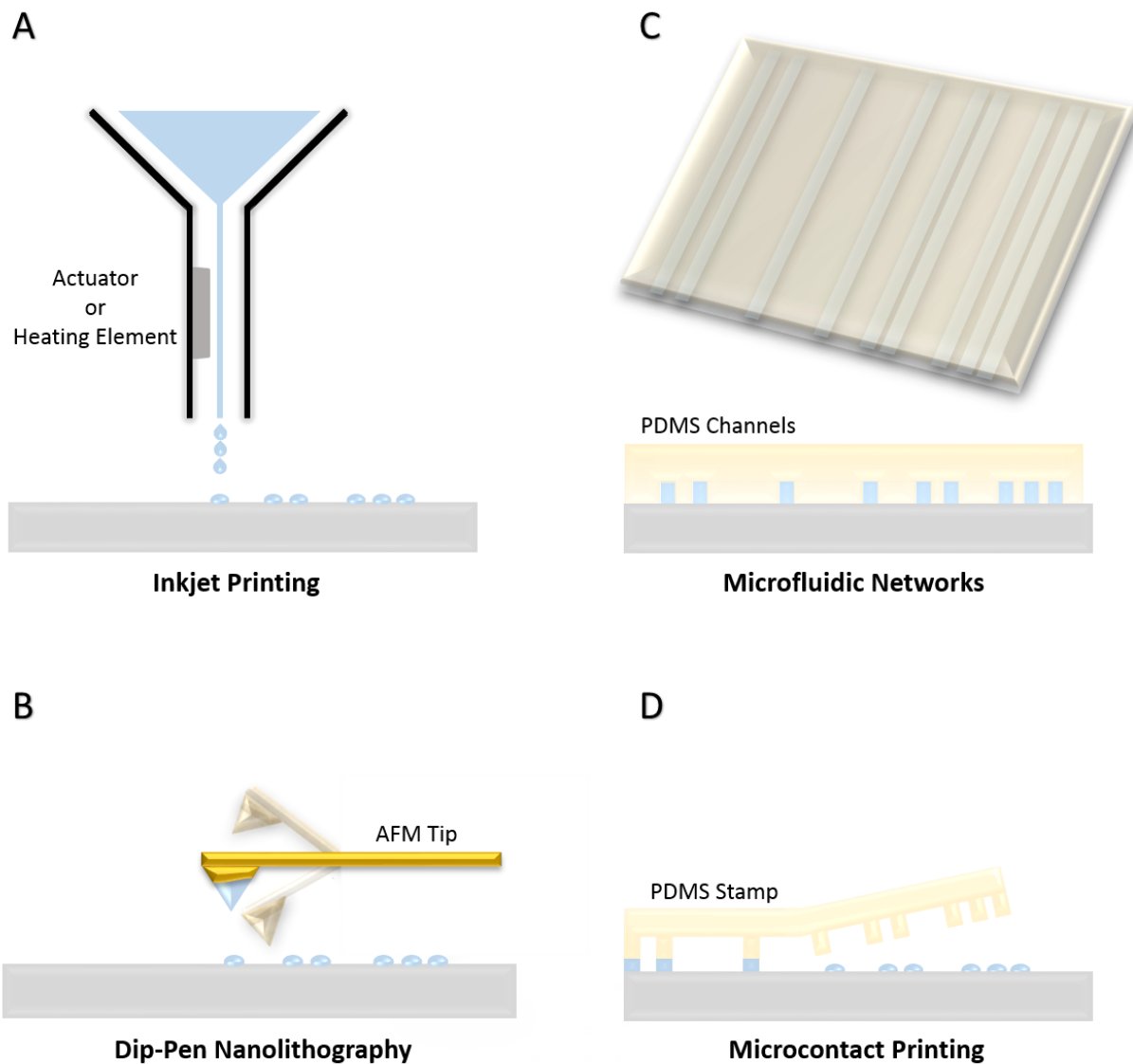


*Figure 1-5. Different patterning techniques.*

Four competing methods of printing biological solutions or bio-inks are depicted. Image (A) shows inkjet printing where either a heating element or piezoelectric actuator is used to create the ink droplets. Image (B) shows the coated AFM tip used for patterning in dip-pen nanolithography. Image (C) shows two perspectives of a microfluidic network, wherein physical adsorption in the channels is used for patterning. Image (D) shows microcontact printing, with the inked PDMS stamp being removed from conformal contact with the substrate.

As described previously,  $\mu$ CP has a number of advantages. Once a master is created, stamps can be rapidly and inexpensively produced, without the need of special equipment or expertise [43]. Moreover, patterns with features as small as 50 nm have been accurately printed using this technique, in a wide range of geometries [68, 69]. However, the PDMS stamps used in  $\mu$ CP can be a limiting factor. In order to ensure accurate pattern transfer, the stamps must be correctly designed with appropriate aspect ratios to prevent any sagging or collapse during printing, and this places a limit on the resolution of any printed patterns [45, 69]. Additionally, each stamp can only print a single solution at any given time; thus, a second solution can only be added through a carefully aligned second stamping. Furthermore, it is possible for PDMS stamps to contaminate the printing surface, transferring low molecular weight residuals [45, 49, 50]. Despite these drawbacks,  $\mu$ CP with PDMS stamps still allows the rapid, straightforward patterning of a wide range of molecules, earning its place as a popular bench-top technique in a range of fields, including cell biology [43, 47].

Microfluidic networks ( $\mu$ FN) offer a few additional benefits over  $\mu$ CP. Firstly, they allow for the patterning of multiple solutions within the same device, without the alignment issues that would be seen with  $\mu$ CP and multiple stamps [51]. Moreover, as this technique lacks the drying steps and mechanical forces involved in stamping, delicate materials, including mammalian cells, can be successfully patterned and patterned over using this technique [51]. Additionally, the use of laminar flow can increase the precision and complexity of any pattern designs [51, 64]. That being said,  $\mu$ FN do offer limited pattern geometries, usually requiring continuous designs [51, 65]. Additionally, the use of PDMS  $\mu$ FN on glass substrates involves irreversible binding; however, the presence of the PDMS networks post-patterning may not be

ideal for all applications [65]. Furthermore, the operation of  $\mu$ FN can be capillary driven or pump driven. The latter, however, would require cumbersome tubing and external pumps, making it a less straightforward implementation.

The greatest asset of dip-pen nanolithography (DPN) is its ability to exploit the accuracy of AFM, with resolution beyond 50 nm [61, 66, 70]. As the patterning is mechanized and computer-aided, this allows for high levels of precision and repeatability. Moreover, complex patterns of multiple solutions can be printed in exact positions using one AFM tip sequentially or several multiplexed AFM tips [61, 66]. However, to achieve these results, DPN requires very expensive equipment, unlike the elastomer stamps required for  $\mu$ CP [61, 66]. Moreover, as found with the limited range of normal AFMs, this technique is only capable of patterning very small areas, leading to longer print times [61, 70].

In contrast, inkjet printing is considered a high-throughput patterning method [61, 67]. Building upon standard inkjet printing technology, this technique allows the printing of multiple solutions over large surface areas in a relatively short period of time [67]. Mechanized and computer aided, inkjet printing also allows for the accurate replication of complex design patterns. However, unlike DPN, the hardware required for inkjet printing is relatively inexpensive – even standard office printers can often be repurposed for biological applications [71]. To that end, inkjet printing has previously been used to deposit materials such as proteins and mammalian cells for a variety of applications, ranging from biosensors to tissue engineering [62, 67]. Despite these strengths, a major limiting factor for inkjet printing is resolution, dependent on ink droplet size. By and large, the average resolution is limited to 10-30  $\mu$ m, making  $\mu$ CP a far more precise method of patterning [61, 62, 67]. Moreover, the solutions used

for inkjet printing are slightly more restrictive, specifically in terms of viscosity and cell concentration, in order to prevent clogging or inconsistencies in the printing process [72, 73].

Taken as a whole, each technique has its own merits. However,  $\mu$ CP appears to be one of the best suited methods for bench-top protein patterning projects requiring high speeds, low costs, and microscale resolution.

#### 1.2.4. Applications of Microcontact Printing

With such capabilities, the  $\mu$ CP of proteins and bioactive molecules is being used in a number of applications, especially in the biomedical engineering field [44]. These range from immunoassays and biosensors [49] to tissue engineering [74] to cell development [75]. Cell development in particular is widely studied, using a variety of bio-inks [47, 62, 76], solutions containing biological material such as proteins, antibodies, and growth factors. These studies examine a number of elements in cell culture ranging from simply controlling cell adhesion to regulating cell function to monitoring developments in cell morphology, polarity and division [5, 9, 43, 60, 75, 77-81].

For example, in the field of tissue engineering, Atmanli and Domian [74] utilized microcontact printing to try and re-create *in vivo* cellular architectures within *in vitro* cultures. In their 2013 study, the authors used the  $\mu$ CP of fibronectin to provide appropriate extracellular cues over cellular growth and organization, enabling cardiac progenitor cells to differentiate into rod shaped cardiac myocytes [74]. This behaviour is thought to be key as directionally controlled growth has shown to improve the mechanical and electrophysiological properties of

cardiac myocytes [74]. Thus, the authors suggest this type of scaffold free,  $\mu$ CP approach to controlling cellular architecture may even be “pivotal” to cardiac tissue bioengineering [74].

Similarly, Elloumi Hannachi *et al.* [10] developed a method of culturing and transferring cell sheets for use in tissue engineering. Within this method, the  $\mu$ CP of fibronectin was employed to control the growth of cellular co-cultures within these cell sheets. Although other micropatterning techniques had been investigated by the authors, none could sufficiently match the simplicity and speed of  $\mu$ CP [10]. By and large, tissues require co-cultures of multiple cell types in specific arrangements in order to maintain function [82]. In this study, liver tissues were examined using hepatocytes and endothelial cells as hepatocyte function is known to improve when in such a co-culture environment [82]. Thus, their use of co-culture should allow for appropriate communication between the cell types, aiding in the maintenance of hepatocyte function and viability over longer terms and the formation of key cellular junctions [10]. Moreover, their use of micropatterning, seen in Figure 1-6 (B) and (C), should allow for more accurate tissue micro-architectures, a key step in the tissue engineering field [10].

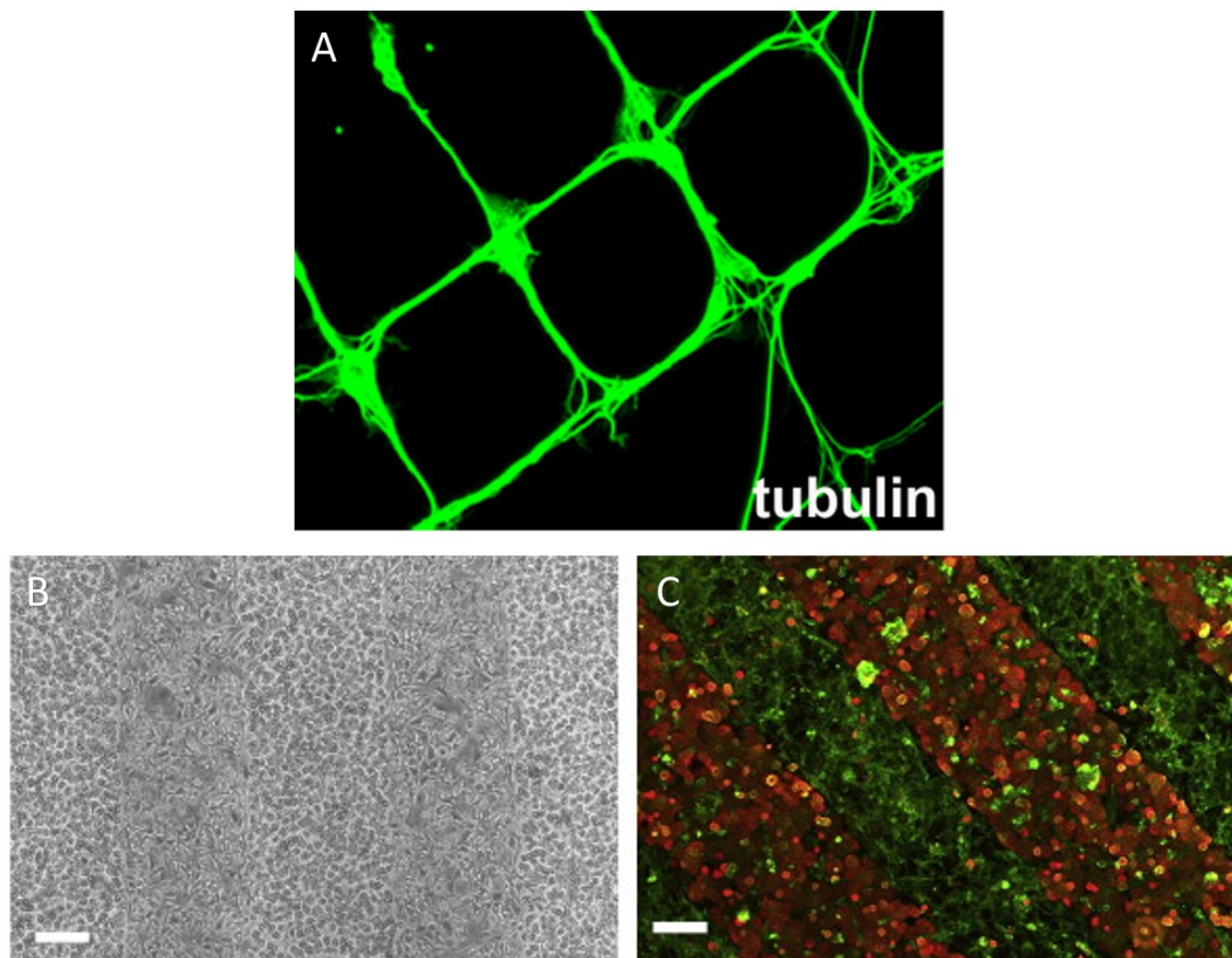


Figure 1-6. Examples of controlling cell growth using microcontact printing.

In image (A), Belkaid *et al.* [7] show the ability to direct neuron growth along printed patterns. (Neurons are stained green using tubulin.) In images (B) and (C), Elloumi Hannachi *et al.* [10] show the patterned co-culture of hepatocytes and endothelial cells, respectively stained red and green in (C). (Scale is 200  $\mu\text{m}$  for images (B) and (C).) Image (A) is adapted from [7] under the creative commons license, copyright © 2013, BioMed Central Ltd. Images (B) and (C) are adapted with permission from [10], copyright © 2009, Elsevier.

Additionally,  $\mu\text{CP}$  has found utility in the study of the central nervous system as well. Being a versatile and adaptable technique, Hsiao *et al.* [83] incorporated  $\mu\text{CP}$  into their novel preparation method of patterning extra-cellular matrix proteins onto collagen hydrogels. These printed proteins were then used to direct astrocyte growth along the patterned designs. This

aligned growth has been shown to decrease the astrocyte expression of neuronal regeneration inhibitors [83]. Thus, this finding may be applicable to studies of regeneration of nervous system tissue, especially those already employing collagen hydrogels.

In a similar vein, Belkaid *et al.* [7] investigated the control over central nervous system cells using the  $\mu$ CP of growth promoting and inhibiting biomolecules, poly-L-lysine and myelin. First, they investigated the growth and alignment of neurons onto printed poly-L-lysine patterns, as seen in Figure 1-6 (A). They found that such controlled growth permits normal neuron polarization and can direct neurite extension along the printed patterns, with axons much more strictly guided than dendrites [7]. Such findings are important as the printed patterns have been shown to permit normal neuron maturation while controlling growth on a single cell level. Secondly, they found the addition of printed myelin patterns onto poly-L-lysine can inhibit the process outgrowth of oligodendrocyte-like cells [7]. However, *in vivo*, such process outgrowth, often in the presence of inhibitory biomolecules such as myelin, is required for nerve repair following trauma [7]. Thus, the use of microcontact printing here can also create an organized platform for testing therapies to aid in overcoming myelin related growth inhibition.

Finally, in their 2013 paper, Yaka *et al.* [84] utilized  $\mu$ CP to study axonal regeneration. That is, neuron growth and neurite extension were controlled by a printed pattern of extracellular matrix proteins and to simulate injury, neuronal processes were removed from specific areas, leaving the underlying pattern intact. Thus, as the regenerating neurites could only grow along the microcontact printed patterns, the resultant qualitative and quantitative

measurements were simplified due to this restricted growth [84]. As such, through the use of  $\mu$ CP, the authors offer a unique platform for studying neuronal injuries.

With such precedence,  $\mu$ CP has become one of the most popular patterning techniques used by cell biologist [43].

### 1.3. Structured *In Vitro* Myelination Co-Cultures

#### 1.3.1. Recent Examples in the Literature

Structured myelination co-cultures have become more and more prevalent within the last 10 years [4, 18, 23, 24, 30, 33, 35, 85]. The rise of micropatterning techniques has undoubtedly aided in this development, with microcontact printing already shown to be useful in other structured studies of the CNS. However, it is far from the only method of structure being employed.

One area of particular focus is in the use of microfluidic platforms. Building upon systems such as Campenot chambers [86], which allow neuron cell bodies to be in fluidic isolation from neurite extensions, these microfluidic systems are generally designed with multiple PDMS chambers and connecting channels. This allows for both the independent control of the fluidic microenvironment of each chamber as well as directed cell growth through the channels.

In their 2012 study, Higashimori and Yang [30] developed such a microfluidic system with two compartments, one housing glial cells and one housing neuronal cell bodies, and several parallel microchannels, connecting the two chambers and directing individual axon extension. The narrowness of these microchannels prevents the fluid in the soma compartment from reaching the glial compartment. By separating neuron cell bodies, *in vivo* conditions are more closely mimicked, as axons generally extend a significant distance from neuronal somas. Not only does the structure provided by the microchannels allow analysis of axons at a single cell level but the isolation of neuronal cell bodies may also provide a more accurate method of

studying signalling pathways between axons and glial cells –two results that are far more difficult to achieve in conventional co-cultures [30]. It should be noted that although this platform was initially tested using astrocyte glial cells, its authors believe it can be easily extended to neuron-oligodendrocyte co-cultures.

Similarly, in their 2009 and 2012 studies, Park *et al.* [4, 24] developed two multi-compartment microfluidic platforms for investigating CNS co-cultures. In both platforms, compartment(s) containing neuronal cell bodies are connected to a series of microchannels, with each microchannel directing axon extension, as seen in Figure 1-7 (A), into a compartment containing oligodendrocytes. The latter axon-glial compartment is isolated from the neuronal soma compartment through both physical (i.e. separated compartments) and fluidic (i.e. hydrostatic pressure due to a small fluidic difference between compartments) means. Through their use of structure, Park *et al.* created the means of controlling the physical and biochemical culture microenvironments [4, 24]. This allows for the localized treatment of axons with a variety of compounds or stimuli and exhaustive studies of axon-glial interactions without the presence of the neuronal somas [4, 24]. Moreover, the number of microchannels and the casting method of fabrication greatly increases the reproducibility and throughput of any experiments utilizing this structured platform. It should be noted that the myelination, possible in the axon-glial compartment, is not structured as once the axons have exited the microchannels, their growth is no longer directed. Perhaps continuing the microchannels into the axon-glial compartment could be another useful route of investigation. However, Park *et al.* also commented on the possible negative effects of enclosed environments, such as that of microfluidic channels. Although their platforms are constructed from the gas permeable, inert

PDMS, primary cells are often highly sensitive to environmental changes [24]. Thus, the complications added by PDMS enclosure, specifically with regard to CO<sub>2</sub> exchange and mechanical stress during media changes, are points worth considering [24].

Finally, in their 2012 study, Yang *et al.* [33] also developed a structured microfluidic platform with separate neuron and glial compartments connected by rows of parallel microchannels. However, in this study, Yang *et al.* investigated the effect of electrical stimulation on myelination. Through their structured design, they were able to selectively stimulate only DRGs with axon extensions running through their microchannels [33]. This was accomplished by exploiting the impedance within the microchannels, but it would also be possible to have electrode arrays incorporated into the platform design. This would be feasible in any similarly structured platform because the microchannels would guide axon extensions into pre-defined positions, such as along the electrode components.

In addition to the microfluidic approaches, microfabrication and micropatterning techniques have also been used to develop structured co-culture platforms, focusing primarily on directing cell growth rather than fluidic isolation. Although not true co-cultures, Rosenberg *et al.* [26] and Lee *et al.* [28] were able to respectively show oligodendrocytes successfully 'myelinating' paraformaldehyde-fixed axons and electrospun nanofibers. In addition to the simplicity of not having to culture live neurons, these platforms, the latter in particular, highlight the benefits of repeatability in structured *in vitro* cultures. For example, the nanofibers created by Lee *et al.* can be consistently adapted to desired densities and patterns, unlike the randomized cell growth found in traditional myelination co-cultures. In a similar vein, Mei *et al.* [8] developed a micropillar array platform, allowing controlled oligodendrocyte

'myelination' around conical micropillars. This is illustrated in Figure 1-7 (B) below. Not only can such a platform be easily re-created between trials, but the micropillar array also allows for a high number of replicates within the platform itself. Such regularity is unlikely to be found in any traditional, unstructured co-culture. Moreover, this regularity can also provide stronger visual identification of myelination, increased automation in quantification, and higher throughput, allowing such a system to act as an effective screening platform for biochemical treatments [8].

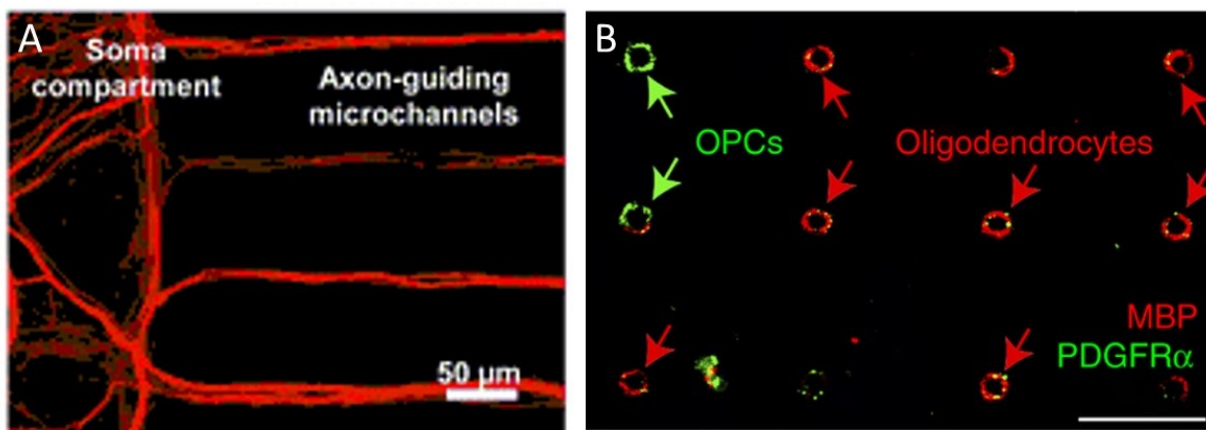


Figure 1-7. Examples of structured cell growth and structured myelination.

Image (A) shows the neuronal axon growth being directed through the microchannels in the microfluidic device created by Park *et al.* [4]. (Scale is 50 µm.) Image (B) shows a myelination microarray on the micropillar device created by Mei *et al.* [8]. The immature OPCs wrapping around micropillars are seen in green, and the mature oligodendrocytes wrapping MBP positive processes around micropillars are seen in red. (Scale is 25 µm.) Image (A) is adapted with permission from [4], copyright © 2012, Royal Society of Chemistry. Image (B) is adapted with permission from [8], copyright © 2014, Nature Publishing Group.

Building upon such ideas, Davis *et al.* (2012) [35] attempted photolithographic micropatterning to control cell growth. That is, alternating regions of specialized cell growth permissive (DETA or N-1[3 (trimethoxysilyl) propyl] diethylenetriamine) and non-permissive

(silane polyethyleneglycol) compounds were patterned in parallel lines onto a substrate using deep ultraviolet light (UV) –the thicknesses and spacing between regions varied. The permissive regions had the desired effect of directing axonal growth along individual lines and permitting oligodendrocyte differentiation. Thus, the significant success of this structured platform is the ability to study neuron-oligodendrocyte interaction on a single cell level [35]. It should be noted that myelination was largely unsuccessful in this study, but the authors suggest this is indicative of the issues with the OPC source as opposed to their platform [35].

Using a similar specialized micropatterning technique and parallel line design, Rumsey *et al.* (2013) [18] also designed a structured platform capable of controlling cell growth, although this study investigated PNS myelination, co-culturing neurons and Schwann cells. In their study, Rumsey *et al.* reported successful myelination and offered their work as one of the first systems for “spatially directed development of DRG myelination” [18]. With this structured co-culture, the authors suggest the spatial control over both myelination and DRG axon extension offers a highly reproducible platform for studying neuron-glia interactions that may lend itself to high-throughput studies of myelination dysfunction and perhaps, related drug discovery [18].

Furthering the micropatterning theme, Liazoghli *et al.* (2012) [23] investigated a controlled co-culture platform utilizing microcontact printing. Using this technique, Matrigel protein mixture was printed in parallel lines 10  $\mu\text{m}$  wide, and the 110  $\mu\text{m}$  spacing between the lines was passivated with a blocking agent. Investigating both CNS and PNS myelination, this platform was used to co-culture DRGs and oligodendrocytes as well as DRGs and Schwann cells, with aims to direct DRG axon extension and permit glial cell maturation and myelination. This system showed encouraging results with a short-term (2 week) CNS myelination study and

highly successful results with a long-term (>6 weeks) PNS myelination study [23]. The use of  $\mu$ CP offers a simple method of patterning proteins and an uncomplicated culture environment, making the development of a structured co-culture platform a much more straightforward process. As with the other described studies, the consistent reproducibility of the platform, the consistent replication of cellular growth patterns within the platform, and the ability to have a single cell level of control are its major benefits. The authors particularly valued the ability to visualize and manipulate the myelin formation and felt the controlled, pre-designed growth patterns offer a great benefit to live-imaging based myelination studies [23].

As a final note, it may be worth observing that these existing structured co-culture systems generally focus on directing the growth of neuronal cells, not glial cells. However, it follows that levels of control over cell-to-cell interactions could be increased by directing the growth of both cell types separately, particularly with oligodendrocytes as they can have more diverse growth patterns due to their interaction with multiple axons. To realize such a platform, the micropatterning of cell-specific bio-molecules is likely necessary. With its speed, simplicity and adaptability, microcontact printing may be the best technique to accomplish this goal.

## Chapter 2. Motivation and Objectives

### 2.1. Motivation

By and large, traditional *in vitro* studies of CNS myelination are plagued by a lack of organization. Comprising dense networks of neurons interlaced with an indiscriminate arrangement of oligodendrocytes, qualitative and quantitative myelination measurements can be made complex by the absence of an underlying order or arrangement within the co-culture system –as can the possibility of consistent replication. As such, there exists a need for a platform capable of controlled myelination –ideally, turning regular, unsystematic myelination cultures into organized systems resembling pseudo-microarrays.

To ensure the utility of such a platform, simplicity of design and ease of fabrication are paramount. For this reason, a proposed strategy is to employ microcontact printing to pattern a rectangular grid –sets of parallel lines in one direction can be patterned with proteins allowing for directed neuronal axon extension, and sets of parallel lines in a perpendicular direction can be patterned with antibodies allowing for the directed growth and differentiation of oligodendrocyte progenitor cells. With this design, illustrated in Figure 2-1 below, regions of myelination would be limited to the discrete points of intersection within the grid pattern – junctions where a neuron and oligodendrocyte(s) meet. Thus, this has the potential to provide means of studying myelination in an organized and reproducible fashion.

Such a pseudo myelination microarray has a multitude of potential applications, aiding the study of numerous effects ranging from neuronal damage to electrical activity to drug delivery. For example, the repeated, structured design is well suited to testing drug responses, and the

pre-designed growth patterns allow such a platform to be paired with commercial electrode arrays in order to provide electrical stimuli or monitor electrical responses. Thus, the utility of such a platform is the main motivation behind this study.

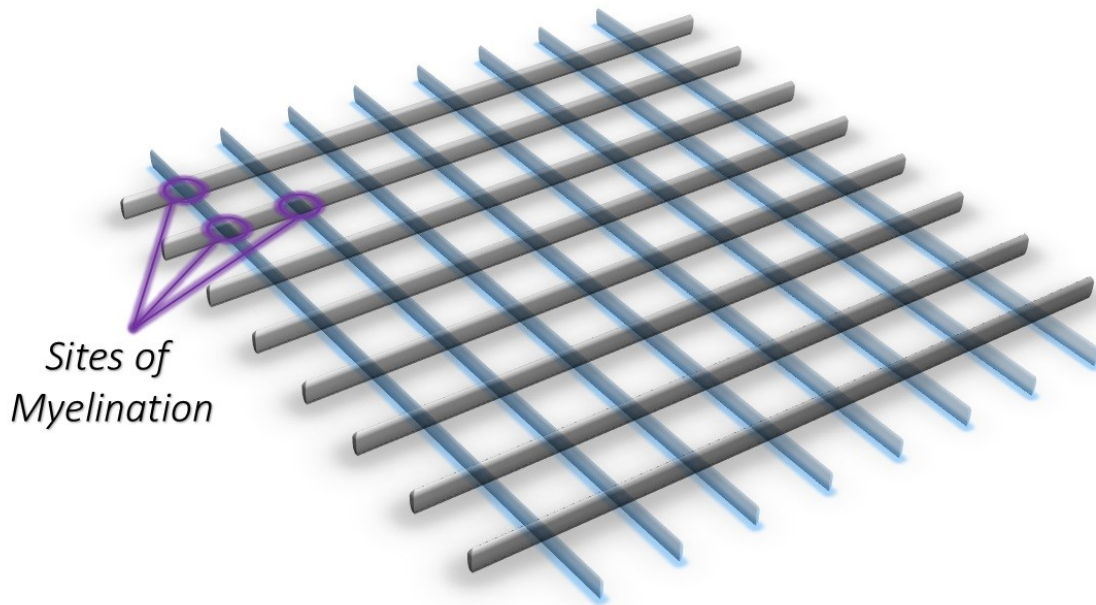


*Figure 2-1. Grid design for a controlled myelination platform.*

The patterns to control oligodendrocyte development and neuron growth are shown in black and blue, respectively. The intersections of these two patterns are potential sites of myelination.

## 2.2. Objectives

Throughout the literature, structured myelination platforms generally attempt to control only neuron growth, allowing unrestrained interaction with glial cells. However, the localization and maturation of both neurons and glial cells must be carefully planned and directed before the possibility of controlled myelination can be considered. For this reason, the primary objective of this study is to address that issue by selectively controlling oligodendrocyte growth

and development using microcontact printed patterns of cell-specific antibodies. The specific aims of this objective can be broken down as follows:

- 1) Determine an appropriate bio-ink for specific OPC attachment meeting the following criteria:
  - a) Microcontact printed bio-inks can be maintained in culture conditions over a long-term period (3 weeks).
  - b) OPCs show specific adherence and strong pattern compliance to the printed bio-ink.
  - c) OPCs successfully differentiate into mature oligodendrocytes on the patterned bio-ink.
  - d) Differentiated OPCs maintain high levels of viability on the patterned bio-ink.

Building upon the results of the primary tier of investigation, the secondary objective can then be further explored. In short, it seeks to apply the acquired knowledge of patterned oligodendrocyte growth to an organized platform for controlled CNS myelination. The specific targets for this objective can be broken down as follows:

- 2) Perform a preliminary investigation into an *in vitro* platform for controlled myelination with the following aims:
  - a) Cross-print the bio-ink for controlled DRG growth with the bio-ink for specific OPC attachment in a pre-designed pattern using microcontact printing.
  - b) Determine cell culture conditions necessary for successful myelination.
  - c) Culture DRGs on a patterned bio-ink, directing axon extension.
  - d) Attempt a long-term patterned co-culture capable of controlled myelination.

## Chapter 3. Materials and Methods

### 3.1. Microcontact Printing

#### 3.1.1. Stamp Photomask

For this study, stamp designs were printed on a transparency photomask (Cad/Art Services, Inc.) with a minimum feature size of 10  $\mu\text{m}$ . All stamp patterns were sets of parallel lines, contained within a 100 mm<sup>2</sup> area. Each line was a rounded rectangle 9.5 mm long, and the width of each line and spacing between successive lines could be varied between stamp designs. The first stamp design contained parallel lines 10  $\mu\text{m}$  in width separated by 100  $\mu\text{m}$  spacing (10x100  $\mu\text{m}$ ). Within the 100 mm<sup>2</sup> parameter, this design contains 86 parallel lines and thus, could pattern a total area of approximately 8.17 mm<sup>2</sup>. This stamp design was used to pattern substrates for neuron culture. The second stamp design contained parallel lines 20  $\mu\text{m}$  in width separated by 100  $\mu\text{m}$  spacing (20x100  $\mu\text{m}$ ). Within the 100 mm<sup>2</sup> parameter, this design contains 80 parallel lines and thus, could pattern a total area of approximately 15.20 mm<sup>2</sup>. This stamp design was used to pattern substrates for oligodendrocyte culture.

#### 3.1.2. Stamp Fabrication

Within microcontact printing, elastomeric stamps are readily and rapidly manufactured through a casting process, and as such, the first step in stamp creation is to fabricate a stamp master. This was carried out in the cleanroom facilities provided by the McGill Nanotool Microfab (MNM), using the standard photolithography techniques summarized in Figure 3-1 below. In brief, a 6" silicon wafer was first cleaned using buffered oxide etch (6:1) for approximately 10 seconds. It was then spin coated (Laurell Spin Coater, MNM) with SU-8 2015

negative photoresist (Microchem Corp) at 1500 rpm for 30 seconds, to achieve a resist thickness of approximately 25-27  $\mu\text{m}$ . To remove solvents from the photoresist, a soft bake was performed for 5 minutes at 95°C. Following this, the SU-8 coated wafer was aligned with the stamp design photomask and exposed to UV light (EVG 620 Contact Aligner, MNM) at approximately 150  $\text{mJ}/\text{cm}^2$ , allowing the UV exposure to cross-link any areas of uncovered photoresist. Following a gradual post-exposure bake of 3 minutes at 65°C and 5 minutes at 95°C, the wafer was then immersed in SU-8 developer for 5 minutes, washing away any non-cross-linked photoresist and thus, creating a stamp master. To end the development process, the wafer was rinsed in isopropanol and dried using compressed nitrogen gas. A final hard bake was then carried out for 30 minutes at 150°C to harden the photoresist layer and strengthen its adhesion to the wafer. Lastly, a silanization step was included to prevent unwanted elastomer adhesion during the casting process. For this step, the stamp master was placed with a drop of triethoxy(1H,1H,2H,2H-perfluoro-1-octyl) silane (Sigma-Aldrich, 667420-5G) in a desiccator under vacuum conditions for one hour, followed by a 15 minute bake at 70°C.

With the stamp master complete, the process of casting PDMS stamps can be carried out outside of the cleanroom, in standard laboratory conditions. Using the Sylgard 184 Silicone Elastomer kits (Dow Corning Corporation), the contained polymer base and curing agent were combined in a ratio, by weight, of 10:1 and thoroughly mixed by hand and using a vortex. To remove resultant bubbles from the PDMS, the mixture was centrifuged at 300 G for 5 minutes [78]. After gently pouring the PDMS mixture onto the master, the uncured stamps were then degassed in a desiccator under vacuum conditions until all remaining bubbles had been removed. The PDMS was baked for 1.5 hours at 70°C, until the PDMS had sufficiently stiffened.

The cured PDMS was then peeled off of the master and cut to size, with the area of each stamp face being approximately 100 mm<sup>2</sup>. They were then cleaned with 70% ethanol and dried with compressed nitrogen gas before being stored in sealed containers, protecting the stamp faces from dust and debris.

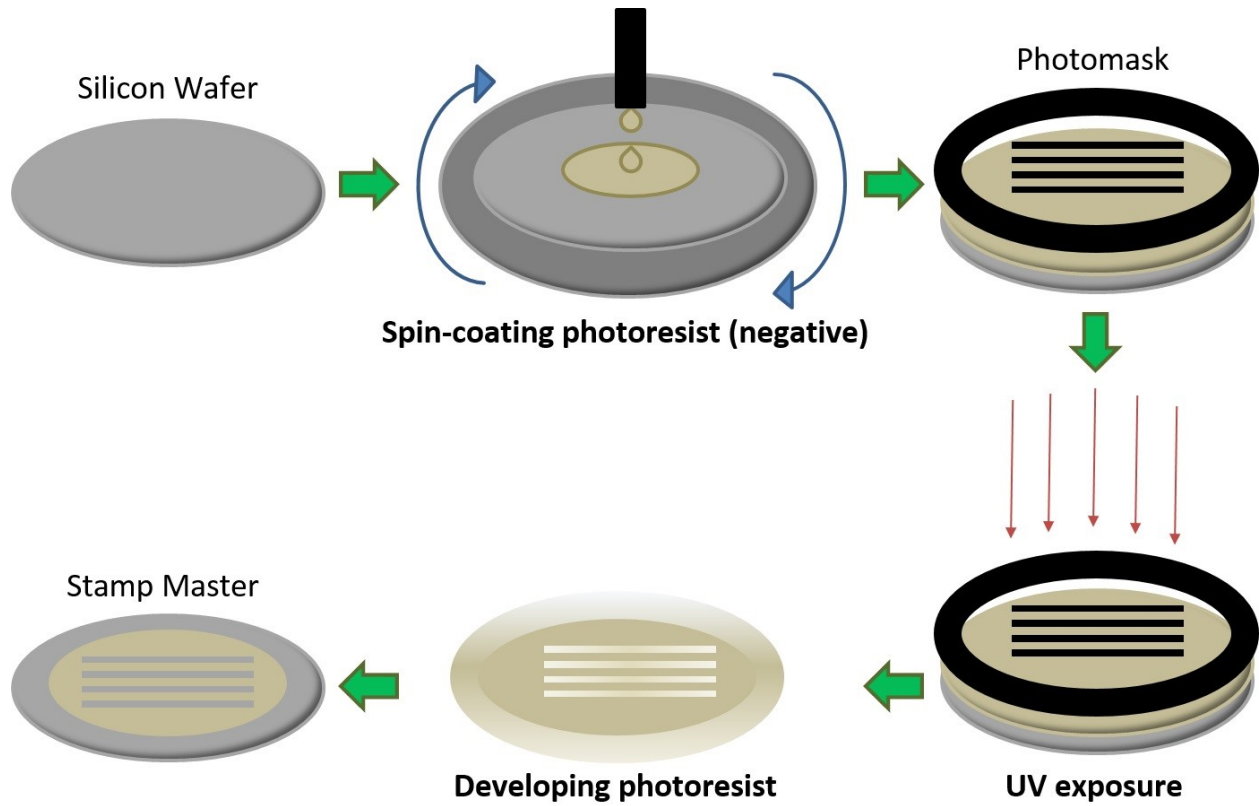


Figure 3-1. Flowchart of the basic photolithography process.

### 3.1.3. Microcontact Printing Procedure

For this study, all microcontact printing was performed on glass or plastic coverslip substrates, using PDMS stamps. All glass coverslips were cleaned first using soap and water. They were then immersed in a 1:1 mixture of ethanol and double distilled water (ddH<sub>2</sub>O) and placed in an ultrasonic bath for 15 minutes at 50°C. Following this, they were soaked in an

ethanol:acetone (1:1) bath for 1.5 hours, followed by three 15 minute washes in 70% ethanol. They were then dried using compressed nitrogen air and baked for 1.25 hours at 100°C, to evaporate any remaining solvent. Following this, a surface activation step to increase the hydrophilicity of the coverslips was required; oxygen plasma treatment (Plasma Etch PE 50) was applied for one minute at 50 W power and 100.7 mTorr pressure. The cleaned coverslips were then stored in dry, sterile conditions until used. All plastic coverslips used were Nunc Thermanox (ThermoScientific, 174950) and purchased pre-sterilized and pre-treated with a hydrophilic surface. Immediately before beginning the printing process, all PDMS stamps were sonicated in 70% ethanol for 7 minutes at 50°C, rinsed, and dried.

The process of microcontact printing was carried out in three phases: inking, stamping, and blocking. In the inking phase, 10  $\mu$ L of the desired bio-ink was pipetted onto the stamp surface. A plasma treated, hydrophilic glass coverslip was then placed atop the stamp, causing the pipetted drop to evenly spread across the surface of the hydrophobic PDMS stamp. The stamp was left to ink for 15 minutes before the coverslip was removed. Before the stamping process, any excess bio-ink was removed from the stamp surface with three washes in phosphate buffered saline (PBS) followed by two washes with ddH<sub>2</sub>O. The stamp was then dried with a short burst of compressed nitrogen, inverted, and gently placed onto a dry, hydrophilic coverslip (Bellco Glass, 1943-10012A) for one minute. Slight pressure was applied to ensure conformal contact between the stamp (1 cm by 1 cm) and coverslip (1.2 cm diameter). Immediately following this, the stamp was removed and the coverslip was transferred to a 24 well plate and immersed in PBS to prevent drying of the stamped bio-ink. Finally, the blocking phase was implemented in order to passivate the unstamped surface of the coverslip. The

surface was backfilled with a monolayer of the blocking agent through incubation in the blocking solution for 30 minutes. Following three washes with PBS, the  $\mu$ CP process, illustrated in Figure 3-2, was complete. Following the printing process, substrates can be used for cell culture immediately or stored in PBS at 4°C for up to 7 days (pre or post the blocking step).

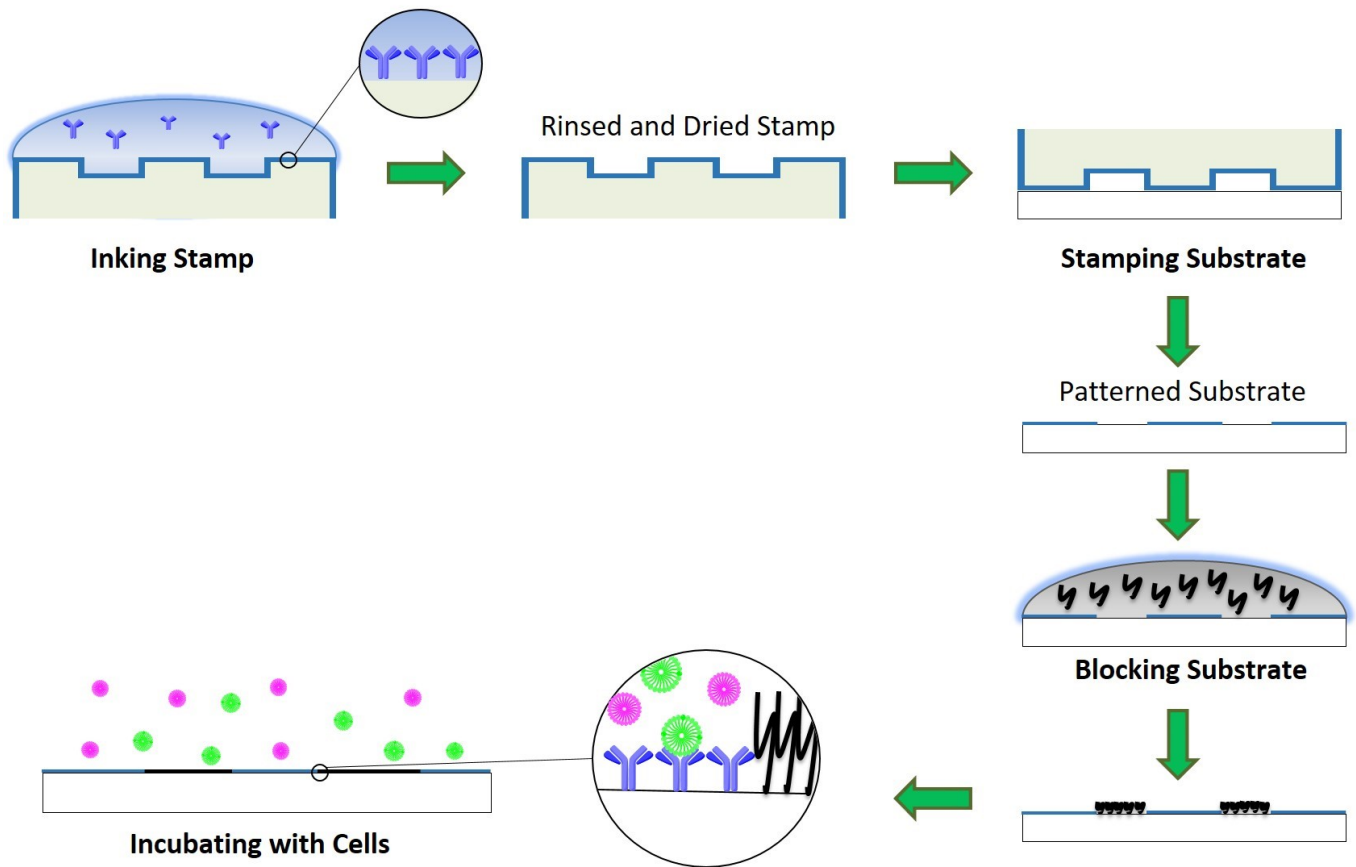


Figure 3-2. Flowchart of the microcontact printing process.

The three main steps of the microcontact printing process (inking, stamping, and blocking) are illustrated, as is the application of the patterned substrates, cell seeding.

### 3.1.4. Bio-inks and Blocking Agents

For bio-inks and blocking agents, the following materials were used: alpha platelet derived growth factor receptor antibody (anti-PDGFr- $\alpha$ ) (Novus Biologicals, NBP1-67666), oligodendrocyte marker O4 antibody (anti-O4) (R&D Systems, MAB1326), A2B5 antibody (anti-A2B5) (kindly supplied by the lab of Dr. Guillermina Almazan, produced in-house from hybridoma), poly-L-ornithine hydrobromide, (Sigma Aldrich, P3655-50MG), collagen-I from rat tail (kindly supplied by the lab of Dr. Guillermina Almazan, extracted and purified in-house), N-Cyclohexyl-N'-(2-morpholinoethyl)carbodiimide metho-p-toluenesulfonate (crosslinking agent) (Sigma-Aldrich, C1011), laminin (Sigma-Aldrich, L2020), tropomyosin receptor kinase A antibody (anti-trkA) (Abcam, ab43416 ), and poly(L-lysine)-grafted-poly(ethylene glycol) (PLL-g-PEG) (SuSos AG, PLL(20)-g[3.5]- PEG(2)) .

For the OPC culture, four bio-inks, in concentrations  $< 50 \mu\text{g}/\text{mL}$ , were tested: anti-PDGFr- $\alpha$  in PBS; anti-PDGFr- $\alpha$  and anti-O4 in PBS; anti-A2B5 in serum-free media; anti-A2B5 and anti-O4 in serum-free media. In future, the four bio-inks will be referred to as anti-PDGFr- $\alpha$ , anti-PDGFr- $\alpha$ /O4, anti-A2B5, and anti-A2B5/O4, respectively. As a non-printed control, poly-L-ornithine was used. The coverslips were immersed for 30 minutes in a  $20 \mu\text{g}/\text{mL}$  solution of poly-L-ornithine in ddH<sub>2</sub>O and washed three times with PBS before use.

For the DRG culture, two bio-inks, in concentrations  $\leq 100 \mu\text{g}/\text{mL}$ , were tested: collagen-I in ddH<sub>2</sub>O ( $50 \mu\text{g}/\text{mL}$ ) and laminin in PBS with magnesium and calcium (PBS\*) ( $100 \mu\text{g}/\text{mL}$ ). For the non-printed collagen-I control, the coverslips were immersed in the bio-ink solution overnight. For both controls and microcontact printed substrates, the collagen was fixed in a solution of

the crosslinking agent at 130  $\mu\text{g}/\text{mL}$  for 2 hours followed by three washes with ddH<sub>2</sub>O. For the non-printed laminin control, the coverslips were immersed in the bio-ink solution for 2 hours at 37°C and washed three times with PBS\* before use. For the microcontact printing of laminin, the previously outlined method was used except the inking step was done at 37°C instead of room temperature, the stamping was done for 2 minutes instead of 1, and PBS\* was used in place of PBS.

In all cell cultures, PLL-g-PEG was used as a blocking agent, dissolved in PBS at a concentration of 100  $\mu\text{g}/\text{mL}$ .

### 3.2. Cell Culture

All primary cells and media formulations were provided by the lab of Dr. Guillermina Almazan. All references to culture conditions denote incubation at 37°C and 5% CO<sub>2</sub>. Immediately prior to plating, all microcontact printed substrates were rinsed in the appropriate media for that cell type. All media changes were done using a pipette.

For cell culture, the following materials were used: Dulbecco's modified Eagle medium (DMEM) (Wisent Inc., 319-005-CL); Dulbecco's modified Eagle medium/Ham's F12 medium (DMEM/F12) (Wisent Inc., 319-085-CL); 7.5% bovine serum albumin fraction V (Wisent Inc., 809-095-EL); nerve growth factor (mouse) (NGF) (Alomone, N-100); fetal bovine serum (Invitrogen, 10082-147); phosphate buffered saline, penicillin/streptomycin, transferrin, putrescine, and insulin purchased from Invitrogen; and 4-(2-hydroxyethyl)-1-piperazineethanesulfonic acid (HEPES) purchased from Sigma-Aldrich. All other reagents were purchased from VWR or Fisher Scientific.

### 3.2.1. Oligodendrocyte Culture

Primary oligodendrocyte progenitor cells were kindly supplied by the lab of Dr. Guillermina Almazan, having being purified from newborn Sprague-Dawley rats through the procedure previously described by Almazan *et al.* [87]. In brief, post-dissection, the mixed culture, primarily of microglia and OPCs, is grown atop an astrocyte monolayer, and a shake-off followed by repeated culturing on bacterial grade petri dishes is used to enrich the OPC population before use in any experiment.

For the differentiation of OPCs, serum-free media (SFM) is used. (SFM is composed of a mixture of DMEM/F12 (1:1) and the components listed in Table 3-1 below.) If OPCs require expansion, the SFM is supplemented with the mitogens platelet-derived growth factor (PDGF<sub>AA</sub>) and basic fibroblast growth factor (bFGF) at a concentration of 2.5 ng/mL each. In this augmented media, the OPCs can be proliferated for a maximum of six days on poly-D-lysine coated culture dishes.

For all pure oligodendrocyte cultures, OPCs were cultured on glass coverslips in 24 well plates, with an approximate density of  $0.75 \times 10^5$  cells/well. Directly after purification, the OPCs are contained in a medium of DMEM with 6-12% fetal bovine serum, and this medium is retained for the initial plating to aid in cell attachment. The following day, the medium is replaced with SFM and this is considered day 0 of any experiment. Subsequent media changes occurred every 2 days. Approximately 3-5 days are required for differentiation into oligodendrocytes in these conditions. Unless otherwise stated, 5 days were allowed for differentiation.

SFM Component	Concentration
<b>4-(2-hydroxyethyl)-1-piperazineethanesulfonic acid (HEPES)</b>	10 mM
<b>Bovine Serum Albumin</b>	0.1%
<b>Penicillin/Streptomycin</b>	1%
<b>Transferrin</b>	25 µg/mL
<b>Triiodothyronine</b>	30nM
<b>Hydrocortisone-21-phosphate</b>	20 nM
<b>Progesterone</b>	20 nM
<b>Biotin</b>	10 nM
<b>Selenium</b>	30 nM
<b>Putrescine</b>	16.2 µg/mL
<b>Insulin</b>	5 µg/mL

*Table 3-1. Serum-free media components.*

### 3.2.2. Neuron Culture

Primary dorsal root ganglia were kindly supplied by the lab of Dr. Guillermina Almazan, having being obtained from Sprague-Dawley rat embryos at day 15-16 of gestation through the procedure previously described in Giasson and Mushynski [88] and Hossain *et al.* [89].

For all pure DRG cultures, DRGs were cultured on glass or plastic coverslips in 24 well plates, with an approximate density of  $2.25 \times 10^4$  cells/well. Cells were maintained in a serum free N1 media, also containing NGF at 12.5 ng/mL. (The N1 used in this experiment is composed

of a mixture of DMEM/F12 (1:1) and the components listed in Table 3-2 below.) To obtain a purified DRG culture (free from contaminating endogenous proliferating cells, such as fibroblasts or Schwann cells), the anti-mitotic cytosine-1-b-D-arabinofuranoside (AraC) (Sigma Aldrich, C-6645) was added to the medium three times, on alternating days. That is, AraC was added at a concentration of 1  $\mu$ M on days 1, 3, and 5, and an 80% media change was performed after 24 hours, on days 2, 4 and 6. Subsequently, 50% media changes were done every 3 days. For DRGs at this stage of development, approximately 21 days are required for maturation.

<b>N1 Component</b>	<b>Concentration</b>
<b>4-(2-hydroxyethyl)-1-piperazineethanesulfonic acid (HEPES)</b>	10 mM
<b>Bovine Serum Albumin</b>	0.1%
<b>Penicillin/Streptomycin</b>	1%
<b>Nerve Growth Factor (mouse)</b>	12.5 ng/mL
<b>Insulin (bovine)</b>	25 $\mu$ g/mL
<b>Transferrin (bovine)</b>	75 $\mu$ g/mL
<b>Selenium</b>	5 $\mu$ g/mL
<b>Progesterone</b>	6.3 $\mu$ g/mL
<b>Putrescene</b>	16.1 $\mu$ g/ mL

*Table 3-2. N1 media components.*

### 3.2.3. Neuron-Oligodendrocyte Co-Culture

For neuron-oligodendrocyte co-cultures, a neuron culture (as described above) was allowed to mature for 21 days. The OPCs were then re-suspended in N1 media and added directly to the mature neuron culture, in the same concentration as pure oligodendrocyte cultures. Subsequently, a 50% media change was performed every 2 days. Approximately 3-7 days are required for OPCs to differentiate into oligodendrocytes and for oligodendrocytes to begin myelination of mature neurons in these conditions. Unless otherwise stated, 7 days were allowed for myelination.

## 3.3. Analysis

### 3.3.1. Immunostaining

The following primary and secondary antibodies were utilized for immunostaining: mouse monoclonal galactocerebroside antibody (anti-GalC) (kindly supplied by the lab of Dr. Guillermina Almazan, produced in-house from hybridoma), mouse monoclonal myelin basic protein SMI-99 antibody (anti-MBP) (BioLegend, 808402), mouse monoclonal neurofilament N52 antibody (anti-N52) (Chemicon, MAB5266), Hoechst 33342 (Life Technologies), and Alexa Fluor 594, 488 conjugated secondary antibodies from Life Technologies for goat anti-Mouse - IgG1 (A-21121), -IgG2b (A-21145), -IgM (A-21044), and goat anti-Rabbit - IgG (H+L) (R37117).

Labeling with anti-GalC was performed on live cells (OPCs) for 30 minutes in culture conditions. Cells were then fixed in 4% paraformaldehyde in PBS for 30 minutes, followed by post-fixation in 100% methanol for 5 min at -20°C. A permeabilization and blocking step was then performed using a buffer of 10% horse serum and 0.1% triton X-100 in PBS. For

intracellular markers, cells were then incubated overnight with anti-MBP (for OPCs) and/or anti-N52 (for DRGs), diluted in the above buffer. Following this, incubation at room temperature with the appropriate secondary antibodies was applied for 1 hour, followed by Hoechst nuclear staining for 15 minutes. All coverslips were then mounted in Permafluor mountant (ThermoScientific, TA-030-FM) and stored at 4°C. Unless otherwise stated, labelled secondary antibodies were used to obtain all fluorescent images.

### 3.3.2. Cell Survival

A live/dead double staining kit (VWR, CA80503-904) was utilized to quantify cell survival. This staining was carried out on live oligodendrocyte cultures after 5 days of differentiation. As it is required that cells are immediately imaged post staining, the cells were moved to a secondary facility with fluorescence imaging capabilities 24 hours prior to staining. Although the disturbance caused by this move may have a slightly negative impact on cell viability, all samples should be equally affected and thus, this should still be able to provide a representative measure of relative cell survival.

## 3.4. Imaging

Unless otherwise stated, all imaging was done using an inverted fluorescence microscope (Nikon TE 2000-E) and analyzed using ImageJ software (U. S. National Institutes of Health).

### 3.4.1. OPC Differentiation Quantification

In order to quantify OPC differentiation, 5 images at 10x magnification were analyzed per stain per well. First, images with Hoechst nuclear staining were used to count the total number of cells. The cells were initially counted and outlined using built-in ImageJ functionality

(see Appendix A), followed by manually correction. These corrected outlines were then overlaid on images with anti-GalC staining or anti-MBP staining, and the number of cells positively stained for each antibody was manually counted.

### 3.4.2. OPC Viability Quantification

Using the live/dead fluorescent staining kit, both alive and dead cells are stained 'green' with the cell permeable Cyto-dye, and only dead cells are stained 'red' with propidium-iodide. For images with staining of each fluorescent dye, positively stained cells were counted and outlined using built-in ImageJ functionality (see Appendix A), followed by manual correction. The cell viability was then calculated as follows:

$$\% \text{ living cells} = \frac{\# \text{ cells Cyto-dye}^+ - \# \text{ cells propidium-iodide}^+}{\# \text{ cells Cyto-dye}^+}$$

### 3.5. Statistical Analysis

Unless otherwise stated, results are expressed as mean  $\pm$  standard error of the mean with cell culture experiments comprising three independent tests performed in triplicate. Anderson-Darling tests were used to measure data normality. Statistical differences were then measured using a one way ANOVA or Kruskal–Wallis test (for normally or non-normally distributed data, respectively) followed by a Turkey-Kramer *post-hoc* test. Standard MATLAB (MATLAB R2014a, The MathWorks, Inc.) functions (adtest, anova1, kruskalwallis, multcomp) were used for all statistical computations. Differences were considered significant when *p* values were found to be  $< 0.05$ .

## Chapter 4. Experimental Rationale

### 4.1. Stamp Design

In order to create a platform for the study of controlled myelination, cell growth would need to be restricted to a simple, repeatable pattern so that the resultant, organized myelination can be easily analyzed and quantified. To that end, a basic grid design was chosen as the inspiration for this investigation. For that reason, all microcontact printing stamps investigated were designed as sets of parallel lines, with varying widths and/or spacings.

#### 4.1.1. Oligodendrocyte Culture

For oligodendrocyte cultures, a line thickness of 20  $\mu\text{m}$  and a spacing of 100  $\mu\text{m}$  was chosen. In terms of width, 10  $\mu\text{m}$  would be the minimum allowable size, as this is on par with the cell body diameter of OPCs [7]. A microcontact printed line width of 10  $\mu\text{m}$  would result in stronger pattern adherence as the restrictive size would limit the points of attachment for OPCs, forcing them into a straight line. However, a thicker line width would allow for the attachment of a higher density of OPCs which would help stabilize the cells' attachment, albeit at a slight cost to pattern adherence. Additionally, the normal functionality of OPCs is density dependent, with a higher concentration of cells encouraging differentiation [26]. Furthermore, the increased width would also be less restrictive to the developing OPC cell morphology. Thus, a thicker line was preferred, and 20  $\mu\text{m}$  was chosen. In terms of line spacing, several studies have suggested that in order to minimize the chance of cell spreading between patterns, a spacing of 50  $\mu\text{m}$  or larger is required [7, 23, 24, 90-92]. As such, a spacing of 100  $\mu\text{m}$  was chosen to minimize the possibility of crossover and accentuate pattern compliance.

#### 4.1.2. Neuron Culture

For neuron cultures, a line width of 10  $\mu\text{m}$  and a spacing of 100  $\mu\text{m}$  was chosen. By and large, investigations have suggested that patterned lines of smaller widths result in better directional alignment, although dependent on sufficient spacing between lines [93-96]. Several recent studies have successfully directed axon extension using patterns with widths between 10 to 15  $\mu\text{m}$  [7, 23, 97]. Thus, it was decided that the line width used for this project would be 10  $\mu\text{m}$ , a width appropriate for the neuron body size of 7-18  $\mu\text{m}$  [93]. Moreover, it was decided that a 100  $\mu\text{m}$  spacing would be the most fitting as it is most likely to prevent neurite bridging between patterns. Moreover, it provides a low enough ratio of line width to line spacing in order to encourage pattern parallel axon growth, as opposed to randomized or perpendicular growth [95].

#### 4.2. Bio-Ink Choice

##### 4.2.1. Oligodendrocyte Culture

For oligodendrocyte cultures, the bio-inks chosen reflect the markers typically expressed by oligodendrocyte progenitor cells and immature oligodendrocytes, as illustrated in Figure 4-1 below.

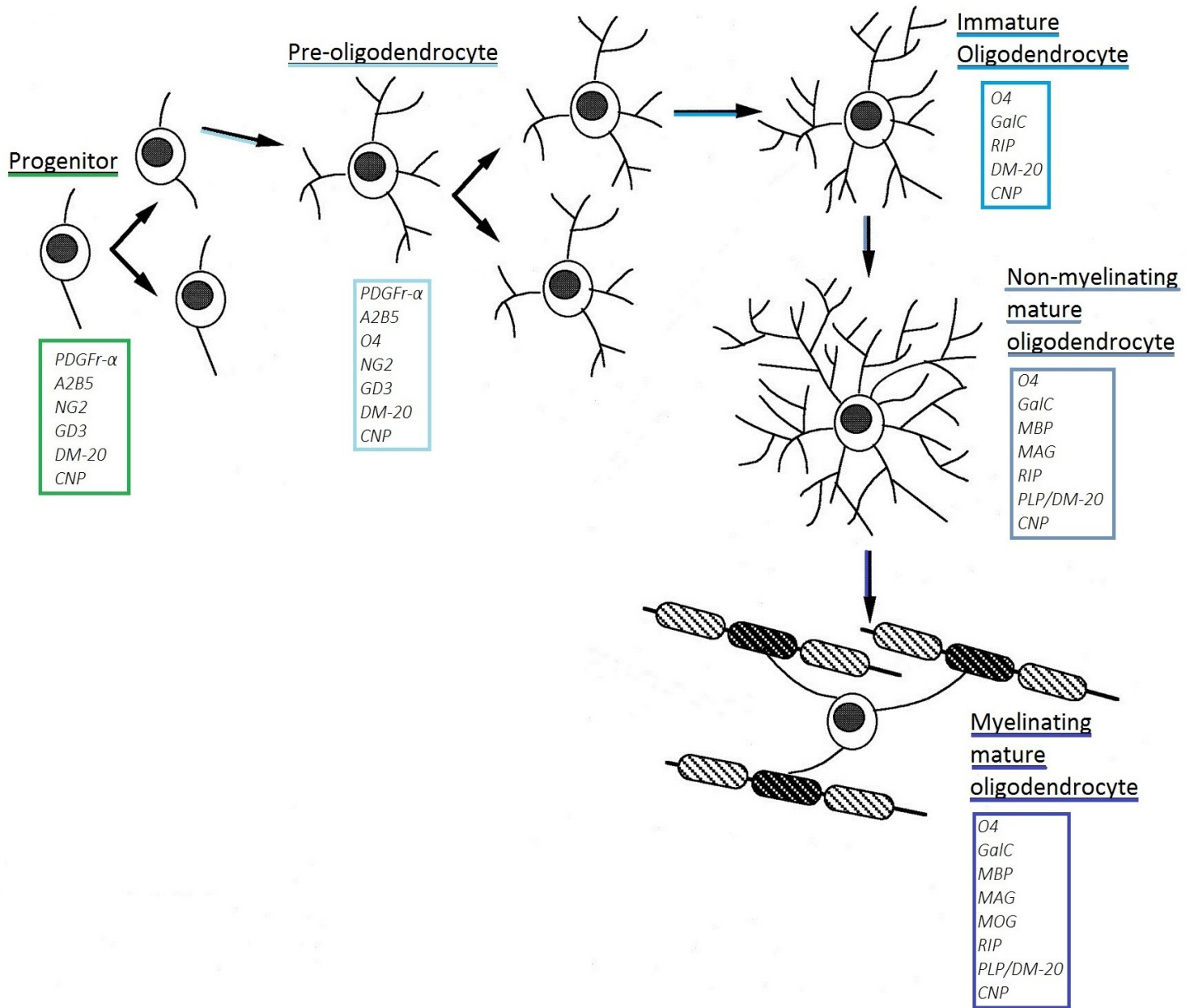


Figure 4-1. Markers present at different developmental stages of the oligodendrocyte cell lineage, in rodents.

This image, provided by Baumann and Pham-Dhim [3], illustrates the morphological features and markers at different stages of the oligodendrocyte lineage. Adapted from [3], copyright © 2001, The American Physiological Society.

OPCs are regularly identified by their specific expression of two markers: alpha platelet derived growth factor receptor (*PDGFr-α*) and the ganglioside epitope *A2B5* [1, 98]. In fact, they

are among the most common markers used for the identification of the earliest progenitor cells in the rodent oligodendrocyte lineage [25, 99]. As such, antibodies for PDGFr- $\alpha$  and A2B5 were used as two separate bio-inks in this study. It should be noted that although these markers are primarily used to identify cells in the early stages of the oligodendrocyte lineage (i.e. progenitors), they can continue to be expressed in later stages (i.e. pre- to immature oligodendrocytes) [100]. However, as the cells further mature, they can experience a gradual loss of markers for both PDGFr- $\alpha$  and A2B5; by this point, the cells have become notably positive for the oligodendrocyte marker O4 [1, 3]. With this in mind, mixtures of antibodies for PDGFr- $\alpha$  and O4 and A2B5 and O4 were used as the final two bio-inks in this study. In short, it was reasoned that if the cells were to experience a loss of the early markers, the presence of anti-O4 would allow the cells to have additional binding points.

As discussed previously, in a co-culture environment, neurons would be cultured on patterned substrates for 21 days prior to OPC seeding. Thus, it is necessary that the oligodendrocyte bio-ink is highly specific, preventing neurons from attaching to the areas patterned for oligodendrocyte attachment. It is for this reason that oligodendrocyte-specific antibodies were used, as opposed to poly-lysine [101] or other commonly used but non-specific proteins. Moreover, Didar *et al.* (2014) [102] previously demonstrated the feasibility of culturing cells on microcontact printed patterns of antibodies, including the ability of OPCs to proliferate and differentiate over several days on printed patterns of anti-PDGFr- $\alpha$ . Thus, this offers some precedence for the use of antibody based bio-inks to direct cell culture.

Finally, it should be recalled that the first two bio-inks, anti-PDGFr- $\alpha$  and anti-PDGFr- $\alpha$ /O4, were diluted in PBS whereas the second two, anti-A2B5 and anti-A2B5/O4, were diluted

in SFM. Although the dilution of all bio-inks in PBS was desired, the anti-A2B5 being used was produced in-house, pre-diluted in SFM. To address this discrepancy, a small comparison was done between anti-PDGFr- $\alpha$  diluted in PBS and anti-PDGFr- $\alpha$  diluted in SFM, and these results will be presented in the later sections.

#### 4.2.2. Neuron Culture

For neuron cultures, it was decided that the patterning of a neuron-specific antibody (e.g. anti-trkA) would be unlikely to provide sufficient long-term attachment and stability for DRG neurons, which are particularly sensitive to cellular conditions such as coating substrates [5, 103]. As such, extra-cellular matrix proteins were considered far more suitable anchoring substrates [92]. In fact, Lauer *et al.* [104] suggest the microcontact patterning of extra-cellular proteins is “one of the most effective techniques to control neuronal cell growth *in vitro*.” As the supply of DRGs would be limited, it was decided that only two bio-inks should be tested. Due to both their ready availability and regular use in neuron cultures, collagen-I and laminin were selected. Collagen, often cross-linked, is commonly used as a substrate coating for DRG cultures [88, 105, 106]. In addition, it has been shown to be successfully microcontact printed [107]. As such, this was the first bio-ink attempted for neuron cultures. In a similar vein, laminin has also been successfully microcontact printed in a number of studies directing neuron growth [92, 104, 108]. This is due, in large part, to laminin being considered growth promoting; as laminin is capable of initiating and supporting neurite outgrowth, many neuron types have been found to readily allow axon extension on laminin coated substrates [93, 96, 109-111]. Thus, with its strong track record, laminin was chosen as the final bio-ink used in this study.

## Chapter 5. Results

### 5.1. Oligodendrocyte Culture

In the following section, the four bio-inks under investigation are anti-PDGFr- $\alpha$ , anti-PDGFr- $\alpha$ /O4, anti-A2B5, and anti-A2B5/O4. In all tests, OPCs were seeded on patterned glass substrates and allowed to differentiate for 5 days.

#### 5.1.1. Pattern Adherence

In this study, clear OPC pattern adherence was seen for all four bio-inks under investigation. That is, the seeded OPCs successfully attached to the microcontact printed 20x100  $\mu\text{m}$  patterns and remained on the patterns through five days of differentiation. This pattern adherence can be observed in Figures 5-1 to 5-4 below. Figure 5-5 shows images from the unpatterned positive control, poly-L-ornithine, and can be used as a point of comparison.

Through qualitative investigation, the most consistent pattern adherence was observed when using the bio-inks of anti-A2B5 and anti-A2B5/O4; that is, at the lowest magnification, the cells were seen to attach to nearly the entire pattern surface, with few to no gaps or holes in coverage (i.e. areas devoid of cells, where the pattern could not be identified). In contrast, cell coverage on the patterned bio-inks of anti-PDGFr- $\alpha$  and anti-PDGFr- $\alpha$ /O4 consistently contained a small number of gaps, generally limited to <20%. It should be noted that the pattern adherence to anti-PDGFr- $\alpha$ /O4 was found to be more regular than with anti-PDGFr- $\alpha$  alone. That is, larger gaps were only ever seen with anti-PDGFr- $\alpha$  patterns, not with anti-PDGFr- $\alpha$ /O4.

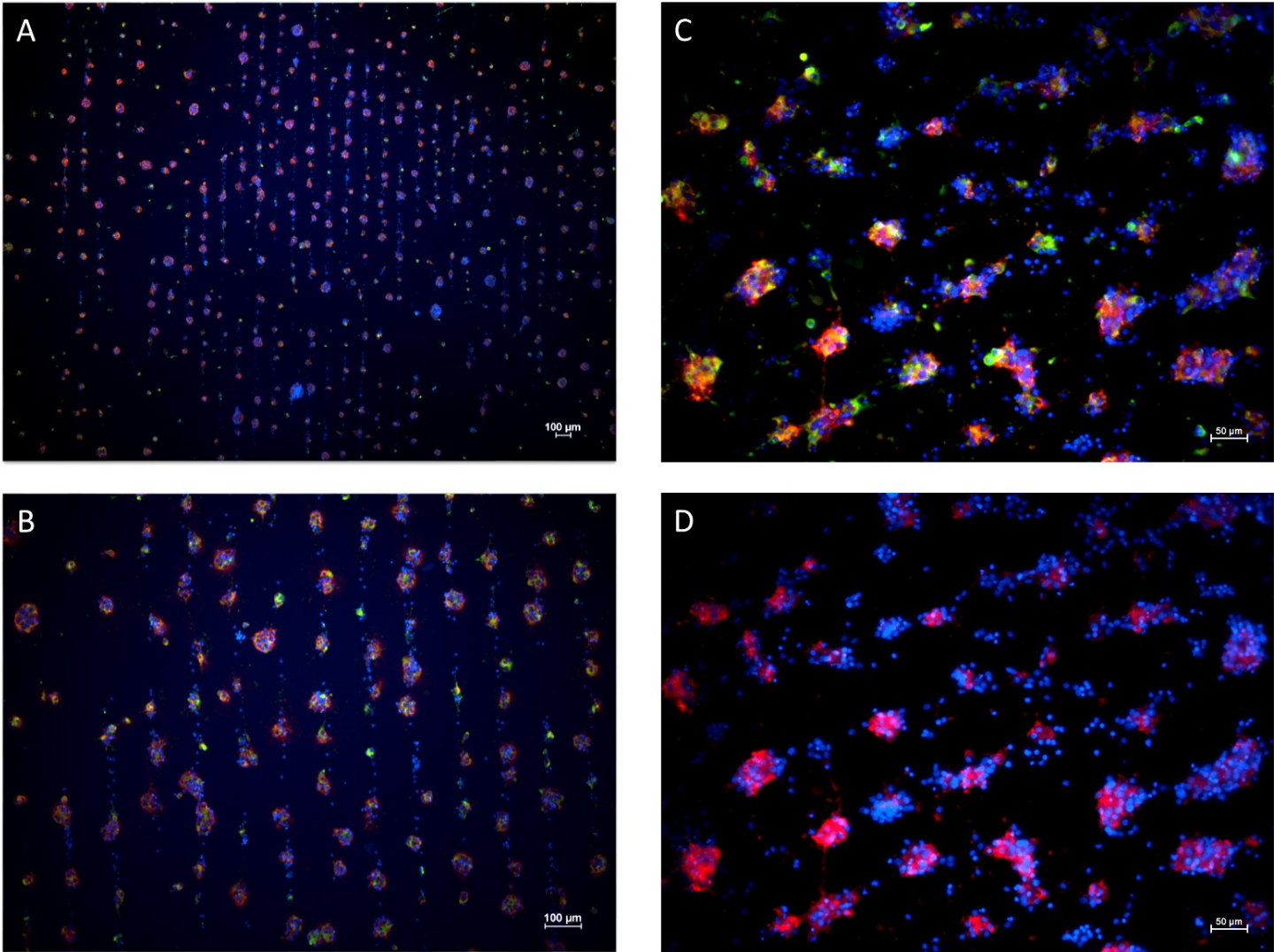


*Figure 5-1. Oligodendrocyte adherence to patterned anti-PDGFr- $\alpha$ .*

For all images, the following stains were used: blue = Hoechst, green = anti-GalC, and red = anti-MBP. Images (A) and (B) are representative of the pattern at 4x and 10x. Images (C) and (D) show the same 20x zoomed image, with the former containing one more stain, anti-GalC, than the latter. Scale is 100  $\mu\text{m}$  for images (A) and (B) and 50  $\mu\text{m}$  for images (C) and (D).

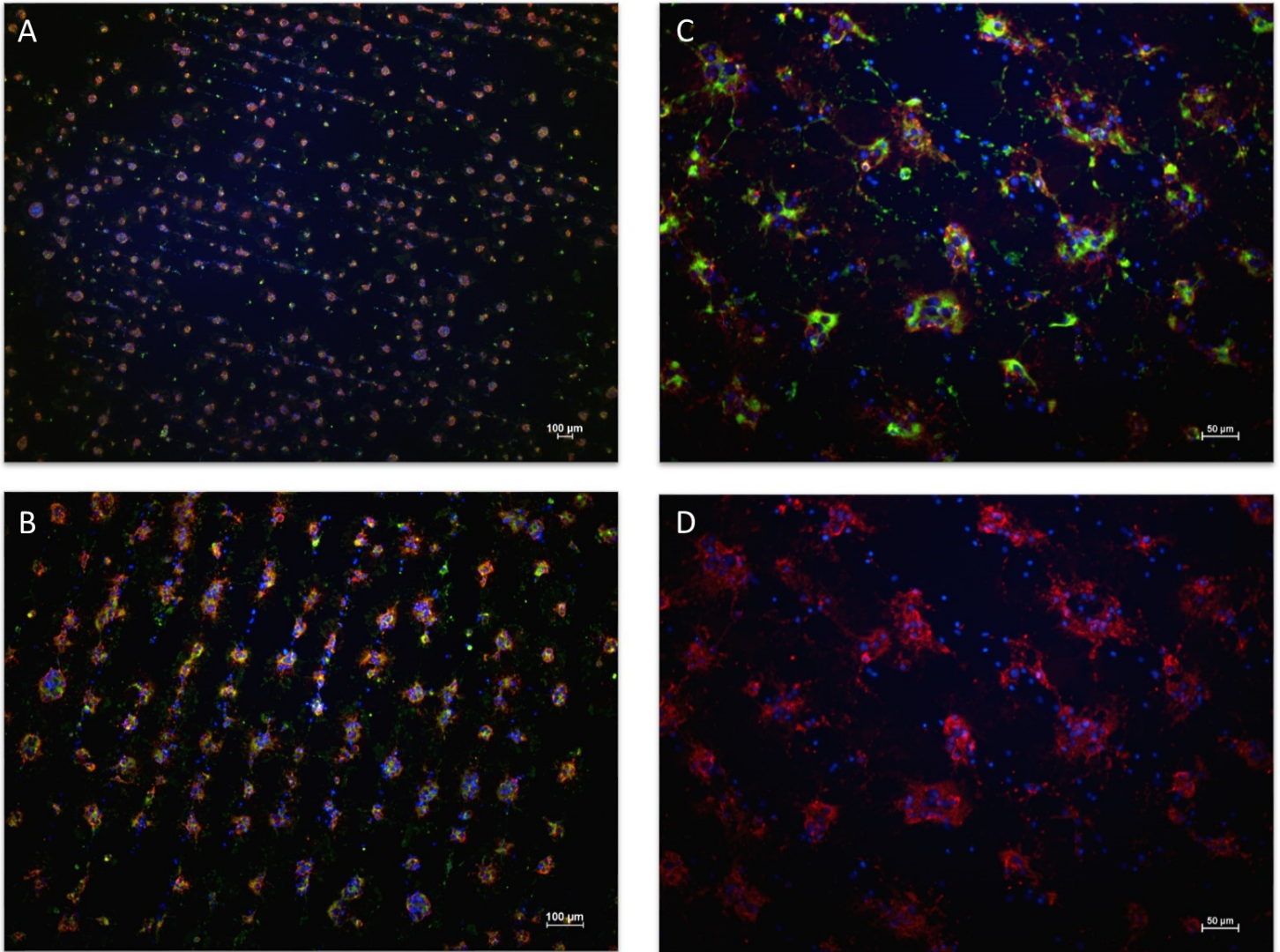


*Figure 5-2. Oligodendrocyte adherence to patterned anti-PDGFr- $\alpha$ /O4.*

For all images, the following stains were used: blue = Hoechst, green = anti-GalC, and red = anti-MBP. Images (A) and (B) are representative of the pattern at 4x and 10x. Images (C) and (D) show the same 20x zoomed image, with the former containing one more stain, anti-GalC, than the latter. Scale is 100  $\mu$ m for images (A) and (B) and 50  $\mu$ m for images (C) and (D).

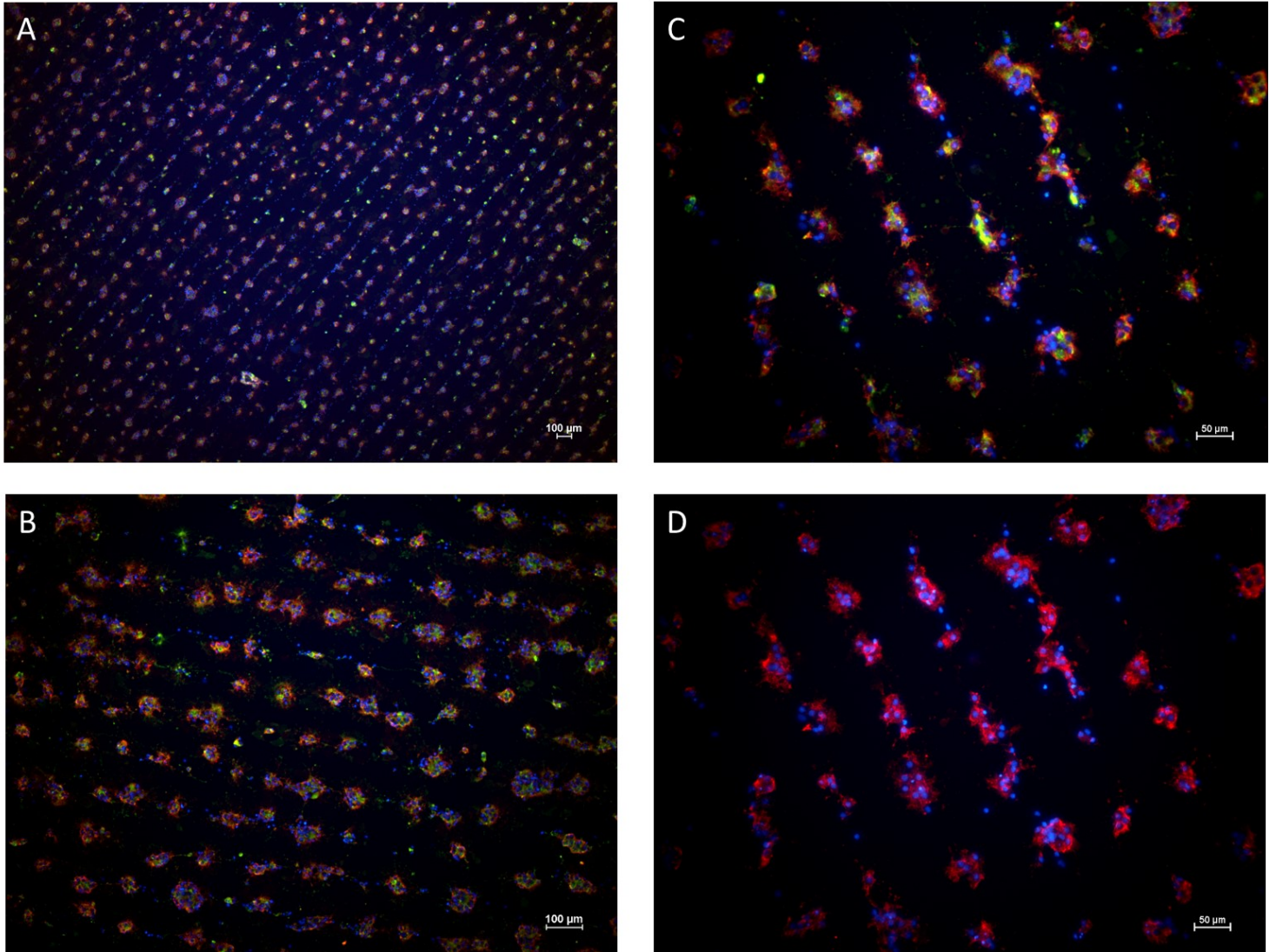


*Figure 5-3. Oligodendrocyte adherence to patterned anti-A2B5.*

For all images, the following stains were used: blue = Hoechst, green = anti-GalC, and red = anti-MBP. Images (A) and (B) are representative of the pattern at 4x and 10x. Images (C) and (D) show the same 20x zoomed image, with the former containing one more stain, anti-GalC, than the latter. Scale is 100 μm for images (A) and (B) and 50 μm for images (C) and (D).

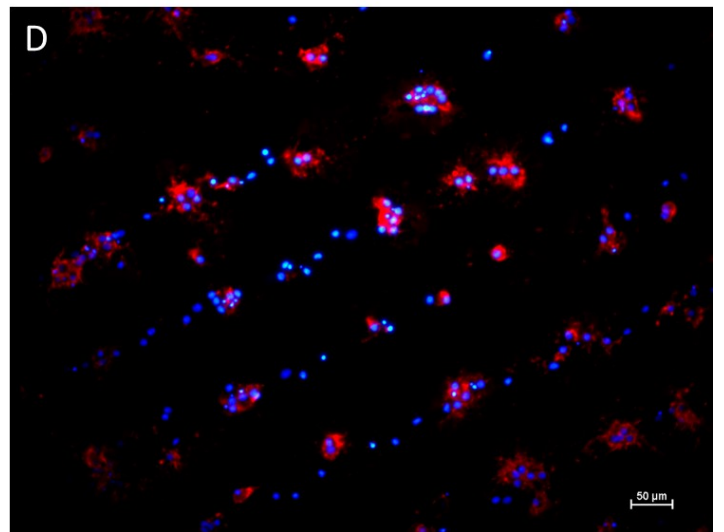
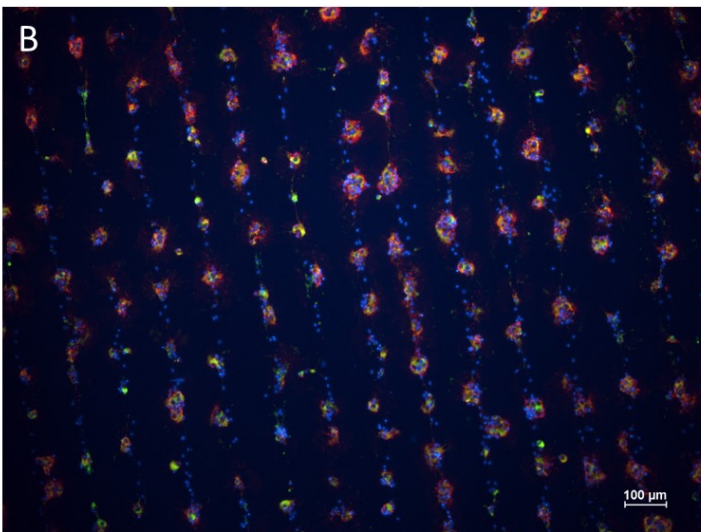
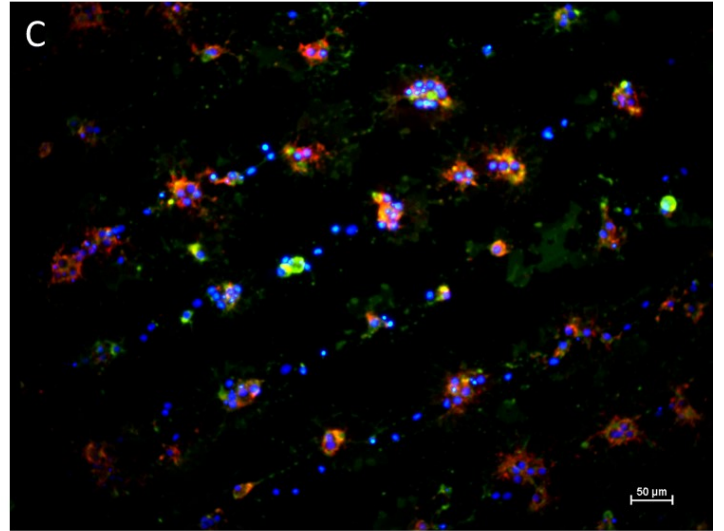
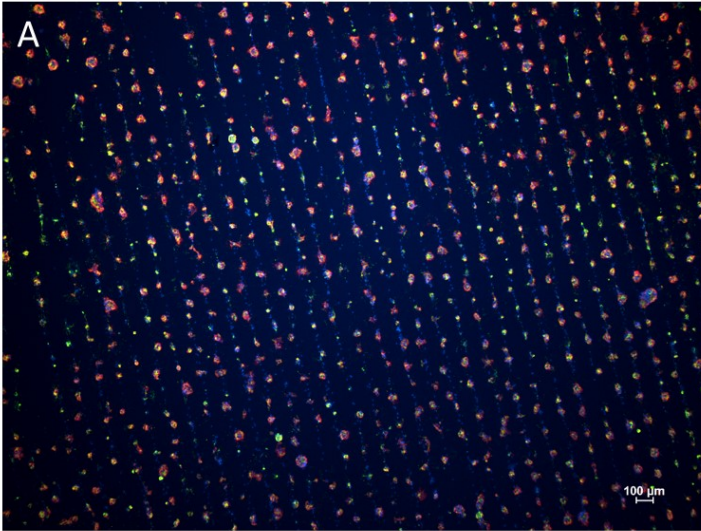


*Figure 5-4. Oligodendrocyte adherence to patterned anti-A2B5/O4.*

For all images, the following stains were used: blue = Hoechst, green = anti-GalC, and red = anti-MBP. Images (A) and (B) are representative of the pattern at 4x and 10x. Images (C) and (D) show the same 20x zoomed image, with the former containing one more stain, anti-GalC, than the latter. Scale is 100  $\mu\text{m}$  for images (A) and (B) and 50  $\mu\text{m}$  for images (C) and (D).

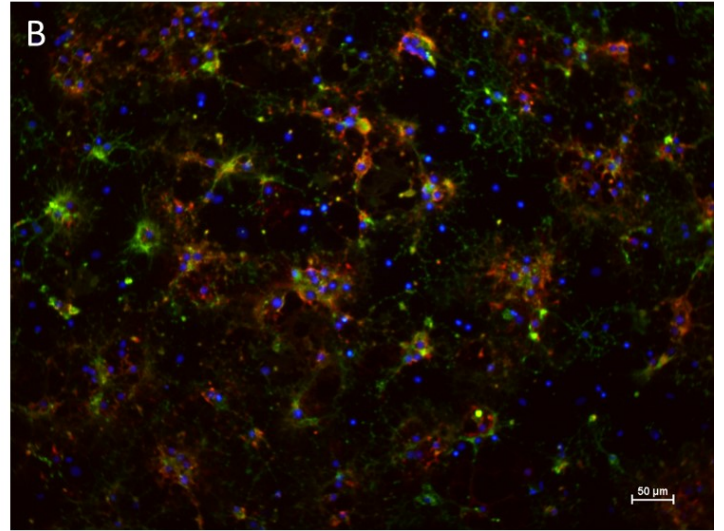
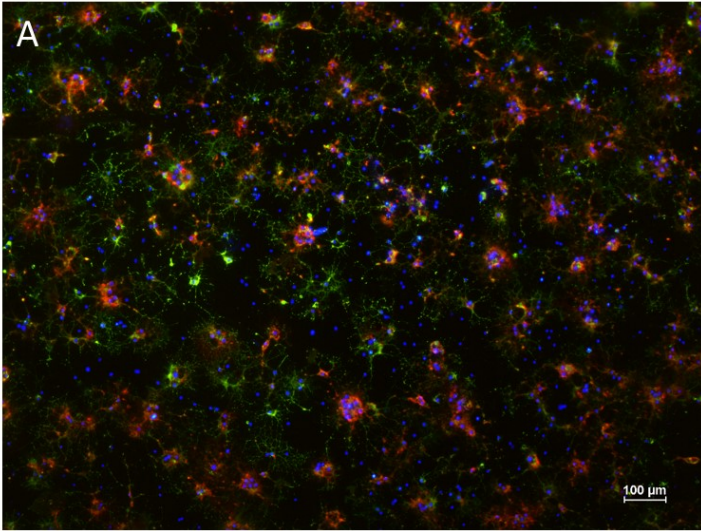


*Figure 5-5. Oligodendrocyte adherence to the positive control, unpatterned poly-L-ornithine.*

For all images, the following stains were used: blue = Hoechst, green = anti-GalC, and red = anti-MBP. Images (A) and (B) are representative of the pattern at 10x and 20x. Scale is 100  $\mu\text{m}$  for image (A) and 50  $\mu\text{m}$  for image (B).

Finally, to observe the effects of the dilutant, bio-inks of anti-PDGFr- $\alpha$  diluted in PBS and anti-PDGFr- $\alpha$  diluted in SFM were compared. In general, no obvious qualitative differences could be observed in the cell adherence to either bio-ink pattern. This is shown below in Figure 5-6.

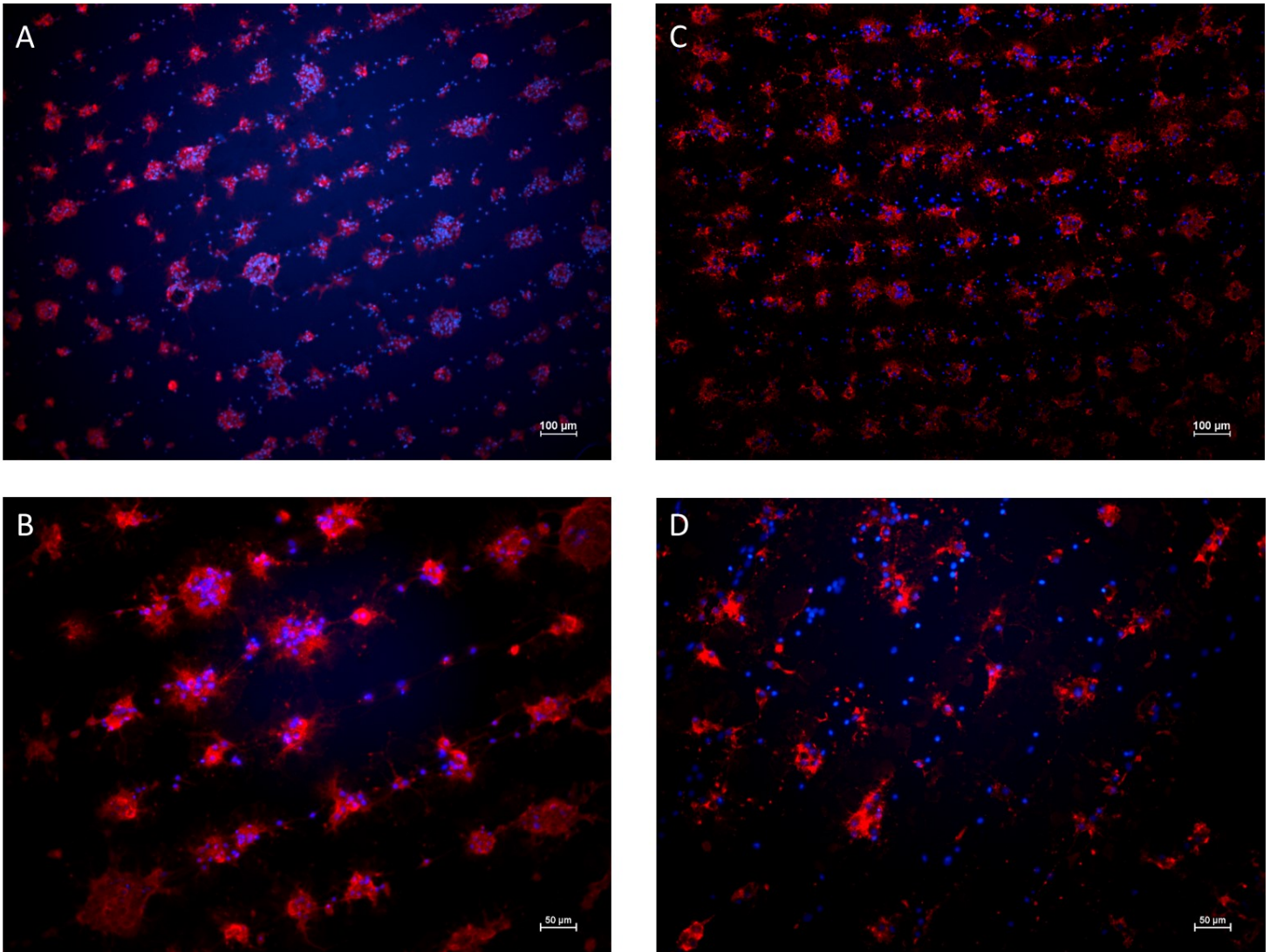


*Figure 5-6. Oligodendrocyte adherence to patterned anti-PDGFr- $\alpha$  diluted in PBS and SFM.*

For all images, the following stains were used: blue = Hoechst and red = anti-MBP. (A) and (B) respectively show 10x and 20x images of cells on the pattern of anti-PDGFr- $\alpha$  diluted in PBS. (C) and (D) respectively show 10x and 20x images of cells on the pattern of anti-PDGFr- $\alpha$  diluted in SFM. Scale is 100  $\mu\text{m}$  for images (A) and (C) and 50  $\mu\text{m}$  for images (B) and (D).

### 5.1.2. OPC Differentiation

Once successful pattern adherence was observed, it was necessary to quantify the effect of patterned growth on OPC differentiation. The results are summarized in Figure 5-7 below. OPCs differentiated into mature oligodendrocytes are positive for the MBP marker, and cells confirmed to be differentiating in the oligodendrocyte lineage, both immature and mature, are positive for the GalC marker [17]. (This was illustrated previously in Figure 4-1.) Thus, the measure of differentiation used was MBP positive cells (MBP+) over GalC positive cells (GalC+). As can be seen, there is no significant difference in OPC differentiation on any of the tested bio-inks. However, all four bio-inks show a small but significantly higher differentiation percentage than that observed on the positive control, poly-L-ornithine. (The same data is presented in Appendix B with the measure of differentiation as simply MBP positive cells (MBP+).)

Furthermore, a single trial, performed in triplicate, was used to compare bio-inks of anti-PDGFr- $\alpha$  diluted in PBS and SFM. It was observed that the differentiation of OPCs on both patterns were found to be on par, with the average MBP+/GalC+ cell percentages at 89.88% for anti-PDGFr- $\alpha$  diluted in PBS and 84.45% for anti-PDGFr- $\alpha$  diluted in SFM. As such, the dilutant does not appear to have a major observable effect on cell differentiation.

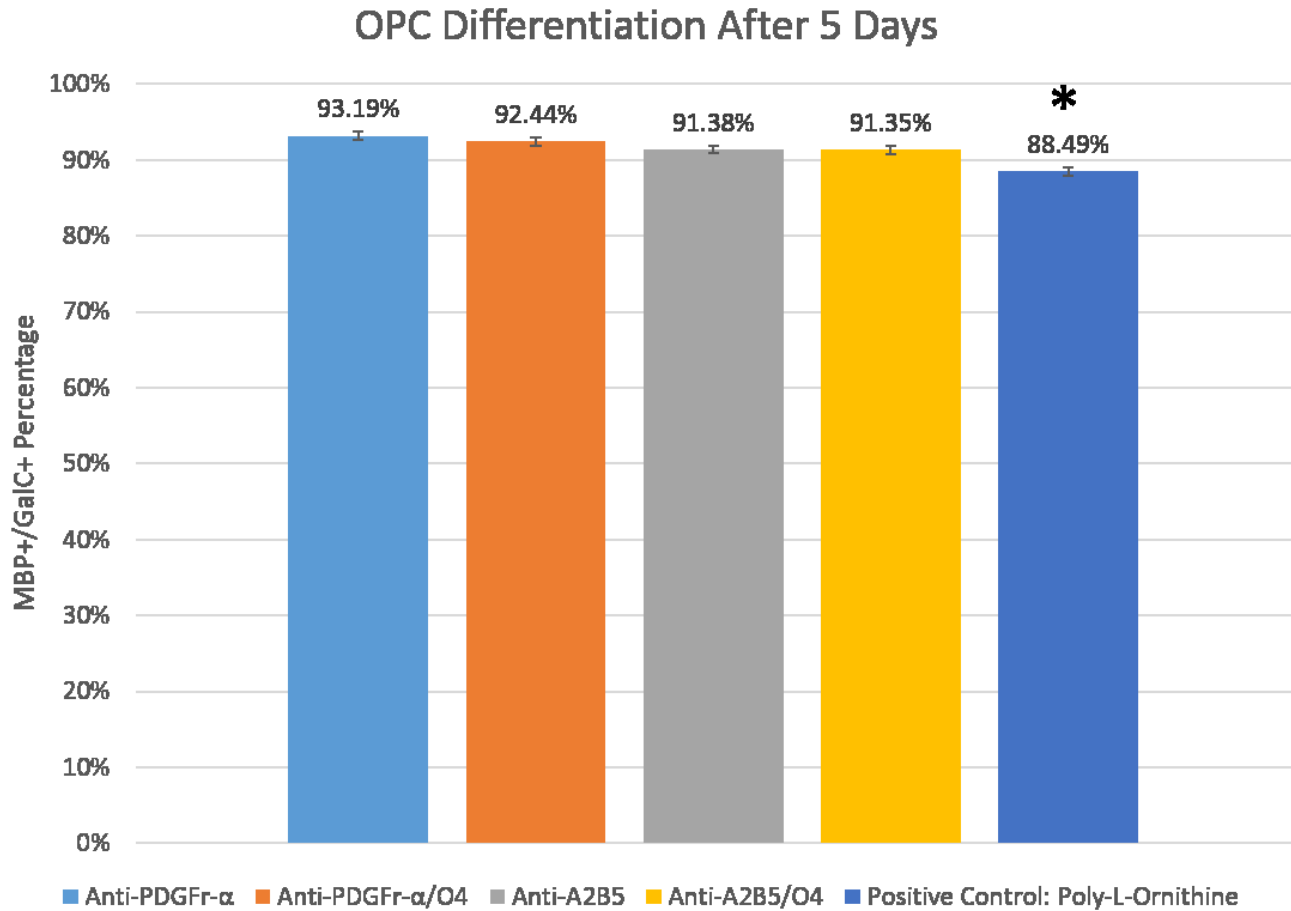


Figure 5-7. OPC differentiation after 5 days on patterned bio-inks.

The measure of differentiation used was the number of MBP+ cells over GalC+ cells. Results are listed as mean  $\pm$  standard error of the mean, with three independent trials performed in triplicate. The positive control had a significantly lower value than all other samples. (For significance, \*  $p < 0.05$ ).

### 5.1.3. OPC Viability

Finally, the viability of the OPCs was measured after five days of differentiation on the patterned bio-inks. As can be seen in Figure 5-8 below, the levels of viability were  $\geq 90\%$  on all bio-inks and the positive control of poly-L-ornithine. Thus, for all four bio-inks, the patterned growth of the cells had no significant impact on cell viability.

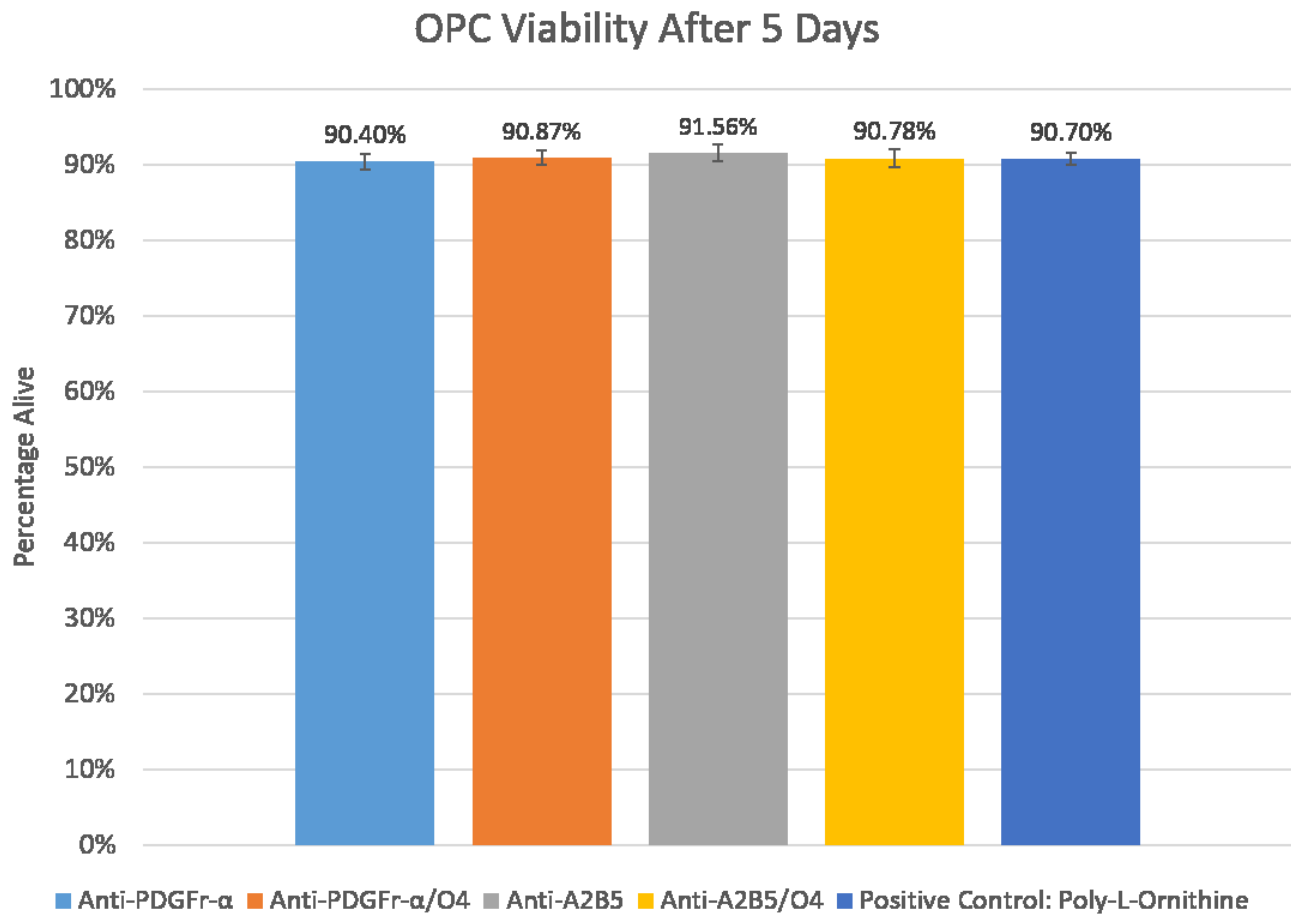


Figure 5-8. OPC viability after 5 days on patterned bio-inks.

Results are listed as mean  $\pm$  standard error of the mean, with three independent trials performed in triplicate.

## 5.2. Neuron Culture

In the following section, the two bio-inks under investigation are collagen-I and laminin, printed in 10x100  $\mu\text{m}$  patterns. In all tests, DRGs were seeded onto the patterned bio-inks and allowed to mature and develop for up to four weeks.

### 5.2.1. Neuron Attachment and Pattern Adherence

For the collagen-I bio-ink on glass substrates, very poor long-term neuron attachment was seen. After initial seeding, DRG attachment and preliminary neurite extension was observed on the patterned collagen. However, by day 7, catastrophic neuron detachment, >90%, consistently occurred for the patterned collagen-I. This, however, was not the case for the positive control, a uniform surface coating of collagen-I, which showed strong long-term neuron attachment and maturation. Both cases are illustrated in Figure 5-9 below. It may be worth noting that neuron detachment during the first week is not entirely unexpected, as the culture encounters somewhat adverse conditions, with an anti-mitotic agent AraC being added to prevent the proliferation of any endogenous non-neuronal cell types.

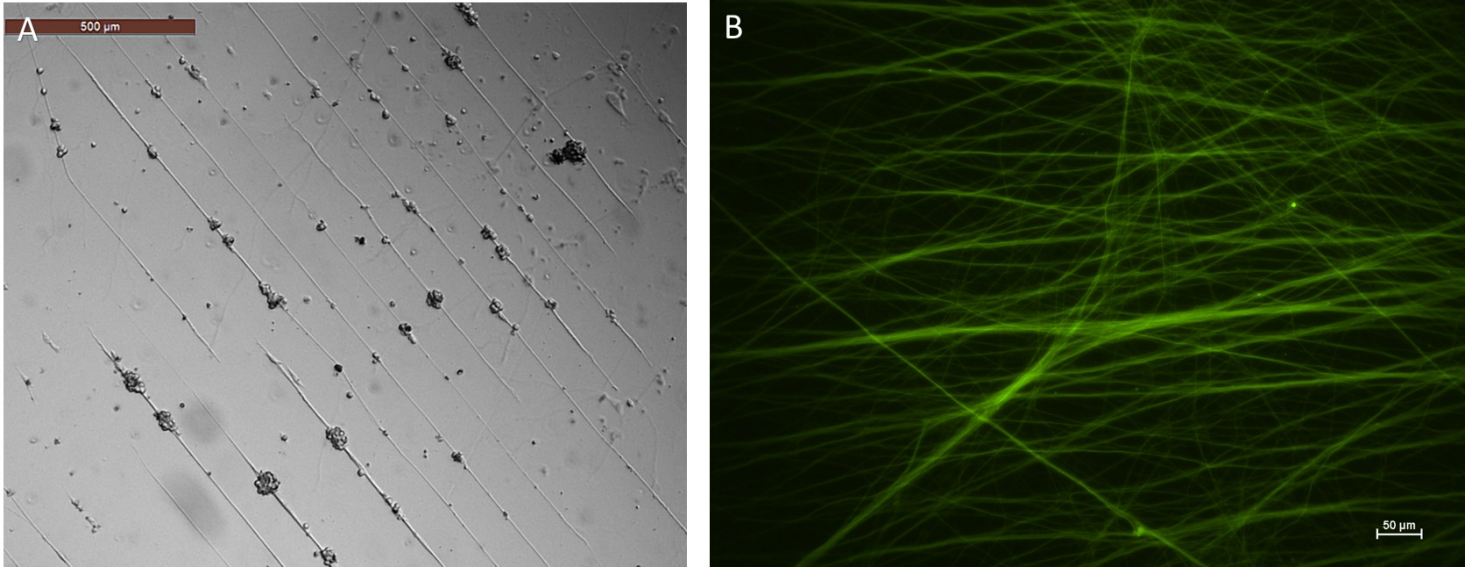


*Figure 5-9. Neuron attachment to collagen-I.*

Neuron growth on collagen-I is shown for the microcontact printed pattern on day 3 in (A) and the positive control on day 28 in (B). For (B), a neurofilament stain was used, green = anti-N52. Scale is 500 μm for image (A) and 50 μm for image (B).

For the laminin bio-ink on glass substrates, stronger long-term neuron attachment was possible, although the problems of cell detachment were still present. As seen in Figure 5-10, the neuron attachment and axon extension was very strong for the first two weeks. However, by the fourth week, discrete areas of pattern overgrowth and neuron detachment were observed. It should be noted that, by and large, neither factor was enough to completely obscure the neurons' adherence to the laminin pattern. That is, the neuron detachment was not necessarily catastrophic, as can be seen in Figure 5-11 (A). Moreover, any major pattern overgrowth was limited to distinct regions, and only minor cell bridging was observed. As such, the patterned samples were generally still distinguishable from the positive controls, shown in Figure 5-11 (B). By and large, the laminin bio-ink was much more successful than collagen-I for

long-term neuron patterning on glass substrates. However, the 10x100  $\mu\text{m}$  pattern of laminin was still not able to provide consistent long-term (>2 weeks) pattern adherence.

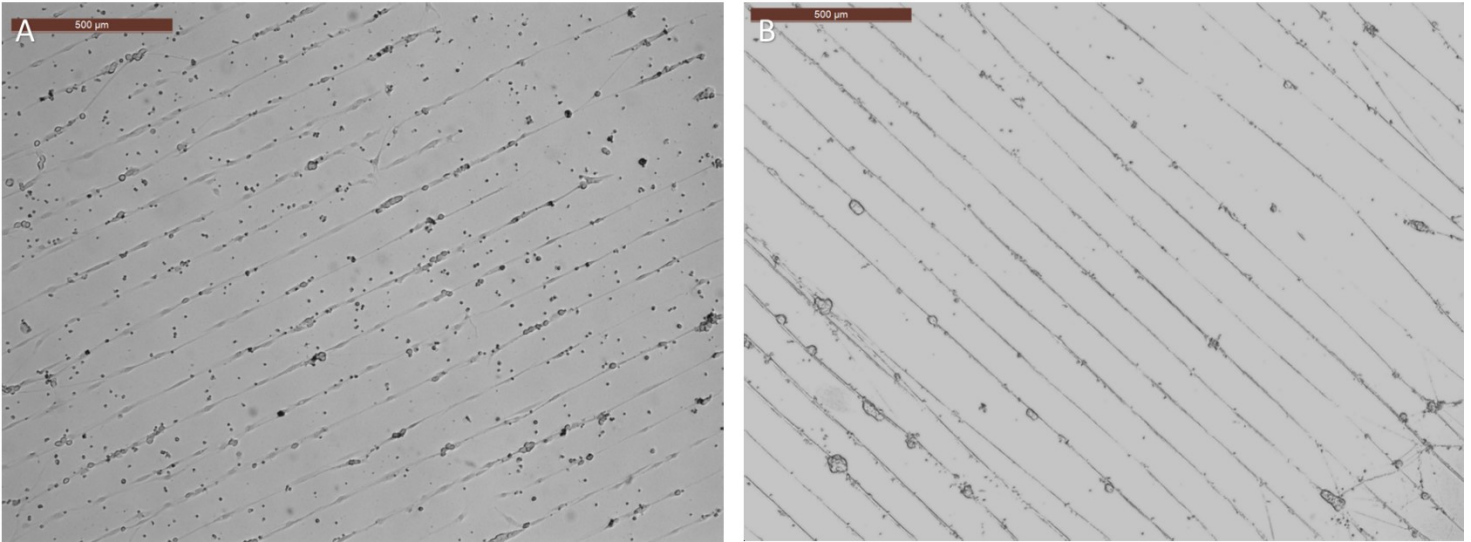


*Figure 5-10. Neuron attachment to laminin patterns at day 3 and day 13.*

Neuron growth on the microcontact printed laminin patterns shown at day 3 (A) and day 13 (B). Scale is 500  $\mu\text{m}$  for all images.

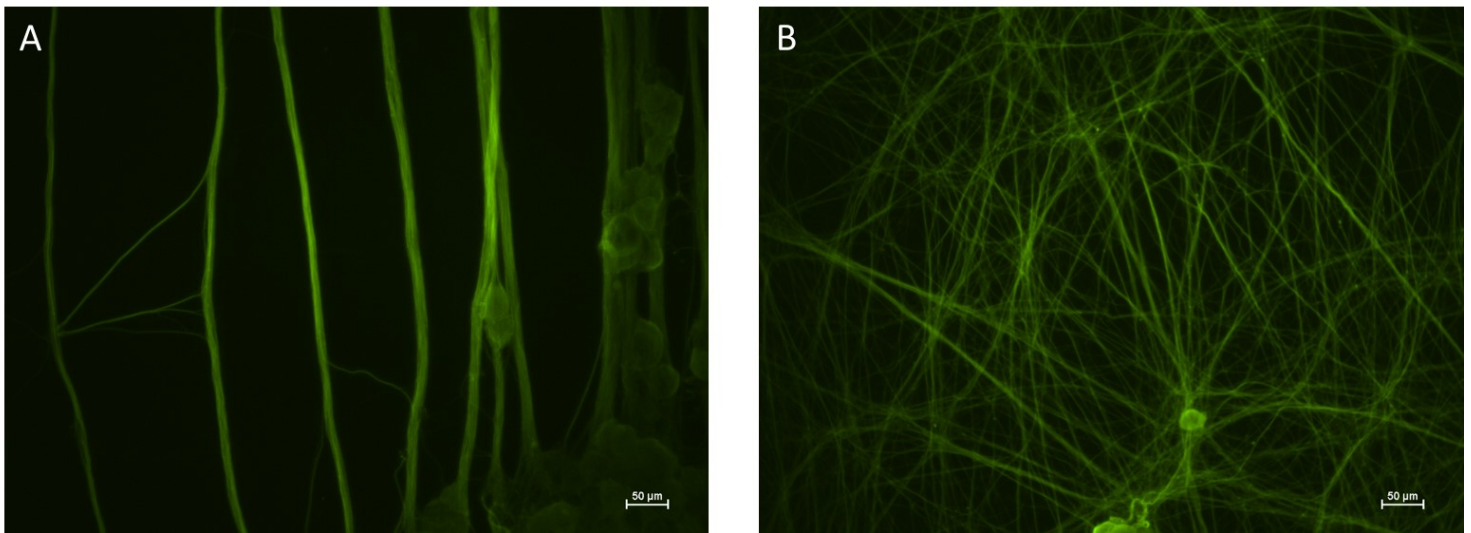


*Figure 5-11. Neuron attachment to laminin at day 28.*

For all images, a neurofilament stain was used, green = anti-N52. Neuron growth at 20x magnification is shown for the microcontact printed laminin in (A) and the positive control, uniform laminin coating, in (B). Scale is 50  $\mu\text{m}$  for all images.

A second set of tests was performed using *Thermanox* plastic coverslips to investigate their effect on neuron attachment. Surprisingly, for both bio-inks on plastic coverslips, little to no cell detachment or pattern adherence was seen. That is, the neurons immediately branched and overgrew the patterned bio-inks, despite the passivation with PLL-g-PEG. (It should be noted that Fink *et al.* [112] also found other cell types capable of weakly attaching to PLL-g-PEG passivated areas on plastic substrates.) Although the pattern was not adhered to, the neurons seemed to flourish, maturing and forming intricate networks. As illustrated in Figure 5-12, the patterned plastic substrates for collagen-I and laminin were indistinguishable from each other or from their respective positive controls. As such, these results may suggest that long-term, unpatterned DRG attachment may also be encouraged using plastic coverslips.

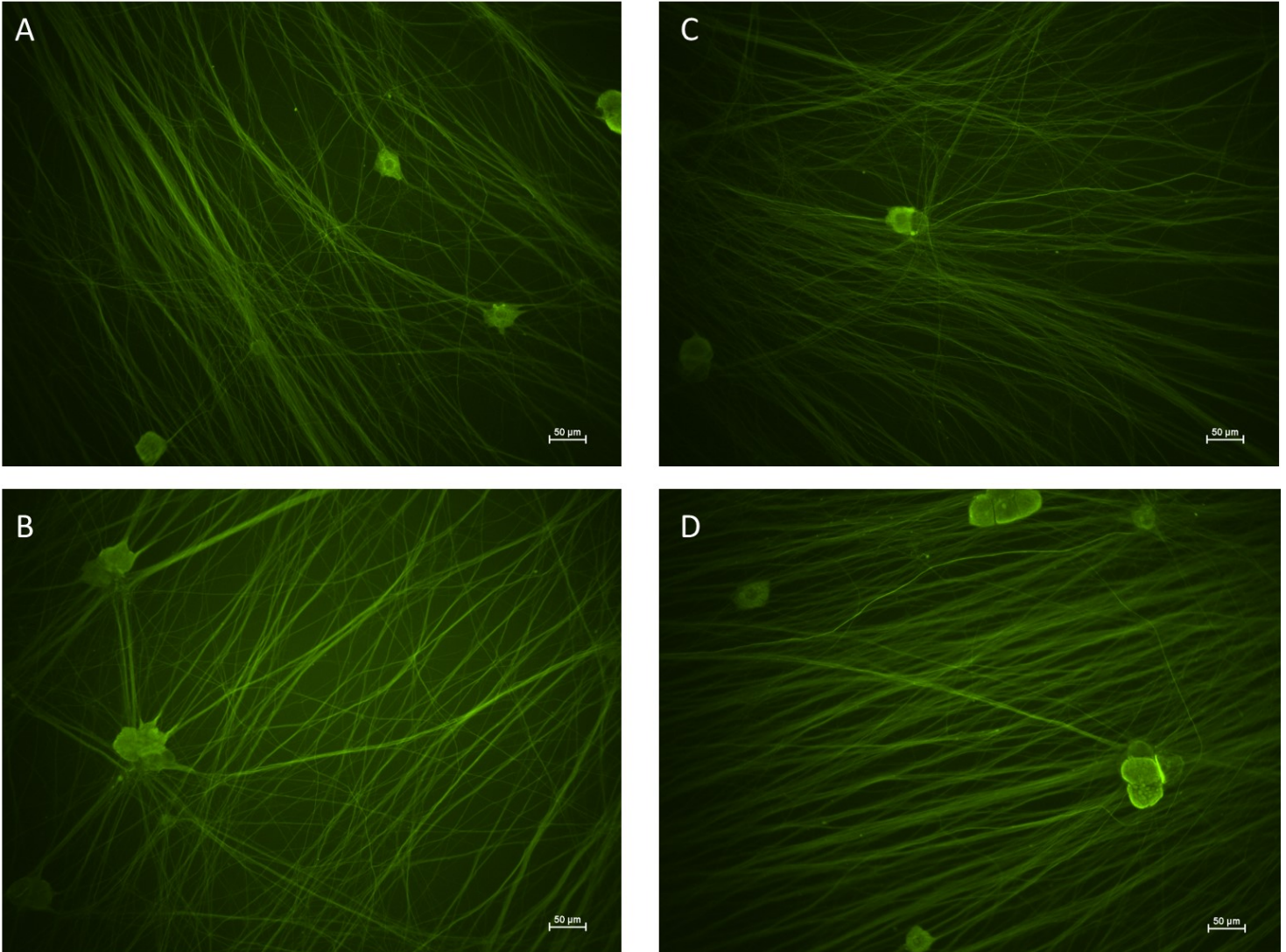


*Figure 5-12. Neuron culture on plastic coverslips.*

For all images, a neurofilament stain was used, green = anti-N52. Images (A) and (C) show neuron growth on patterned collagen-I and laminin, respectively. Images (B) and (D) show neuron growth on unpatterned positive controls of collagen-I and laminin, respectively. All cultures had grown for 4 weeks on plastic substrates. Scale is 50  $\mu\text{m}$  for all images.

### 5.3. Neuron-Oligodendrocyte Co-Culture

In the following section, two bio-inks were consecutively printed. First, one of the two neuron culture bio-inks were printed in one direction followed by one of the four oligodendrocyte culture bio-inks being printed in the perpendicular direction. In all tests, DRGs were initially seeded and allowed 21 days to mature. Following this maturation, OPCs were then seeded and allowed 7 days to differentiate. Unless otherwise stated, glass coverslips were employed.

#### 5.3.1. Cross-Printing

In order to create a patterned co-culture, two separate microcontact printed bio-inks need to be applied to the same substrate. To demonstrate the feasibility of this process, laminin mixed with anti-trkA (added for visualization purposes only) was printed in one direction followed by the successive printing of anti-A2B5 in the perpendicular direction. The successful results are illustrated in Figure 5-13 below.

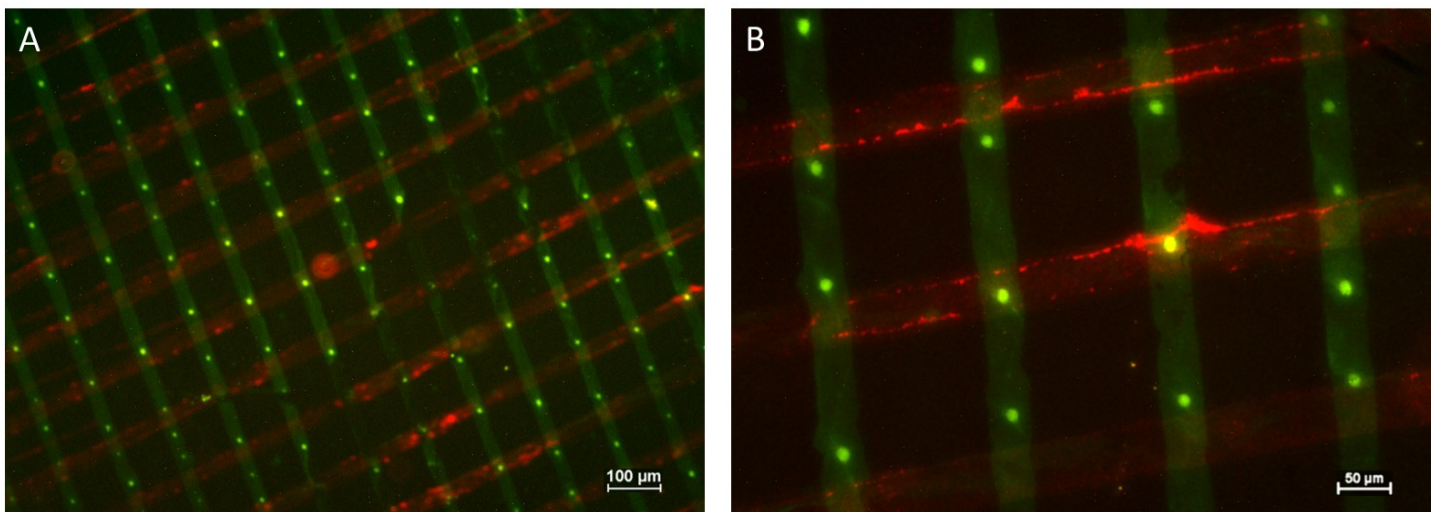


*Figure 5-13. Cross-printed pattern.*

Laminin and anti-trkA is stained in green (vertical) and anti-A2B5 is stained in red (horizontal). Scale is 100 μm for image (A) and 50 μm for image (B).

### 5.3.2. Pattern Maintenance

As explained earlier, a patterned neuron-oligodendrocyte co-culture would require initial DRG seeding followed by up to three weeks of neuron maturation before OPCs are to be added. As such, it is important that the microcontact printed bio-inks designed for OPC attachment are able to withstand cell culture conditions for up to three weeks without significant pattern degradation. As such, all four bio-inks were tested. They were printed onto glass substrates and kept in oligodendrocyte cell culture conditions, with media changes every two days, for a total of 23 days. Following this, OPCs were seeded and allowed to differentiate for 5 days. As seen in Figure 5-14 below, the printed pattern did not seem to be adversely affected by the extended time in culture conditions. That is, for all bio-inks, the OPCs still showed clear pattern adherence and comparable differentiation capabilities, at 89-90%. (Differentiation data shown in Appendix C.) It should be noted that this experiment was carried out as a single independent trial, performed in triplicate.

Furthermore, patterned co-culture experiments were tried in which, before the three week mark, the DRGs detached. However, OPCs were still added to that co-culture at the three week mark and allowed 7 days for differentiation, in co-culture conditions. In this case, strong pattern maintenance could still be seen, predominantly in the direction of the patterned oligodendrocyte antibody-based bio-ink. This was especially seen to be the case for the O4 antibody bio-inks, as see in Figure 5-15 below. As such, these findings offer further support to the idea that the patterned oligodendrocyte bio-inks can be successfully maintained in co-culture conditions over the required time period.

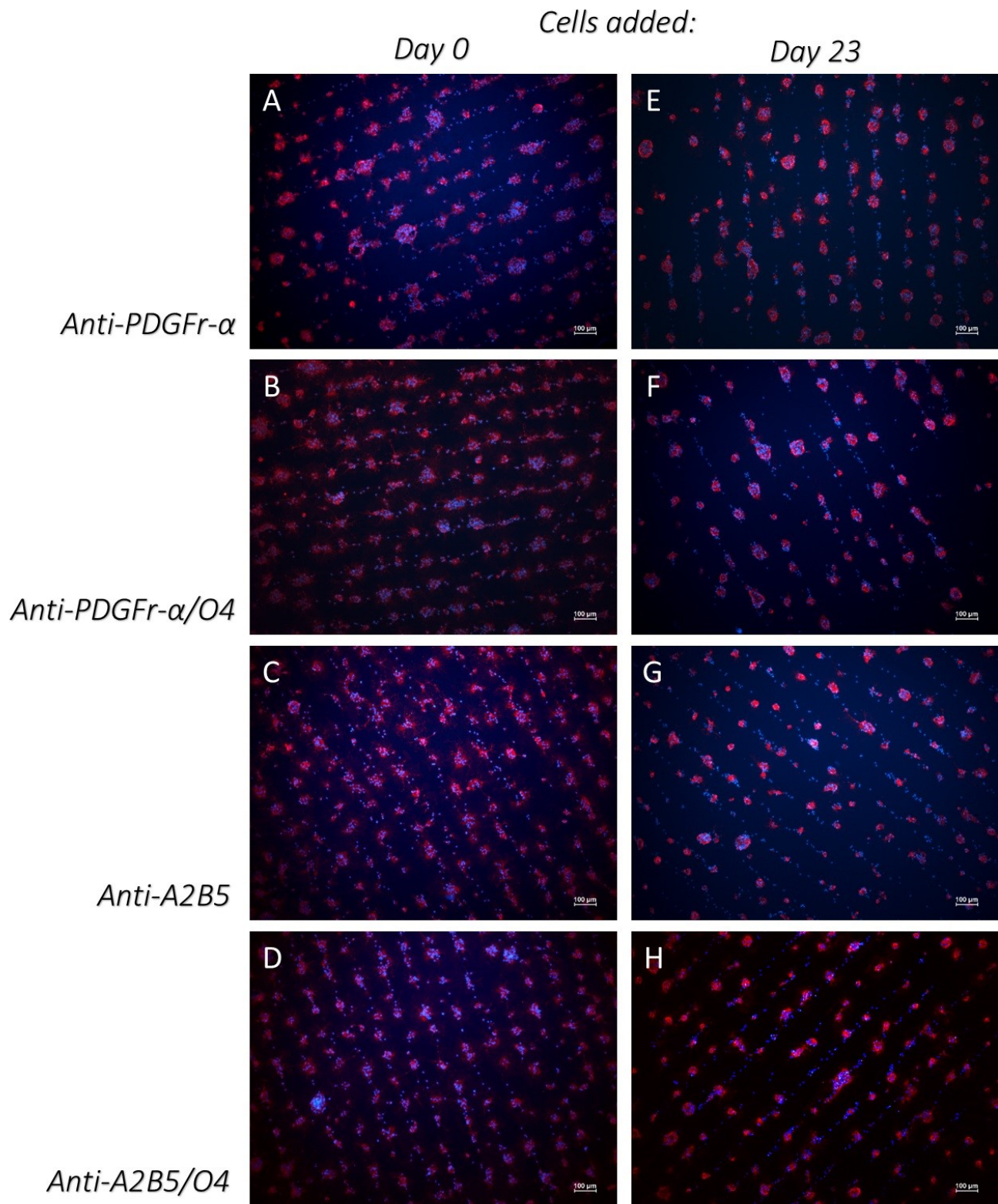


*Figure 5-14. Oligodendrocyte adherence to patterns printed 0 days and 23 days before cell seeding.*

For all images, the following stains were used: blue = Hoechst and red = anti-MBP. The rows show the different patterned bio-inks, and from left to right, the columns show patterns printed at 0 days and 23 days prior to cell seeding. Scale is 100  $\mu$ m for all images.

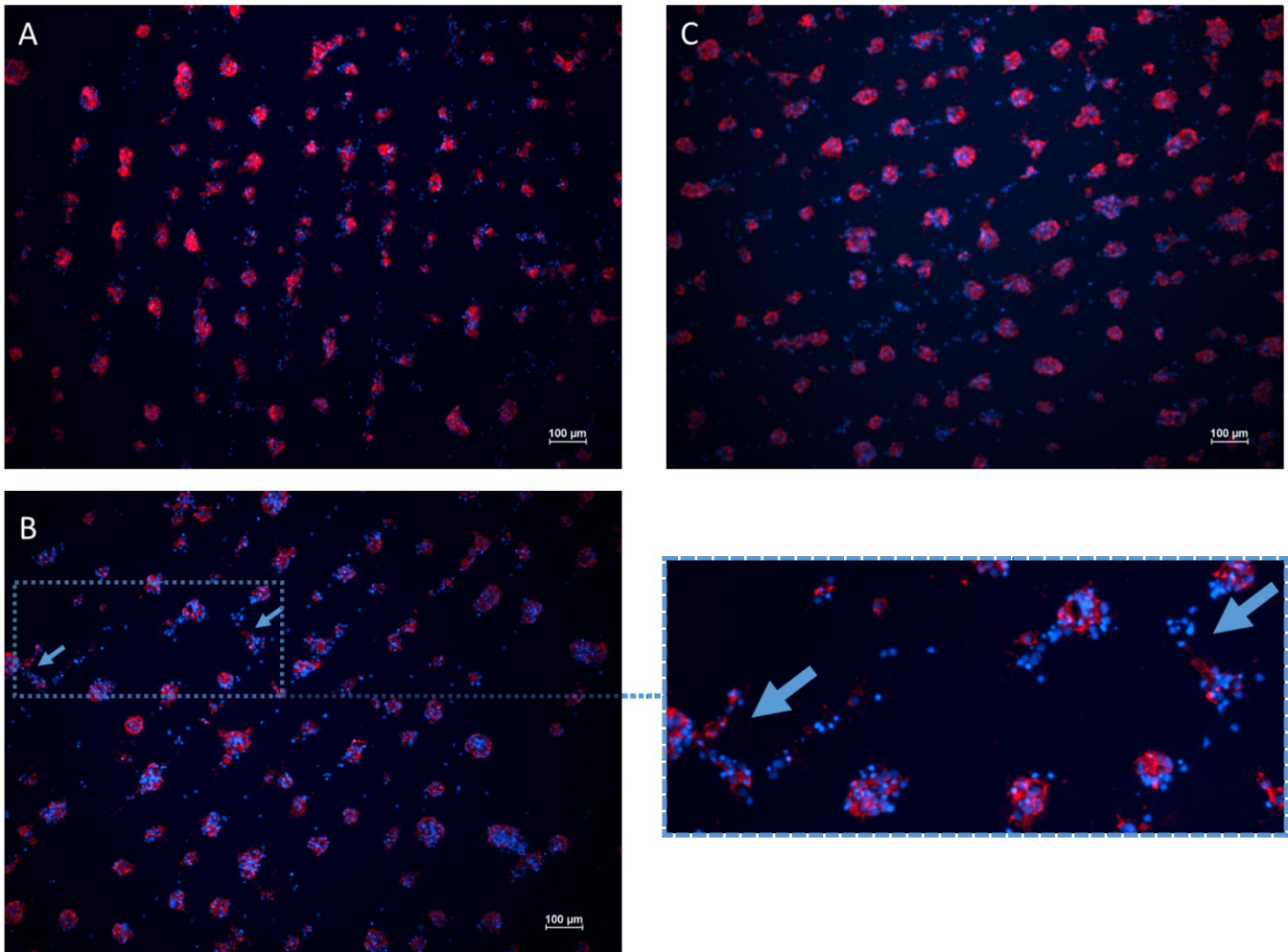


*Figure 5-15. Oligodendrocyte adherence to antibodies on co-culture substrates, patterned 21 days before cell seeding.*

For all images, the following stains were used: blue = Hoechst and red = anti-MBP. Images (A) and (B) show oligodendrocyte attachment to the anti-PDGFr- $\alpha$ /O4 pattern. The arrows on image (B) show a small amount of oligodendrocyte attachment to the cross-patterned collagen-I. Image (C) shows the oligodendrocyte attachment to anti-A2B5/O4 pattern. Scale is 100  $\mu$ m for all images.

### 5.3.3. Myelination

Due to the problems of neuron detachment, the feasibility of a patterned co-culture capable of myelination could not be tested. However, two observations could be used from the co-culture positive controls on glass substrates and all co-culture samples on plastic substrates. Firstly, the chosen media (N1), length of time for neuron maturation (21 days), and the length of time for OPC differentiation and myelination (7 days) was shown to successfully result in myelination. Moreover, from the tests on plastic substrates (subject to strong neuron attachment without any pattern compliance), it can be reasoned that the presence of patterned bio-inks did not prevent myelination from occurring, as myelination was present in samples testing all six bio-inks. Figure 5-16 below illustrates the presence of myelination in these cases.

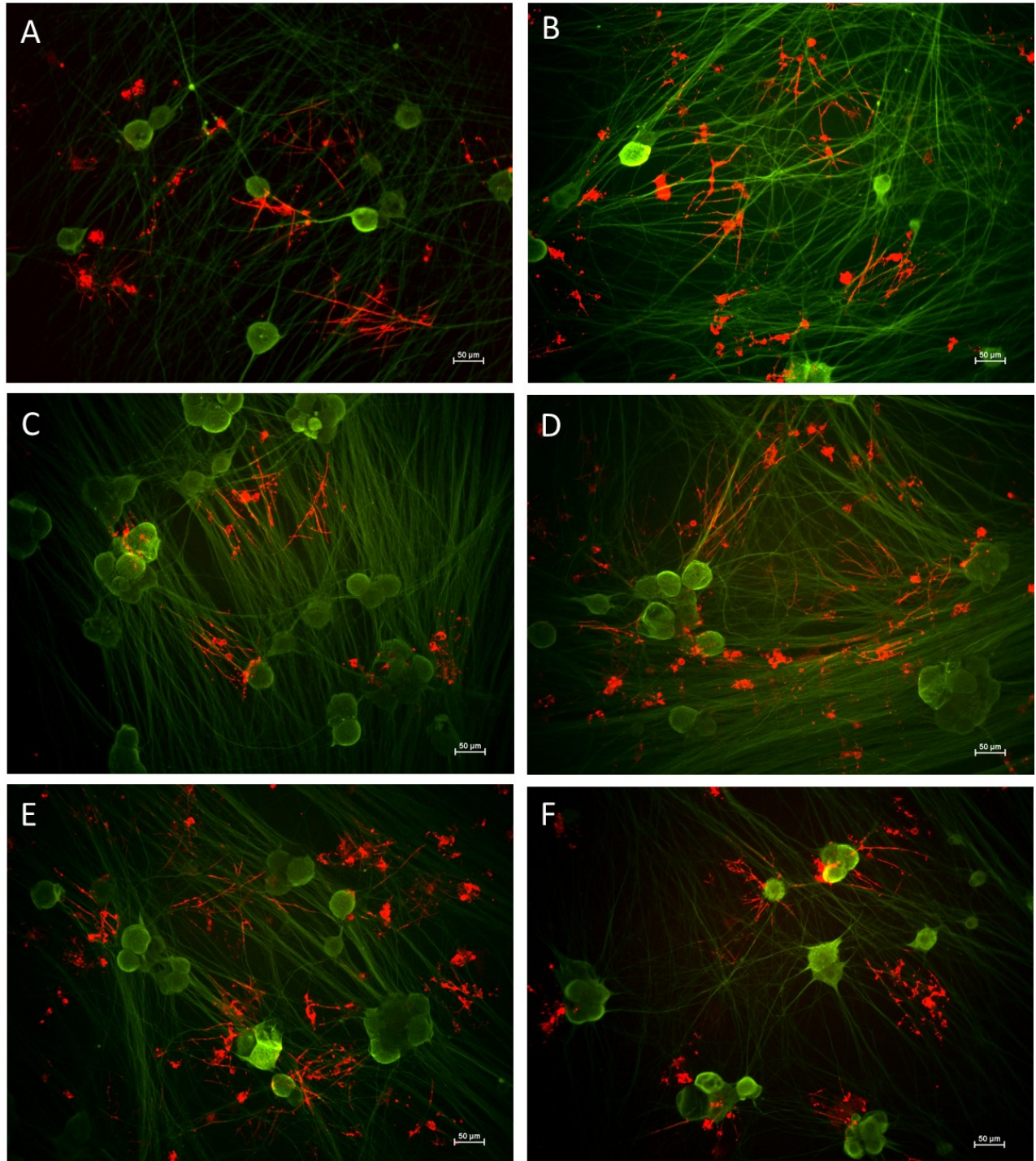


Figure 5-16. Successful myelination of mature axons by oligodendrocytes.

For all images, the following stains were used: green = anti-N52 and red = anti-MBP. Myelination is shown as thin red (MBP+) lines overlapping the green (N52+) neurite extensions. Respectively, images (A) and (B) show myelination of laminin positive controls on glass and plastic substrates. The remaining images show myelination on plastic substrates co-patterned with laminin and anti-PDGFr- $\alpha$  (C), anti-PDGFr- $\alpha$ /O4 (D), anti-A2B5 (E), or anti-A2B5/O4 (F). Scale is 50  $\mu$ m for all images.

## Chapter 6. Discussion

### 6.1. Oligodendrocyte Culture

In this study, all bio-inks tested with oligodendrocyte cultures provided very encouraging results. In terms of permitting cell differentiation and maintaining cell viability, no significant differences could be seen between the four investigated bio-inks. Coupled with average differentiation and survival results of approximately 90%, any of the four bio-inks tested appear to be suitable choices for achieving patterned oligodendrocyte growth. Although the quantitative measures of successful development showed no obvious differences between the bio-inks, qualitative measures did in fact offer reasonable means of differentiation between the four patterned substrates.

By and large, the OPCs were shown to attach specifically to the microcontact printed patterns such that the patterned designs were clearly visible. Moreover, the cells continued to adhere to these microcontact printed patterns over five days of differentiation. This successful oligodendrocyte attachment was found using both classes of bio-ink, those containing anti-PDGFr- $\alpha$  and those containing anti-A2B5. This was hypothesized to be the case because although markers for these two antibodies are more commonly used to identify progenitor cells, their selectivity is not necessarily limited to this phase of the oligodendrocyte lineage [100]. In terms of morphology in rodents, oligodendrocyte progenitor cells are characterized by their bipolarity whereas in the latter stages of differentiation, cells develop multiple processes, characteristic of the pre- to mature oligodendrocyte phases (see Figure 1-2 and Figure 4-1) [3]. Experimentally, PDGFr- $\alpha$  and A2B5 antibodies have been found to bind to cells in both the

bipolar and multi-process phases of development [3, 100]. This suggests that although these markers have the most significant presence in the first stages of development, a sizeable, albeit downregulated, presence can still be expected in later stages. Thus, this can explain how it is possible to maintain the attachment of mature oligodendrocytes to bio-inks designed to bind to markers of progenitor cells.

Generally speaking, the pattern adherence of cells on bio-inks containing anti-A2B5 was noticeably stronger than on bio-inks containing anti-PDGFr- $\alpha$ . Moreover, it was observed that the presence of anti-O4 increased the pattern adherence when added to the anti-PDGFr- $\alpha$  bio-ink, whereas it had no discernible effect when added to the anti-A2B5 bio-ink. Many factors may contribute to these results, including the initial levels of expression of each antibody receptor as well as the different affinity levels of each antibody. However, one possible explanation may also be found by looking at markers for the stages of oligodendrocyte maturation. It is suggested that the PDGF- $\alpha$  receptors “disappear” at the pre-oligodendrocyte stage, the second stage of development characterized by the newfound presence of O4 markers [3]. In contrast, the “loss of expression” of the A2B5 antigen is considered to occur at the immature oligodendrocyte stage, the third stage of development [1, 3]. This suggests that the downregulation of PDGFr- $\alpha$  begins much sooner than that of A2B5 markers. As such, it seems reasonable to expect differentiating cells attaching to the anti-A2B5 bio-ink have more time to establish secure attachment points than those attaching to the anti-PDGFr- $\alpha$  bio-ink. This may explain why more cells are able to maintain adherence to the anti-A2B5 bio-inks over the anti-PDGFr- $\alpha$  bio-inks. Similarly, it may explain why the effect of anti-O4 is apparent only in anti-PDGFr- $\alpha$  bio-inks. As the A2B5 marker persists well past the appearance of O4 markers, the

additional potential binding points provided by anti-O4 may be superfluous in this case. However, as the respective appearance and disappearance of the O4 markers and PDGF- $\alpha$  receptors begin at roughly the same stage, the utility of the potential binding points provided by anti-O4 is far more conceivable. Moreover, it may be possible that differentiating cells may have found significantly decreased PDGF- $\alpha$  receptors before the appearance of O4 markers and thus, may not have been able to create any firm attachment. This may account for the gaps in coverage characteristic of the anti-PDGFr- $\alpha$  bio-inks.

These results suggest that anti-A2B5 bio-inks may be preferable to those containing anti-PDGFr- $\alpha$ . However, the A2B5 marker is expressed by glial cells and by neurons, including embryonic dorsal root ganglia [3, 113]. Moreover, a preliminary co-culture test showed a very small number of DRGs weakly cross-attaching to anti-A2B5 patterned areas. This attachment was considered weak as it did not promote neurite outgrowth and was quickly followed by high levels of neuron detachment. Taken together, all this evidence suggests that for patterned neuron- oligodendrocyte co-cultures, anti-PDGFr- $\alpha$ /O4 may be the preferred oligodendrocyte bio-ink.

Additionally, it should be noted that OPC density at initial seeding plays a large role in subsequent pattern adherence. If too low, the pattern adherence may not be clearly visible, and if too high, the possibility of pattern overgrowth exists. In this study, approximately  $0.75 \times 10^5$  cells were seeded into each well, and this seemed a sufficient concentration to prevent the issues associated with both extremes. Moreover, this concentration seems to provide a cell density suitable for differentiation on the patterned substrates. Differentiation has been suggested to result from intercellular interactions, with OPCs required to reach a “critical

density” before the onset of differentiation can occur [26]. For patterned substrates, the restrictive nature of the printed pattern confines cells to a much smaller surface area than with positive controls (< 0.5). As a result, the necessary critical density and OPC interaction is more easily met on patterned substrates. This may explain why the percentage of fully differentiated OPCs on the positive control was found to be significantly lower than on the patterned bio-inks. Instead of indicating a difference between poly-L-ornithine and the four bio-inks, it is likely to simply be a consequence of patterned growth and cell density. As the patterned substrates have a higher number of cells per unit of surface area than the positive control, it follows that they would have higher levels of differentiation. However, it should be noted that Rosenberg *et al.* [26] found the required “critical density” of OPCs to be approximately 500-600, and in this study, that number was met or exceeded in all cases, patterned bio-inks and positive controls. More specifically, the cell density on the positive controls was estimated to be closer to 500-cells/mm<sup>2</sup> across the entire substrate whereas cell densities on the patterned bio-inks were estimated to be closer to 1000 cells/mm<sup>2</sup>, although only on the patterned areas.

## 6.2. Neuron Culture

Using microcontact printing to maintain long-term cell cultures, specifically for primary neurons, can be considered quite a challenge [5, 23]. In fact, many studies investigating patterned neuron growth maintain cell cultures for less than one week, with a majority observing cell growth for only 2-4 days [7, 95-97, 104, 109]. As a result, it can be difficult to determine the most efficient patterning substrate. Through this study, laminin was shown to provide reasonably encouraging results, maintaining strong pattern adherence for up to two weeks and preventing catastrophic cell detachment for over three weeks. It must be noted that

after two weeks, although some areas of neuron growth could still be seen to match the original pattern design, regions of pattern overgrowth and cell detachment were observed. These factors suggest this current iteration of a 10x100  $\mu\text{m}$  laminin pattern alone may not be enough for long-term, controlled neuron growth.

One possible reason for the lack of pattern maintenance may be the limited cell-to-cell interactions. When observing the positive control on laminin (e.g. Figure 5-11), the normal growth patterns of the DRGs seem to be to form complex networks, which were easily maintained for up to 4 weeks. Similarly, on the microcontact printed samples, areas of pattern overgrowth (e.g. Figure 6-2) were found to be quite stable points of attachment, not at all prone to detachment. As such, a microcontact printed pattern with greater connectivity may help stabilize the neuron culture. In the literature, Hardelauf *et al.* [5] and Vogt *et al.* [9] both presented micropatterned networks for neuronal growth, as seen in Figure 6-1, which offered stability for at least three weeks. Hardelauf *et al.* were able to achieve high levels of pattern compliance for cultures exceeding one month; however, it should also be noted that they did not use laminin, but printed poly-lysine on a PLL-g-PEG covered substrate [5]. Vogt *et al.*, however, did use laminin as a printing bio-ink and found three weeks of stable network growth, without pattern overgrowth [9]. Similarly, both studies had wide ( $>10 \mu\text{m}$ ) nodes within their microcontact printed patterns; these thick nodes were designed to provide strong attachment points for neuronal cell bodies and the thin portions ( $< 10 \mu\text{m}$ ) of the patterns were meant to direct neurite outgrowth, specifically axon extension. As such, perhaps incorporating these two design factors into the patterns used in this study may improve long-term neuron culture maintenance.

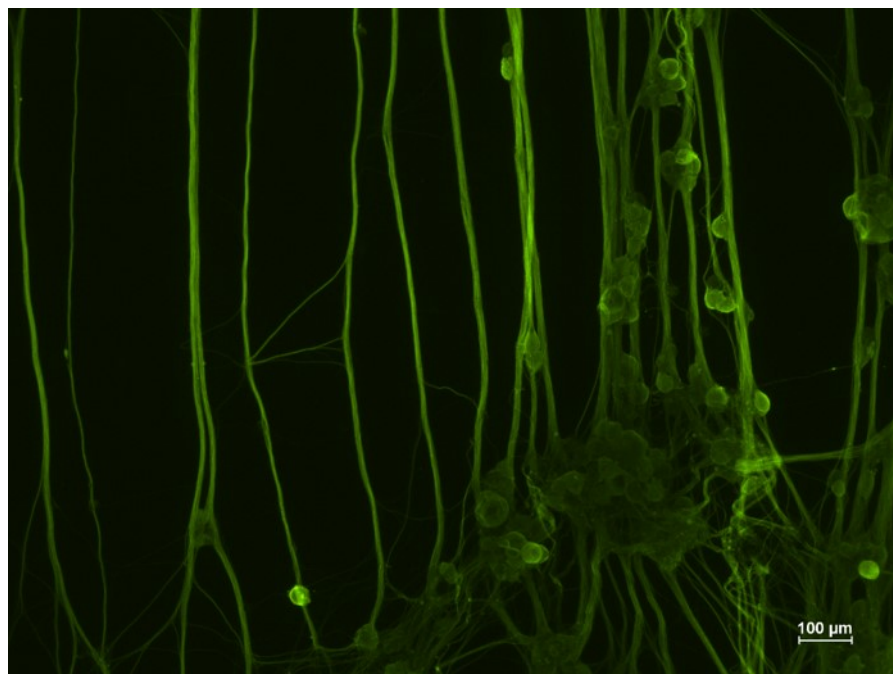


Figure 6-2. Overgrowth of neuron attachment on patterned laminin at day 28.

Neuron overgrowth is seen on the microcontact printed laminin, at the bottom right of the image. A neurofilament stain was used, green = anti-N52. Scale is 100  $\mu\text{m}$ .

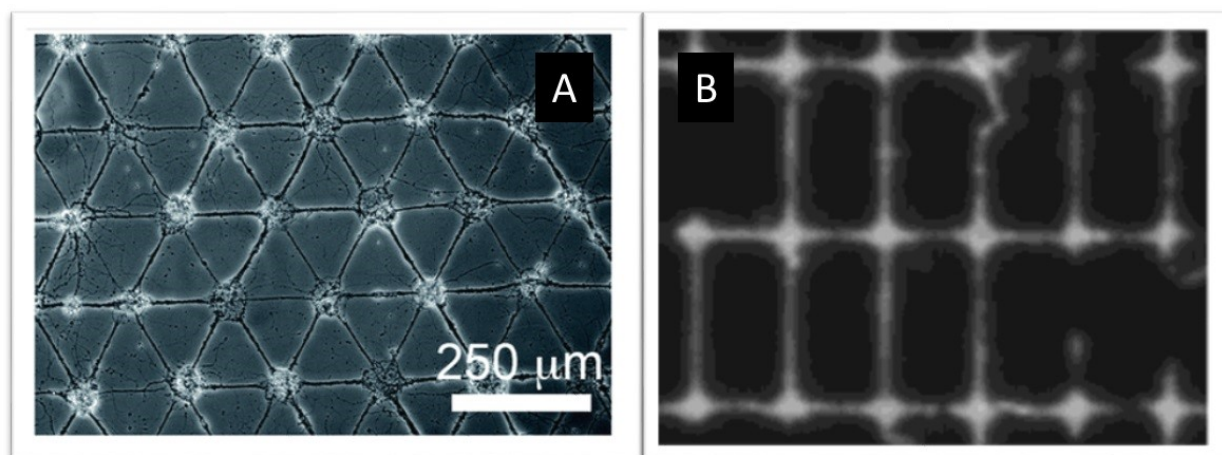


Figure 6-1. Designs for networked neuronal growth.

Image (A) shows the neuronal growth on the printed pattern suggested by Hardelauf *et al.* [5] and image (B) shows the printed pattern of laminin suggested by Vogt *et al.* [9]. Image (A) is adapted with permission from [5], copyright © 2014, Royal Society of Chemistry. Image (B) is adapted with permission from [9], copyright © 2003, John Wiley and Sons (American Institute of Chemical Engineers).

In this study, the laminin bio-ink has shown itself to offer strong results for at least two weeks, as seen in Figure 5-10. Moreover, a number of studies on neuronal growth suggest the benefits of using laminin [93, 96, 97, 109-111]. Being a prominent extra-cellular matrix protein, laminin is suggested to play a “key role” [93] in nerve development and is known to act as a signalling cue guiding axon growth, similar to that encountered *in vivo* [97, 111]. For these reasons, it seems that the laminin component is worth maintaining. However, some studies have suggested a mixture of poly-lysine with extra-cellular matrix proteins can provide strong substrates for neuronal culture [5, 91, 109, 111]. The addition of poly-lysine is suggested to not only support directed neuron growth itself, but also act as a stable anchor for extra-cellular matrix proteins, such as laminin [5, 111]. As such, it may be useful in this study to further examine the utility of a poly-lysine/laminin bio-ink.

It should also be noted that initial cell density may be a key factor in a successful patterned neuron culture. The initial seeding density used in this study, approximately  $2.25 \times 10^4$  cells per well, may have been slightly too high. In order to achieve strong initial pattern compliance, a high initial cell density is favoured. However, as the patterned areas of the substrate offer limited room for growth, the high cell number may encounter a lack of attachment points and thus, result in cell detachment. Moreover, the high initial density may contribute to instances of pattern overgrowth. Conversely, when a much lower initial density was attempted, it resulted in very poor initial pattern compliance and reduced cell interaction, a configuration very prone to cell detachment within the first week. Thus, a marginally lower initial seeding density, perhaps  $1 \times 10^4$ , may improve the long-term pattern maintenance of neuron cultures.

Furthermore, addressing the areas of pattern overgrowth in the neuron cultures may also include examining the blocking agent employed, PLL-g-PEG. The ubiquity of PLL-g-PEG as a blocking agent in the literature [5, 102, 114] and its largely successful results in this study, especially with oligodendrocyte cultures, suggest it can be a suitable compound for passivation here. However, it may be that in the areas of overgrowth, the substrate blocking was possibly incomplete or non-uniform, either stemming from the initial passivation or resulting over time. As such, future studies may benefit from an investigation into the uniformity of the blocking layer between samples and over longer terms (>2 weeks).

### 6.3. Neuron-Oligodendrocyte Co-Culture

Due to the issues involved with maintaining long-term (>2 week) patterned DRG cultures, a co-culture with patterned growth was not able to be tested. However, as discussed previously, the positive controls as well as the uncontrolled growth on the patterned plastic substrates showed successful myelination. As such, the co-culture conditions and printed antibodies/proteins used in this experiment have been shown to permit myelination.

As discussed previously, a new design for patterned DRG growth, taking into consideration enhanced connectivity and/or nodes for cell body attachment, may aid in long term growth. Such designs, illustrated in Figure 6-3, can be incorporated into an organized platform for controlled myelination. As can be seen with these designs, distinct points of myelination are still possible. Moreover, the addition of the attachment nodes in (A) and (B) and the central node for added connectivity in (B) may assist in stronger neuron attachment. The central node in (B) can offer a large surface area for cell bodies to form stable attachment points as well as

interact, similar to what is seen in areas of pattern overgrowth. Furthermore, the multiple attachment nodes in (A) and (B) can not only provide slightly larger surface areas, attractive for cell body attachment, but also “intermediate targets” to encourage axon extension over “smaller more manageable steps”, behaviour typical in normal axon development [111].

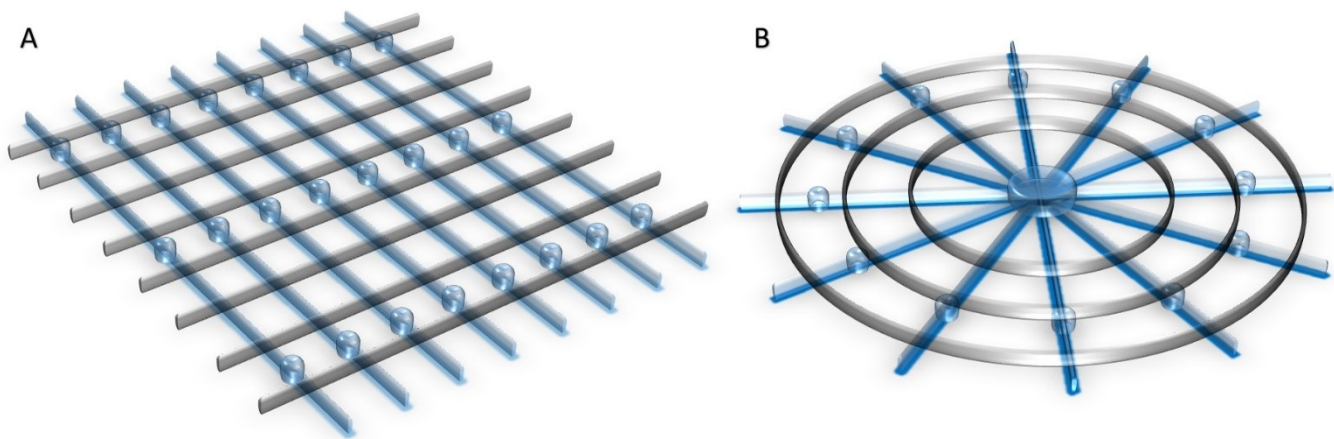


Figure 6-3. Alternate designs for controlled myelination platforms.

Patterns for OPC differentiation are shown in black, and patterns for DRG development are shown in blue. Circular blue areas denote the presences of attachment nodes.

As a final note, it should be recalled that Liazoghli *et al.* [23] were able to successfully microcontact print 10  $\mu\text{m}$  thick lines of Matrigel on which they were able to maintain long term co-cultures. In their neuron-oligodendrocyte co-culture, DRGs were grown on the Matrigel patterns for 7 days before OPCs were added and allowed to differentiate for 7 days. (These OPCs were expected to attach on the same Matrigel patterns, growing on the neurons themselves.) Due to the nature of oligodendrocyte myelination and the set-up of this co-culture, Liazoghli *et al.* could not confirm myelination, but scanning electron microscopy images

were suggested to show the oligodendrocyte plasma membrane wrapped around neurite extensions [23]. In their neuron-Schwann cell co-cultures, DRGs were plated and the endogenous Schwann cell population (PNS glial cells) was kept alive (i.e. no anti-mitotic agents were added). These PNS co-cultures could be maintained for very long terms (>6 weeks) and successfully showed myelination [23]. The presence of glial cells offer axonal support, playing a role in their functional integrity [11]. As such, neuron-glial co-cultures tend to be more stable than neuron cultures alone. Taking all this into account, an additional option for this study may be to utilize slightly more mature DRGs as they would require a shorter maturation time, perhaps two weeks instead of three. As the patterned DRG culture can be maintained successfully for two weeks, adding the OPCs at this time may offer the additional support and stabilization necessary for longer term culture. That being said, timing is very important in myelination co-cultures. Axon maturation is important for complete myelination as axon diameter is an important factor regulating myelination [17]. At the same time, oligodendrocytes only have a limited time period in which they engage in myelination [17]. Thus, it is important not to add OPCs to immature DRGs or else myelination is unlikely to occur.

## Chapter 7. Conclusions and Future Work

In this study, the ability of select bio-inks to permit the patterned growth and differentiation of OPCs into oligodendrocytes was examined. To that end, the four bio-inks tested offered encouraging results as they were each found appropriate for the differentiation of OPCs into oligodendrocytes. Qualitatively, the oligodendrocyte cells showed strong pattern adherence after five days of differentiation on each of the four bio-inks tested, with an estimated pattern compliance of >80% in all cases. In terms of ranking, the anti-A2B5 and anti-A2B5/O4 bio-inks had the strongest pattern compliance with each showing nearly complete coverage, closely followed by anti-PDGFr- $\alpha$ /O4 which showed small gaps in pattern adherence, and finally tailed by anti-PDGFr- $\alpha$  which showed small to large gaps in pattern coverage. Moreover, these microcontact printed patterns were shown able to withstand culture conditions for over 21 days before cell seeding without exhibiting any qualitative differences in cell adherence or pattern compliance capabilities. Quantitatively, the four patterned bio-inks did not appear to present any negative effects to normal cell development, maintaining strong levels of cell viability and OPC differentiation. In fact, the restrictive nature of the patterned substrates may have had a positive effect on differentiation. The small surface area covered by the printed bio-ink resulted in a higher cell density on that pattern, and this has been found necessary for oligodendrocyte differentiation. To further understand the role of the patterned bio-inks, future investigations may also focus on examining the effect of the bio-inks on cell signaling and/or gene expression.

Using these findings on patterned oligodendrocyte growth, the feasibility of a platform for controlled myelination was investigated. This initial study produced a number of promising

preliminary results which can help shape any future investigations. The first major finding was the successful culturing and neurite direction of DRGs on microcontact printed laminin patterns for approximately 2 weeks. Such an ability to maintain patterned DRG attachment and maturation over long terms (2-3 weeks) is a necessary pre-requisite for any controlled myelination platform. However, as maintaining strong pattern compliance post two weeks was not successful, future investigations may focus on increasing the long-term efficacy of a pure culture of patterned DRGs by adding an anchoring polyamine, such as poly-lysine, to the bio-ink or by incorporating large nodes within the printed patterns to offer sufficient attachment points for the neuron cell bodies. In a similar vein, future patterned co-culture investigations may concentrate on culturing DRGs for a shorter period of time before adding OPCs, as the addition of glial cells may act to stabilize the culture and increase its long-term viability. Furthermore, this investigation confirmed a number of points necessary for a successful controlled myelination platform. These include the feasibility of cross-printing bio-inks for controlled DRG and OPC attachment and the confirmation of cell conditions and development time frames necessary for myelination. Building upon these findings, future work in this area can focus on developing a prototype platform capable of controlled myelination.

## References

- [1] A. Barateiro and A. Fernandes, "Temporal oligodendrocyte lineage progression: in vitro models of proliferation, differentiation and myelination," *Biochim Biophys Acta*, vol. 1843, pp. 1917-29, 2014.
- [2] K. A. Nave and H. B. Werner, "Myelination of the nervous system: mechanisms and functions," *Annu Rev Cell Dev Biol*, vol. 30, pp. 503-33, 2014.
- [3] N. Baumann and D. Pham-Dinh, "Biology of oligodendrocyte and myelin in the mammalian central nervous system," *Physiol Rev*, vol. 81, pp. 871-927, 2001.
- [4] J. Park, H. Koito, J. Li, and A. Han, "Multi-compartment neuron-glia co-culture platform for localized CNS axon-glia interaction study," *Lab Chip*, vol. 12, pp. 3296-304, 2012.
- [5] H. Hardelauf, S. Waide, J. Sisnaiske, P. Jacob, V. Hausherr, N. Schobel, *et al.*, "Micropatterning neuronal networks," *Analyst*, vol. 139, pp. 3256-64, 2014.
- [6] B. Sobottka, U. Ziegler, A. Kaech, B. Becher, and N. Goebels, "CNS live imaging reveals a new mechanism of myelination: the liquid croissant model," *Glia*, vol. 59, pp. 1841-9, 2011.
- [7] W. Belkaid, P. Thostrup, P. T. Yam, C. A. Juzwik, E. S. Ruthazer, A. S. Dhaunchak, *et al.*, "Cellular response to micropatterned growth promoting and inhibitory substrates," *BMC Biotechnol*, vol. 13, p. 86, 2013.
- [8] F. Mei, S. P. Fancy, Y. A. Shen, J. Niu, C. Zhao, B. Presley, *et al.*, "Micropillar arrays as a high-throughput screening platform for therapeutics in multiple sclerosis," *Nat Med*, vol. 20, pp. 954-60, 2014.
- [9] A. K. Vogt, L. Lauer, W. Knoll, and A. Offenhausser, "Micropatterned substrates for the growth of functional neuronal networks of defined geometry," *Biotechnol Prog*, vol. 19, pp. 1562-8, 2003.
- [10] I. Elloumi Hannachi, K. Itoga, Y. Kumashiro, J. Kobayashi, M. Yamato, and T. Okano, "Fabrication of transferable micropatterned-co-cultured cell sheets with microcontact printing," *Biomaterials*, vol. 30, pp. 5427-32, 2009.
- [11] K. A. Nave and B. D. Trapp, "Axon-glia signaling and the glial support of axon function," *Annu Rev Neurosci*, vol. 31, pp. 535-61, 2008.
- [12] Kathryn K. Bercury and Wendy B. Macklin, "Dynamics and Mechanisms of CNS Myelination," *Developmental Cell*, vol. 32, pp. 447-458, 2015.
- [13] M. Simons and K. A. Nave, "Oligodendrocytes: Myelination and Axonal Support," *Cold Spring Harb Perspect Biol*, 2015.
- [14] N. Takahashi and T. Sakurai, "Roles of glial cells in schizophrenia: possible targets for therapeutic approaches," *Neurobiol Dis*, vol. 53, pp. 49-60, 2013.
- [15] N. Snaidero and M. Simons, "Myelination at a glance," *J Cell Sci*, vol. 127, pp. 2999-3004, 2014.
- [16] A. R. Scholze and B. A. Barres, "A Nogo signal coordinates the perfect match between myelin and axons," *Proc Natl Acad Sci U S A*, vol. 109, pp. 1003-4, 2012.
- [17] M. Bradl and H. Lassmann, "Oligodendrocytes: biology and pathology," *Acta Neuropathol*, vol. 119, pp. 37-53, 2010.

- [18] J. W. Rumsey, C. McAleer, M. Das, A. Bhalkikar, K. Wilson, M. Stancescu, *et al.*, "Myelination and node of Ranvier formation on sensory neurons in a defined in vitro system," *In Vitro Cell Dev Biol Anim*, vol. 49, pp. 608-18, 2013.
- [19] T. Ishibashi, K. A. Dakin, B. Stevens, P. R. Lee, S. V. Kozlov, C. L. Stewart, *et al.*, "Astrocytes promote myelination in response to electrical impulses," *Neuron*, vol. 49, pp. 823-32, 2006.
- [20] A. Alizadeh, S. M. Dyck, and S. Karimi-Abdolrezaee, "Myelin Damage and Repair in Pathologic CNS: Challenges and Prospects," *Frontiers in Molecular Neuroscience*, vol. 8, 2015.
- [21] M. Mekhail, G. Almazan, and M. Tabrizian, "Oligodendrocyte-protection and remyelination post-spinal cord injuries: a review," *Prog Neurobiol*, vol. 96, pp. 322-39, 2012.
- [22] B. Garbay, A. M. Heape, F. Sargueil, and C. Cassagne, "Myelin synthesis in the peripheral nervous system," *Prog Neurobiol*, vol. 61, pp. 267-304, 2000.
- [23] D. Liazoghli, A. D. Roth, P. Thostrup, and D. R. Colman, "Substrate Micropatterning as a New in Vitro Cell Culture System to Study Myelination," *ACS Chem Neurosci*, vol. 3, pp. 90-95, 2012.
- [24] J. Park, H. Koito, J. Li, and A. Han, "Microfluidic compartmentalized co-culture platform for CNS axon myelination research," *Biomed Microdevices*, vol. 11, pp. 1145-53, 2009.
- [25] R. H. Miller, "Oligodendrocyte origins," *Trends Neurosci*, vol. 19, pp. 92-6, 1996.
- [26] S. S. Rosenberg, E. E. Kelland, E. Tokar, A. R. De la Torre, and J. R. Chan, "The geometric and spatial constraints of the microenvironment induce oligodendrocyte differentiation," *Proc Natl Acad Sci U S A*, vol. 105, pp. 14662-7, 2008.
- [27] J. R. Chan, T. A. Watkins, J. M. Cosgaya, C. Zhang, L. Chen, L. F. Reichardt, *et al.*, "NGF controls axonal receptivity to myelination by Schwann cells or oligodendrocytes," *Neuron*, vol. 43, pp. 183-91, 2004.
- [28] S. Lee, S. Y. C. Chong, S. J. Tuck, J. M. Corey, and J. R. Chan, "A rapid and reproducible assay for modeling myelination by oligodendrocytes using engineered nanofibers," *Nature Protocols*, vol. 8, pp. 771-782, 2013.
- [29] N. Snaidero, W. Mobius, T. Czopka, L. H. Hekking, C. Mathisen, D. Verkleij, *et al.*, "Myelin membrane wrapping of CNS axons by PI(3,4,5)P3-dependent polarized growth at the inner tongue," *Cell*, vol. 156, pp. 277-90, 2014.
- [30] H. Higashimori and Y. Yang, "Imaging analysis of neuron to glia interaction in microfluidic culture platform (MCP)-based neuronal axon and glia co-culture system," *J Vis Exp*, 2012.
- [31] M. A. Preston and W. B. Macklin, "Zebrafish as a model to investigate CNS myelination," *Glia*, vol. 63, pp. 177-93, 2015.
- [32] Z. Wang, H. Colognato, and C. Ffrench-Constant, "Contrasting effects of mitogenic growth factors on myelination in neuron-oligodendrocyte co-cultures," *Glia*, vol. 55, pp. 537-45, 2007.
- [33] I. H. Yang, D. Gary, M. Malone, S. Dria, T. Houdayer, V. Belegu, *et al.*, "Axon myelination and electrical stimulation in a microfluidic, compartmentalized cell culture platform," *Neuromolecular Med*, vol. 14, pp. 112-8, 2012.

- [34] Z. Chen, Z. Ma, Y. Wang, Y. Li, H. Lu, S. Fu, *et al.*, "Oligodendrocyte-spinal cord explant co-culture: an in vitro model for the study of myelination," *Brain Res*, vol. 1309, pp. 9-18, 2010.
- [35] H. Davis, M. Gonzalez, N. Bhargava, M. Stancescu, J. J. Hickman, and S. Lambert, "Rat Cortical Oligodendrocyte-Embryonic Motoneuron Co-Culture: An Axon-Oligodendrocyte Interaction Model," *J Biomater Tissue Eng*, vol. 2, pp. 206-214, 2012.
- [36] A. Gardner, P. Jukkola, and C. Gu, "Myelination of rodent hippocampal neurons in culture," *Nat Protoc*, vol. 7, pp. 1774-82, 2012.
- [37] Y. Pang, B. Zheng, S. L. Kimberly, Z. Cai, P. G. Rhodes, and R. C. Lin, "Neuron-oligodendrocyte myelination co-culture derived from embryonic rat spinal cord and cerebral cortex," *Brain Behav*, vol. 2, pp. 53-67, 2012.
- [38] Z. Wang, J. Xia, Y. Yan, A. C. Tsai, Y. Li, T. Ma, *et al.*, "Facile functionalization and assembly of live cells with microcontact-printed polymeric biomaterials," *Acta Biomater*, vol. 11, pp. 80-7, 2015.
- [39] T. A. Watkins and A. R. Scholze, "Myelinating cocultures of purified oligodendrocyte lineage cells and retinal ganglion cells," *Cold Spring Harb Protoc*, vol. 2014, p. pdb top070839, 2014.
- [40] P. M. Wood and A. K. Williams, "Oligodendrocyte proliferation and CNS myelination in cultures containing dissociated embryonic neuroglia and dorsal root ganglion neurons," *Brain Res*, vol. 314, pp. 225-41, 1984.
- [41] D. Huh, Y. S. Torisawa, G. A. Hamilton, H. J. Kim, and D. E. Ingber, "Microengineered physiological biomimicry: organs-on-chips," *Lab Chip*, vol. 12, pp. 2156-64, 2012.
- [42] G. M. Whitesides, E. Ostuni, S. Takayama, X. Jiang, and D. E. Ingber, "Soft lithography in biology and biochemistry," *Annu Rev Biomed Eng*, vol. 3, pp. 335-73, 2001.
- [43] A. Azioune, M. Storch, M. Bornens, M. Thery, and M. Piel, "Simple and rapid process for single cell micro-patterning," *Lab Chip*, vol. 9, pp. 1640-2, 2009.
- [44] D. Qin, Y. Xia, and G. M. Whitesides, "Soft lithography for micro- and nanoscale patterning," *Nat Protoc*, vol. 5, pp. 491-502, 2010.
- [45] A. Perl, D. N. Reinhoudt, and J. Huskens, "Microcontact Printing: Limitations and Achievements," *Advanced Materials*, vol. 21, pp. 2257-2268, 2009.
- [46] S. Fodor, J. Read, M. Pirrung, L. Stryer, A. Lu, and D. Solas, "Light-directed, spatially addressable parallel chemical synthesis," *Science*, vol. 251, pp. 767-773, 1991.
- [47] T. Kaufmann and B. J. Ravoo, "Stamps, inks and substrates: polymers in microcontact printing," *Polymer Chemistry*, vol. 1, p. 371, 2010.
- [48] C. Wendeln and B. J. Ravoo, "Surface patterning by microcontact chemistry," *Langmuir*, vol. 28, pp. 5527-38, 2012.
- [49] J. A. Wigenius, S. Fransson, F. von Post, and O. Inganas, "Protein biochips patterned by microcontact printing or by adsorption-soft lithography in two modes," *Biointerphases*, vol. 3, pp. 75-82, 2008.
- [50] C. Thibault, C. Severac, A. F. Mingotaud, C. Vieu, and M. Mauzac, "Poly(dimethylsiloxane) contamination in microcontact printing and its influence on patterning oligonucleotides," *Langmuir*, vol. 23, pp. 10706-14, 2007.
- [51] R. S. Kane, S. Takayama, E. Ostuni, D. E. Ingber, and G. M. Whitesides, "Patterning proteins and cells using soft lithography," *Biomaterials*, vol. 20, pp. 2363-76, 1999.

- [52] A. Kumar and G. M. Whitesides, "Features of gold having micrometer to centimeter dimensions can be formed through a combination of stamping with an elastomeric stamp and an alkanethiol "ink" followed by chemical etching," *Applied Physics Letters*, vol. 63, pp. 2002-2004, 1993.
- [53] A. Bernard, E. Delamarche, H. Schmid, B. Michel, H. R. Bosshard, and H. Biebuyck, "Printing Patterns of Proteins," *Langmuir*, vol. 14, pp. 2225-2229, 1998.
- [54] S. G. Ricoult, A. S. Nezhad, M. Knapp-Mohammady, T. E. Kennedy, and D. Juncker, "Humidified microcontact printing of proteins: universal patterning of proteins on both low and high energy surfaces," *Langmuir*, vol. 30, pp. 12002-10, 2014.
- [55] N. Patel, R. Bhandari, K. M. Shakesheff, S. M. Cannizzaro, M. C. Davies, R. Langer, *et al.*, "Printing patterns of biospecifically-adsorbed protein," *J Biomater Sci Polym Ed*, vol. 11, pp. 319-31, 2000.
- [56] E. Delamarche, "Microcontact Printing of Proteins," in *Protein Science Encyclopedia*, ed: Wiley-VCH Verlag GmbH & Co. KGaA, 2008.
- [57] J. P. Renault, A. Bernard, D. Juncker, B. Michel, H. R. Bosshard, and E. Delamarche, "Fabricating microarrays of functional proteins using affinity contact printing," *Angew Chem Int Ed Engl*, vol. 41, pp. 2320-3, 2002.
- [58] M. Fritz and M. Bastmeyer, "Microcontact printing of substrate-bound protein patterns for cell and tissue culture," *Methods Mol Biol*, vol. 1018, pp. 247-59, 2013.
- [59] A. Bernard, J. P. Renault, B. Michel, H. R. Bosshard, and E. Delamarche, "Microcontact Printing of Proteins," *Advanced Materials*, vol. 12, pp. 1067-1070, 2000.
- [60] A. C. von Philipsborn, S. Lang, A. Bernard, J. Loeschinger, C. David, D. Lehnert, *et al.*, "Microcontact printing of axon guidance molecules for generation of graded patterns," *Nat Protoc*, vol. 1, pp. 1322-8, 2006.
- [61] C. D. Eichinger, T. W. Hsiao, and V. Hlady, "Multiprotein microcontact printing with micrometer resolution," *Langmuir*, vol. 28, pp. 2238-43, 2012.
- [62] A. D. Dias, D. M. Kingsley, and D. T. Corr, "Recent advances in bioprinting and applications for biosensing," *Biosensors (Basel)*, vol. 4, pp. 111-36, 2014.
- [63] E. D'Arcangelo and A. P. McGuigan, "Micropatterning strategies to engineer controlled cell and tissue architecture in vitro," *Biotechniques*, vol. 58, pp. 13-23, 2015.
- [64] L. K. Fiddes, H. K. Chan, B. Lau, E. Kumacheva, and A. R. Wheeler, "Durable, region-specific protein patterning in microfluidic channels," *Biomaterials*, vol. 31, pp. 315-20, 2010.
- [65] D. Kim and A. E. Herr, "Protein immobilization techniques for microfluidic assays," *Biomicrofluidics*, vol. 7, p. 41501, 2013.
- [66] K. Salaita, Y. Wang, and C. A. Mirkin, "Applications of dip-pen nanolithography," *Nat Nanotechnol*, vol. 2, pp. 145-55, 2007.
- [67] E. A. Roth, T. Xu, M. Das, C. Gregory, J. J. Hickman, and T. Boland, "Inkjet printing for high-throughput cell patterning," *Biomaterials*, vol. 25, pp. 3707-15, 2004.
- [68] A. Ruiz, M. Zychowicz, L. Ceriotti, D. Mehn, L. Sirghi, H. Rauscher, *et al.*, "Microcontact printing and microspotting as methods for direct protein patterning on plasma deposited polyethylene oxide: application to stem cell patterning," *Biomed Microdevices*, vol. 15, pp. 495-507, 2013.

- [69] S. Alom Ruiz and C. S. Chen, "Microcontact printing: A tool to pattern," *Soft Matter*, vol. 3, pp. 168-177, 2007.
- [70] J. Voskuhl, J. Brinkmann, and P. Jonkheijm, "Advances in contact printing technologies of carbohydrate, peptide and protein arrays," *Curr Opin Chem Biol*, vol. 18, pp. 1-7, 2014.
- [71] K. W. Binder, A. J. Allen, J. J. Yoo, and A. Atala, "Drop-on-Demand Inkjet Bioprinting: A Primer," *Gene Therapy and Regulation*, vol. 06, pp. 33-49, 2011.
- [72] B. Guillotin and F. Guillemot, "Cell patterning technologies for organotypic tissue fabrication," *Trends Biotechnol*, vol. 29, pp. 183-90, 2011.
- [73] C. Khatiwala, R. Law, B. Shepherd, S. Dorfman, and M. Csete, "3D Cell Bioprinting for Regenerative Medicine Research and Therapies," *Gene Therapy and Regulation*, vol. 07, p. 1230004, 2012.
- [74] A. Atmanli and I. J. Domian, "Generation of aligned functional myocardial tissue through microcontact printing," *J Vis Exp*, p. e50288, 2013.
- [75] M. Thery, V. Racine, A. Pepin, M. Piel, Y. Chen, J. B. Sibarita, *et al.*, "The extracellular matrix guides the orientation of the cell division axis," *Nat Cell Biol*, vol. 7, pp. 947-53, 2005.
- [76] S. Ilkhanizadeh, A. I. Teixeira, and O. Hermanson, "Inkjet printing of macromolecules on hydrogels to steer neural stem cell differentiation," *Biomaterials*, vol. 28, pp. 3936-43, Sep 2007.
- [77] S. G. Ricoult, G. Thompson-Steckel, J. P. Correia, T. E. Kennedy, and D. Juncker, "Tuning cell-surface affinity to direct cell specific responses to patterned proteins," *Biomaterials*, vol. 35, pp. 727-36, 2014.
- [78] K. Shen, J. Qi, and L. C. Kam, "Microcontact printing of proteins for cell biology," *J Vis Exp*, 2008.
- [79] T. W. Hsiao, V. P. Swarup, C. D. Eichinger, and V. Hlady, "Cell substrate patterning with glycosaminoglycans to study their biological roles in the central nervous system," *Methods Mol Biol*, vol. 1229, pp. 457-67, 2015.
- [80] J. Albers, K. Toma, and A. Offenhausser, "Engineering connectivity by multiscale micropatterning of individual populations of neurons," *Biotechnol J*, vol. 10, pp. 332-8, 2015.
- [81] G. Csucs, R. Michel, J. W. Lussi, M. Textor, and G. Danuser, "Microcontact printing of novel co-polymers in combination with proteins for cell-biological applications," *Biomaterials*, vol. 24, pp. 1713-1720, 2003.
- [82] S. Kidambi, L. Sheng, M. L. Yarmush, M. Toner, I. Lee, and C. Chan, "Patterned co-culture of primary hepatocytes and fibroblasts using polyelectrolyte multilayer templates," *Macromol Biosci*, vol. 7, pp. 344-53, 2007.
- [83] T. W. Hsiao, P. A. Tresco, and V. Hlady, "Astrocytes alignment and reactivity on collagen hydrogels patterned with ECM proteins," *Biomaterials*, vol. 39, pp. 124-30, 2015.
- [84] C. Yaka, P. Bjork, T. Schonberg, and A. Erlandsson, "A novel in vitro injury model based on microcontact printing demonstrates negative effects of hydrogen peroxide on axonal regeneration both in absence and presence of glia," *J Neurotrauma*, vol. 30, pp. 392-402, 2013.

- [85] M. Shi, D. Majumdar, Y. Gao, B. M. Brewer, C. R. Goodwin, J. A. McLean, *et al.*, "Glia co-culture with neurons in microfluidic platforms promotes the formation and stabilization of synaptic contacts," *Lab Chip*, vol. 13, pp. 3008-21, 2013.
- [86] R. B. Campenot, "Local control of neurite development by nerve growth factor," *Proc Natl Acad Sci U S A*, vol. 74, pp. 4516-9, 1977.
- [87] G. Almazan, D. E. Afar, and J. C. Bell, "Phosphorylation and disruption of intermediate filament proteins in oligodendrocyte precursor cultures treated with calyculin A," *J Neurosci Res*, vol. 36, pp. 163-72, 1993.
- [88] B. I. Giasson and W. E. Mushynski, "Aberrant stress-induced phosphorylation of perikaryal neurofilaments," *J Biol Chem*, vol. 271, pp. 30404-9, 1996.
- [89] S. Hossain, G. Fragoso, W. E. Mushynski, and G. Almazan, "Regulation of peripheral myelination by Src-like kinases," *Exp Neurol*, vol. 226, pp. 47-57, 2010.
- [90] A. Azione, N. Carpi, Q. Tseng, M. Thery, and M. Piel, "Protein micropatterns: A direct printing protocol using deep UVs," *Methods Cell Biol*, vol. 97, pp. 133-46, 2010.
- [91] R. Fricke, P. D. Zentis, L. T. Rajappa, B. Hofmann, M. Banzet, A. Offenhausser, *et al.*, "Axon guidance of rat cortical neurons by microcontact printed gradients," *Biomaterials*, vol. 32, pp. 2070-6, 2011.
- [92] P. Thiebaud, L. Lauer, W. Knoll, and A. Offenhausser, "PDMS device for patterned application of microfluids to neuronal cells arranged by microcontact printing," *Biosens Bioelectron*, vol. 17, pp. 87-93, 2002.
- [93] M. Song and K. E. Uhrich, "Optimal micropattern dimensions enhance neurite outgrowth rates, lengths, and orientations," *Ann Biomed Eng*, vol. 35, pp. 1812-20, 2007.
- [94] K. E. Schmalenberg, H. M. Buettner, and K. E. Uhrich, "Microcontact printing of proteins on oxygen plasma-activated poly(methyl methacrylate)," *Biomaterials*, vol. 25, pp. 1851-1857, 2004.
- [95] S. R. Hart, Y. Huang, T. Fothergill, D. C. Lumbard, E. W. Dent, and J. C. Williams, "Adhesive micro-line periodicity determines guidance of axonal outgrowth," *Lab Chip*, vol. 13, pp. 562-9, 2013.
- [96] P. Clark, S. Britland, and P. Connolly, "Growth cone guidance and neuron morphology on micropatterned laminin surfaces," *J Cell Sci*, vol. 105 ( Pt 1), pp. 203-12, 1993.
- [97] S. Joo, K. Kang, and Y. Nam, "In vitro neurite guidance effects induced by polylysine pinstripe micropatterns with polylysine background," *J Biomed Mater Res A*, vol. 103, pp. 2731-9, 2015.
- [98] A. Almad, F. R. Sahinkaya, and D. M. McTigue, "Oligodendrocyte fate after spinal cord injury," *Neurotherapeutics*, vol. 8, pp. 262-73, 2011.
- [99] R. J. Franklin and C. Ffrench-Constant, "Remyelination in the CNS: from biology to therapy," *Nat Rev Neurosci*, vol. 9, pp. 839-55, 2008.
- [100] K. Kleinsimlinghaus, R. Marx, M. Serdar, I. Bendix, and I. D. Dietzel, "Strategies for repair of white matter: influence of osmolarity and microglia on proliferation and apoptosis of oligodendrocyte precursor cells in different basal culture media," *Front Cell Neurosci*, vol. 7, p. 277, 2013.
- [101] S. Hossain, H. N. Liu, G. Fragoso, and G. Almazan, "Agonist-induced down-regulation of AMPA receptors in oligodendrocyte progenitors," *Neuropharmacology*, vol. 79, pp. 506-14, 2014.

- [102] T. F. Didar, K. Bowey, G. Almazan, and M. Tabrizian, "A Miniaturized Multipurpose Platform for Rapid, Label-Free, and Simultaneous Separation, Patterning, and In Vitro Culture of Primary and Rare Cells," *Advanced Healthcare Materials*, vol. 3, pp. 253-260, 2014.
- [103] M. Lange, Y. Zeng, A. Knight, A. Windebank, and E. Trushina, "Comprehensive Method for Culturing Embryonic Dorsal Root Ganglion Neurons for Seahorse Extracellular Flux XF24 Analysis," *Front Neurol*, vol. 3, p. 175, 2012.
- [104] L. Lauer, C. Klein, and A. Offenhausser, "Spot compliant neuronal networks by structure optimized micro-contact printing," *Biomaterials*, vol. 22, pp. 1925-32, 2001.
- [105] M. L. De Paula, Q. L. Cui, S. Hossain, J. Antel, and G. Almazan, "The PTEN inhibitor bisperoxovanadium enhances myelination by amplifying IGF-1 signaling in rat and human oligodendrocyte progenitors," *Glia*, vol. 62, pp. 64-77, 2014.
- [106] M. J. Mahoney, R. R. Chen, J. Tan, and W. M. Saltzman, "The influence of microchannels on neurite growth and architecture," *Biomaterials*, vol. 26, pp. 771-8, 2005.
- [107] J. Lee, A. A. Abdeen, D. Zhang, and K. A. Kilian, "Directing stem cell fate on hydrogel substrates by controlling cell geometry, matrix mechanics and adhesion ligand composition," *Biomaterials*, vol. 34, pp. 8140-8, 2013.
- [108] T. Leng, P. Wu, N. Z. Mehenti, S. F. Bent, M. F. Marmor, M. S. Blumenkranz, *et al.*, "Directed retinal nerve cell growth for use in a retinal prosthesis interface," *Invest Ophthalmol Vis Sci*, vol. 45, pp. 4132-7, 2004.
- [109] L. Kam, W. Shain, J. N. Turner, and R. Bizios, "Axonal outgrowth of hippocampal neurons on micro-scale networks of polylysine-conjugated laminin," *Biomaterials*, vol. 22, pp. 1049-54, 2001.
- [110] A. A. Oliva, Jr., C. D. James, C. E. Kingman, H. G. Craighead, and G. A. Banker, "Patterning axonal guidance molecules using a novel strategy for microcontact printing," *Neurochem Res*, vol. 28, pp. 1639-48, 2003.
- [111] J. Roy, T. E. Kennedy, and S. Costantino, "Engineered cell culture substrates for axon guidance studies: moving beyond proof of concept," *Lab Chip*, vol. 13, pp. 498-508, 2013.
- [112] J. Fink, M. Thery, A. Azioune, R. Dupont, F. Chatelain, M. Bornens, *et al.*, "Comparative study and improvement of current cell micro-patterning techniques," *Lab Chip*, vol. 7, pp. 672-80, 2007.
- [113] J. Schnitzer and M. Schachner, "Cell type specificity of a neural cell surface antigen recognized by the monoclonal antibody A2B5," *Cell Tissue Res*, vol. 224, pp. 625-36, 1982.
- [114] S. G. Ricoult, J. S. Goldman, D. Stellwagen, D. Juncker, and T. E. Kennedy, "Generation of microisland cultures using microcontact printing to pattern protein substrates," *J Neurosci Methods*, vol. 208, pp. 10-7, 2012.

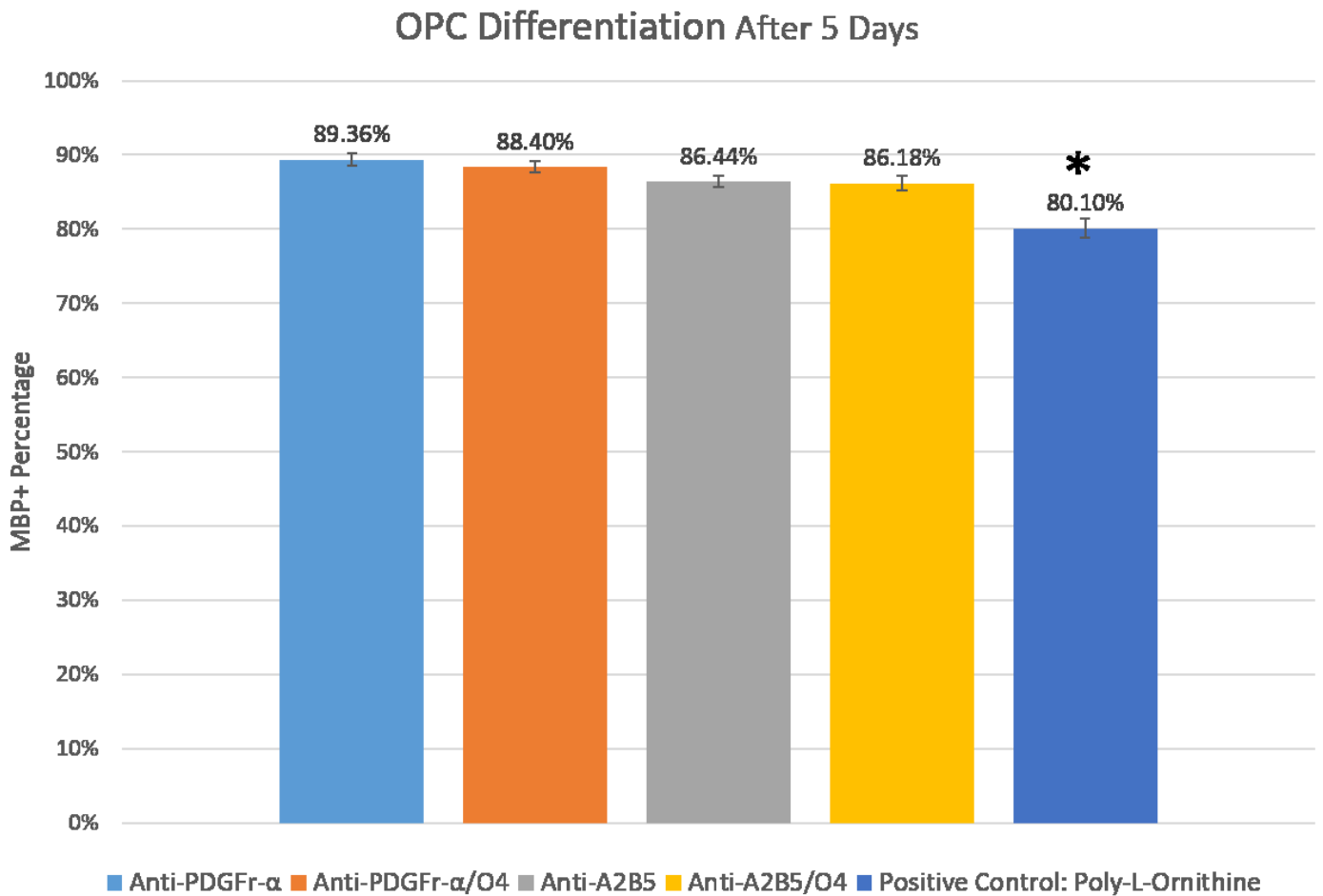
## Appendix A

The following is the ImageJ cell counting macro used in this study.

```
run("8-bit");
setAutoThreshold("Default dark");
run("Threshold...");
setThreshold(17, 255);
setOption("BlackBackground", false);
run("Convert to Mask");
run("Watershed");
run("Watershed");
run("Despeckle");
run("Watershed");
run("Analyze Particles...", "size=10-Infinity show=Outlines display exclude clear include summarize");
```

## Appendix B

The following shows OPC differentiation after 5 days on patterned bio-inks. The measure of differentiation used was the number of MBP+ cells. Results are listed as mean  $\pm$  standard error of the mean, with three independent trials performed in triplicate and five images per sample. The positive control had a significantly lower value than all other samples. (For significance, \*  $p < 0.05$ ).



## Appendix C

The following shows OPC differentiation after 5 days on bio-inks patterned 23 days before cell seeding. The measure of differentiation used was the number of MBP+ cells over GalC+ cells. Results are listed as mean  $\pm$  intra-experimental standard error of the mean, with one trial performed in triplicate.

